frontiers in Earth Science

REVIEW
published: 29 May 2020
doi: 10.3389/feart.2020.00162

High Impact Weather Events in the Andes

Germán Poveda[1]*, Jhan Carlo Espinoza[2], Manuel D. Zuluaga[1], Silvina A. Solman[3,4], René Garreaud[5] and Peter J. van Oevelen[6]

[1] Department of Geosciences and Environment, Universidad Nacional de Colombia, Medellín, Colombia, [2] Université Grenoble Alpes, IRD, CNRS, G-INP, IGE (UMR 5001), Grenoble, France, [3] Universidad de Buenos Aires, Facultad de Ciencias Exactas y Naturales, Departamento de Ciencias de la Atmósfera y los Océanos, Buenos Aires, Argentina, [4] CONICET - Universidad de Buenos Aires, Centro de Investigaciones del Mar y la Atmósfera (CIMA), Buenos Aires, Argentina, [5] Department of Geophysics, Universidad de Chile, Santiago, Chile, [6] International GEWEX Project Office, Washington, DC, United States

Owing to the extraordinary latitudinal extent, a strong orographic variability with very high mountain tops, and the presence of deep valleys and steep slopes, the Andes and the population of the region are highly prone and vulnerable to the impacts of a large suite of extreme weather events. Here we provide a review of the most salient events in terms of losses of human and animal lives, economic and monetary losses in costs and damages, and social disruption, namely: (1) extreme precipitation events and related processes (Mesoscale Convective Systems, lightning), (2) cold spells, frosts, and high winds, (3) the impacts of ENSO on extreme hydro-meteorological events, (4) floods, (5) landslides, mudslides, avalanches, and (6) droughts, heat waves and fires. For our purposes, we focus this review on three distinctive regions along the Andes: Northern tropical (north of 8°S), Southern tropical (8°S-27°S) and Extratropical Andes (south of 27°S). Research gaps are also identified and discussed at the end of this review. It is very likely that climate change will increase the vulnerability of the millions of inhabitants of the Andes, impacting their livelihoods and the sustainable development of the region into the twenty first century amidst urbanization, deforestation, air, soil and water pollution, and land use changes.

Keywords: Andes, extreme weather, storms, ENSO, floods, landslides, droughts, fires

Edited by:
Bryan G. Mark,
The Ohio State University,
United States

Reviewed by:
Francina Dominguez,
University of Illinois at
Urbana-Champaign, United States
Mario Bruno Rohrer,
Meteodat GmbH, Switzerland

****Correspondence:***
Germán Poveda
gpoveda@unal.edu.co

Specialty section:
This article was submitted to
Hydrosphere,
a section of the journal
Frontiers in Earth Science

Received: *04 November 2019*
Accepted: *29 April 2020*
Published: *29 May 2020*

Citation:
Poveda G, Espinoza JC, Zuluaga MD,
Solman SA, Garreaud R and van
Oevelen PJ (2020) High Impact
Weather Events in the Andes.
Front. Earth Sci. 8:162.
doi: 10.3389/feart.2020.00162

INTRODUCTION

Rapid rates of human encroachment, urbanization, deforestation and land use changes are taking place along the Andes (**Figure 1**). These developments make the region and their populations highly vulnerable to extreme weather events and impose a huge toll in terms of socioeconomic, environmental and ecological impacts. Such high vulnerability is associated with diverse natural hazards and risks, poor (or non-existent) preventive and adaptive capabilities and fragile governance. **Figures 2A,B** illustrate the impacts of weather and hydrological extreme events over the Andes. Floods and cold spells lead the rank in human lives losses in the region. Between 1985 and 2014 occurred 150 disasters in the Andes triggered by these extreme events, causing economic losses of 3,138.4 million of US dollars, killing 6,664 people and affecting more than 12 million people (Stäubli et al., 2017). It is highly likely that climate change will increase such vulnerability throughout the Andes (Magrin et al., 2014).

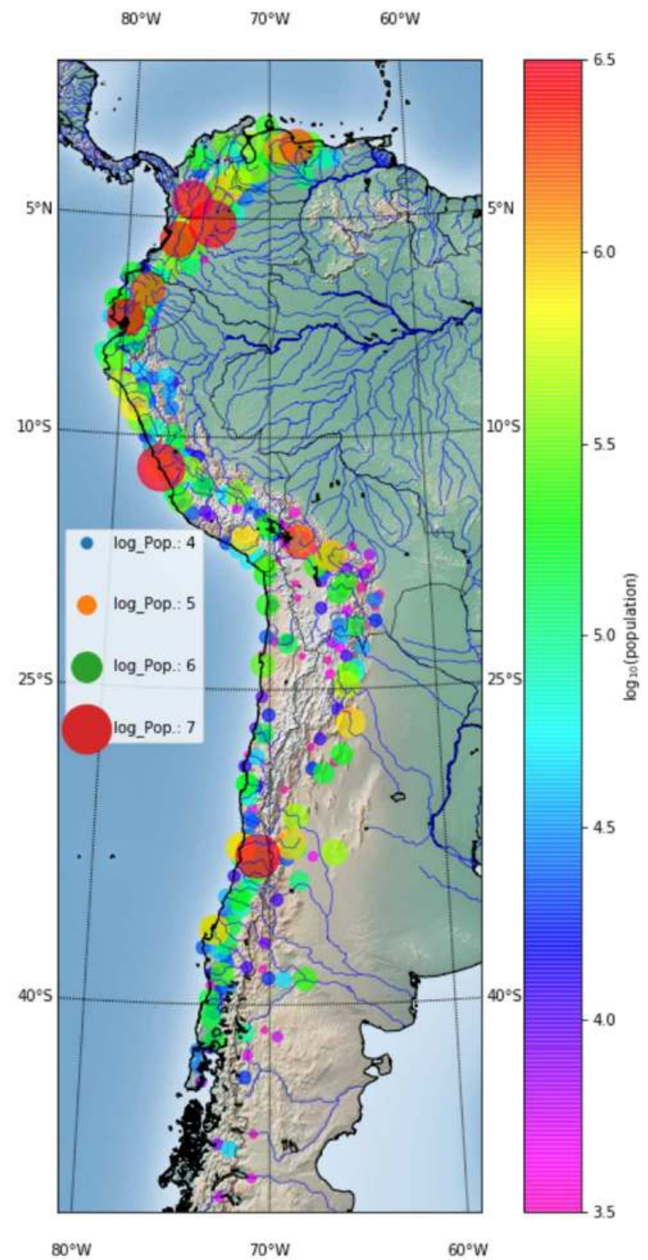

FIGURE 1 | Location and population of cities and towns along the Andes, whose populations are greater that 10,000 inhabitants. Data source: World Cities Database (https://simplemaps.com/data/world-cities).

This paper reviews high impact weather events affecting the livelihoods of millions of people, and compromise the sustainable development of the Andean region amid climate change, urbanization, deforestation, and land use changes. It is a contribution in a series of six to this special issue of Frontiers in Earth Science focused on the Andes climate, weather, hydrology and cryosphere (Condom et al., 2020; Espinoza et al., 2020; Masiokas et al., 2020; Pabón-Caicedo et al., 2020), arising from ANDEX, a prospective Regional Hydroclimate Project (RHP) of the Global Energy and Water Cycle Experiment (GEWEX; https://www.gewex.org/).

For our purposes, the Andean region is divided into three distinctive regions: Northern Tropical (north of 8°S), Southern Tropical (27°S-8°S) and Extratropical Andes (south of 27°S). The work is distributed as follows. Section Extreme Precipitation and Related Processes is focused on extreme precipitation and storm events and related processes, including mesoscale convective systems and lightning. Section Cold Spells, Frosts, and High Winds deals with cold spells, frosts, and high winds, while section ENSO Impacts on Extreme Events discusses the impacts of ENSO on extreme hydro-meteorological events. Section Floods is related to floods, while section Landslides, Mudslides, Avalanches with landslides, mudslides, and avalanches, and section Droughts, Heat Waves and Fires reviews droughts, heat waves and fires. Section Research Gaps provides a summary of main research gaps regarding the monitoring, understanding, modeling, and prediction of the studied processes and phenomena, and some final remarks are pointed out in section Final Remarks.

EXTREME PRECIPITATION AND RELATED PROCESSES

Northern Tropical Andes

Very localized intense storms occur in the tropical Andes during the (annual or semi-annual) wet seasons, with a diurnal cycle shifting with the seasons (Poveda et al., 2005; Bedoya-Soto et al., 2019). Over the Andes of Colombia and Venezuela, most intense storms occur during the two maxima of the annual cycle (April-May and September-November) (Espinoza et al., 2020). The most salient feature of intense storms is a strong spatiotemporal variability, which is caused by steep orography and topographic roughness, local circulations, small and large-scale convective cloud systems acting at different timescales, local circulations and regional valley/mountain breeze systems, katabatic winds (López and Howell, 1967; Bendix et al., 2009), evapotranspiration from the bottom of intra-Andean valleys, orographically-driven moisture transport (Rollenbeck and Bendix, 2011), and anabatic circulations (Bedoya-Soto et al., 2019), which in turn are influenced by synoptic mesoscale and continental conditions. Over the eastern slopes of the Ecuadorian Andes, nocturnal convection and clouds develop in spite of unfavorable large-scale conditions (Bendix et al., 2009; Trachte et al., 2010). Precipitation recycling in the tropical Andes can be 70–90% of total precipitation (Zemp et al., 2014; Bedoya-Soto et al., 2019). The strong variability of tropical Andean storms is evidenced in their fractal and multifractal properties (Poveda and Mejía, 2004; Gómez and Poveda, 2008; Hurtado and Poveda, 2009; Poveda, 2011; Mesa and Peñaranda, 2015; Posadas et al., 2015; Poveda and Salas, 2015; Yarleque et al., 2016; Duffaut-Espinosa et al., 2017).

Intense storms over the tropical Andes are also associated with Mesoscale Convective Systems (MCS) over western Colombia and the far eastern tropical Pacific (Velasco and Fritsch, 1987; Houze et al., 2015; Zuluaga and Houze, 2015). These large and intense convective systems are seen to contribute to explain

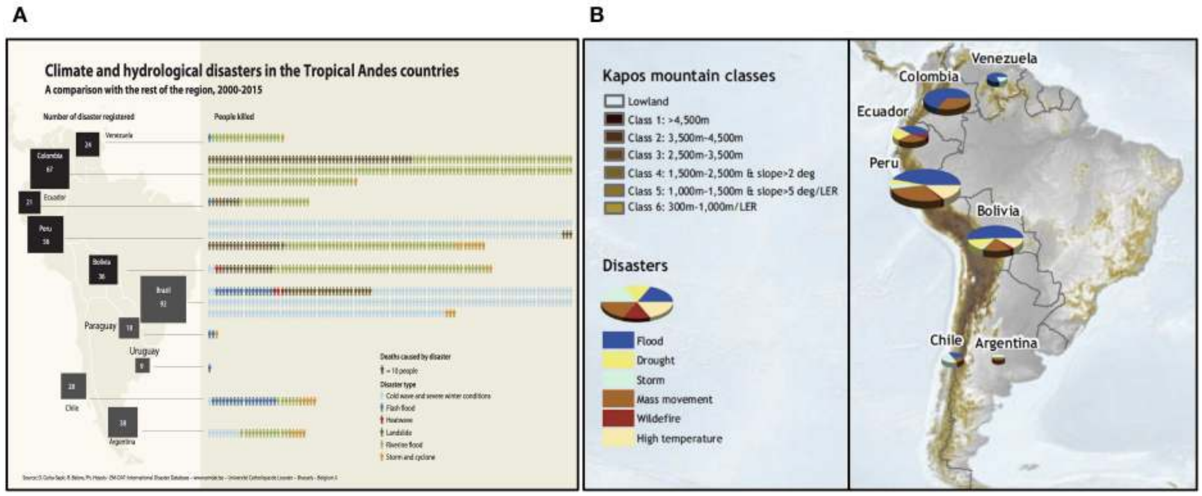

FIGURE 2 | (A) Climate and hydrological disasters in the Andean countries and human fatalities during the period spanning from 2000 to 2015. Source: Schoolmeester et al. (2016), from a figure made by GRID-Arendal and Cartografare il Presente/Riccardo Pravettoni (https://www.grida.no/resource). **(B)** Disasters along the Andes caused by storms, floods, mass movements, extreme temperatures, droughts and wild fires, based on EM-DAT (Guha-Sapir et al., 2015). Cartography by Jürg Krauer, Centre for Development and Environment (CDE), University of Bern, Switzerland. Adapted from Stäubli et al. (2017) by permission from Springer, *Climate Change Extreme Events and Disaster Risk Reduction*, by S. Mal, R. B. Singh, and C. Huggel (eds.), Copyright, 2018.

the existence of one of the rainiest spots on Earth over the Pacific coast of Colombia with average rain rates of 10,000–13,000 mm per year (Poveda and Mesa, 1999; Poveda et al., 2014; Yepes et al., 2019). Over Colombia's far eastern Pacific, the cross-equatorial flow become the south-westerly CHOCO LLJ that interacts with the western Andes (Poveda and Mesa, 2000; Bedoya-Soto et al., 2019; Yepes et al., 2019), exhibiting weaker winds in February-March and stronger winds during September-November (**Figure 3**). Such enhanced ocean-atmosphere-land interactions by the CHOCO LLJ produce world-record breaking rainfall intensities over western Colombia inland and off-shore (Poveda and Mesa, 1999, 2000; Yepes et al., 2019). Mostly focused on the Caribbean and the Orinoco LLJs, easterly trade winds prevail, and their interaction with the ITCZ produce large amounts of rainfall in the Orinoco basin, and the Upper Amazon river basins in Colombia, Venezuela and Brazil (**Figure 3**).

Figure 4 shows the distribution of average (1998–2013) rainfall over most South America during JJA and DJF, using data from the Tropical Rainfall Measuring Mission (TRMM). Most of this rain is produced by different types of convective organization at the regional scale (Houze et al., 2015; Rasmussen et al., 2016), which are often part of large MCSs at different stages. Such types can be classified using reflectivity echoes from the TRMM 3B42 product (Kummerow et al., 1998, 2000; Houze et al., 2007, 2015; Romatschke et al., 2010). **Figure 5A** shows the probability of TRMM Precipitation Radar (PR) observing a wide convective core (WCC), with pixels exceeding 40 dBZ reflectivity over 1,000 km^2 during JJA (Houze et al., 2015). The WWC tend to maximize in the Pacific coast of Colombia and Panama, in the northern region of the Andes of Colombia, as well as in the Orinoco and parts of the Upper Amazon river basin. **Figures S1**, **S2** show the MCS that triggered the flooding of Mocoa, Colombia, in April 1st, 2017, killing at least 336 people, injuring 332, and 70 others missing.

Rainfall over north-western South America exhibits different precipitation features (PF) containing elements associated with their convective life cycle, such as those with and without ice scattering and MCSs. The former two maximize in the afternoon from 12:00 to 18:00 LT at the west of the western Colombian Andes, and the eastern slope of the eastern Andes. The former occurs by the effect of Pacific sea breeze along the valley floor and upslope to the top of the Andes in the afternoon (López and Howell, 1967; Yepes et al., 2019), but also from the Orinoco LLJ during the afternoon. On the other hand, PFs with MCSs mainly occur in the morning (00:00–06:00 LT) offshore in the Pacific at 77.5°W (Mapes et al., 2003; Yepes et al., 2019). Large precipitation features (PFs) associated with MCSs represent <1% of PFs in the eastern Amazonian slopes of the Andes (Jaramillo et al., 2017). The most common PFs exhibit small areas and contribute about 15% to total precipitation, while MCS are observed least but produce more than 50% of the total along the eastern slope of the Central Andes below 2000 m a.s.l. (Chávez and Takahashi, 2017).

Some mesoscale convective units may become broad areas of stratiform rain (BSR; TRMM echoes covering more than 50,000 km^2) at the later stage of MCS (Houze, 2004) (**Figure 5B** for JJA). They are concentrated over the eastern Pacific near Colombia, and less in the Orinoco and Upper Amazon basin. Furthermore, very deep and intense convective cores (DCC) develop over continental regions, with maxima during JJA over the north-eastern Andes of Colombia and Venezuela. **Figure 5C** shows DCCs higher than 10 km, associated with severe weather, lightning and flash floods (Rasmussen and Houze, 2011; Zuluaga and Houze, 2015; Hoyos et al., 2019).

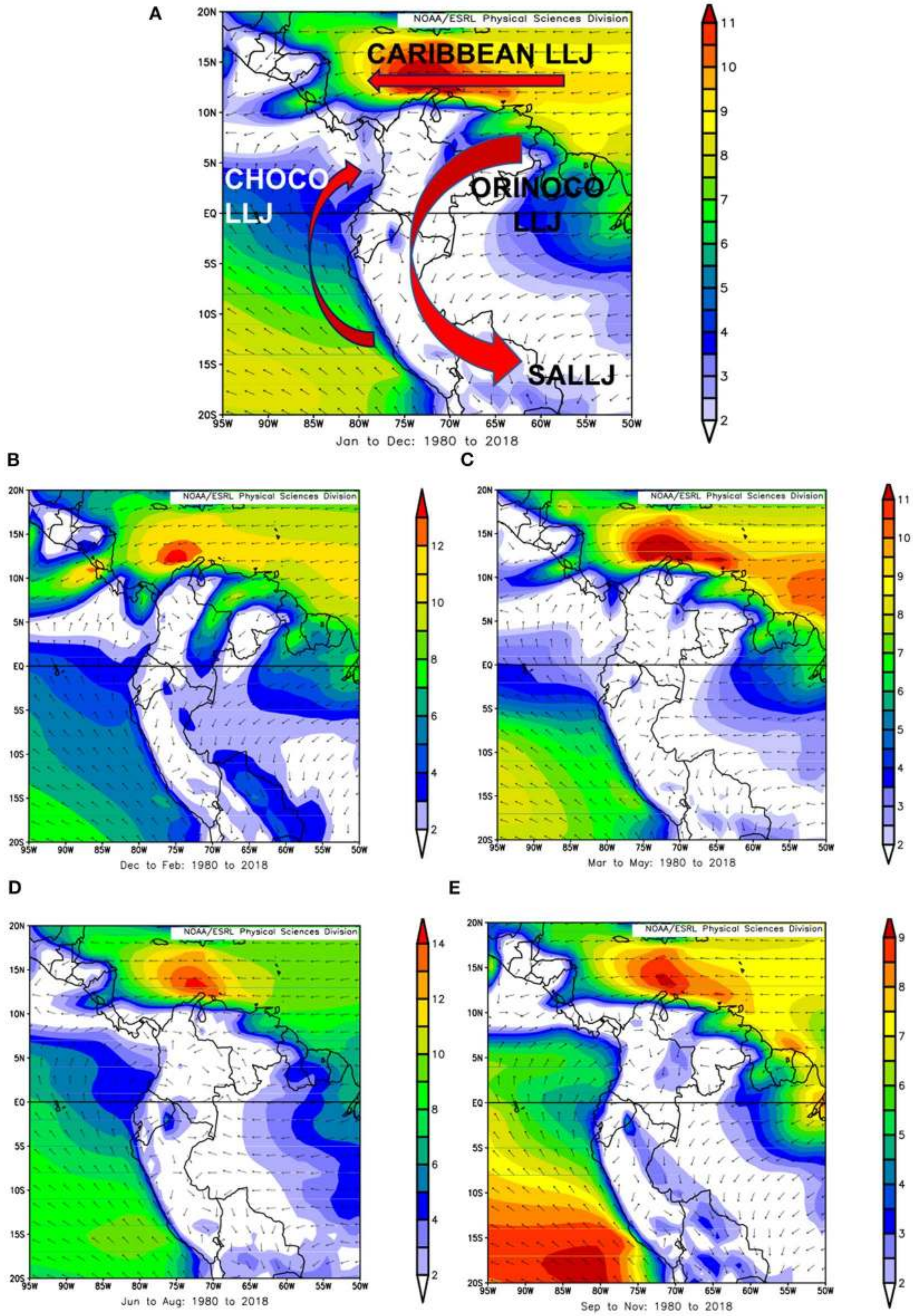

FIGURE 3 | Distribution of the long-term mean (1980-2018) horizontal wind speed (m/s) at 950 hPa over northern South America; **(A)** Mean annual values showing the Choco, Caribbean, and Orinoco low-level jets, and the SALLJ. Mean seasonal values during **(B)** December-January-February; **(C)** March-April-May; **(D)** June-July-August; and **(E)** September-October-November. Images prepared from the NOAA/ESRL Physical Sciences Division, Boulder Colorado; https://www.esrl.noaa.gov/psd/.

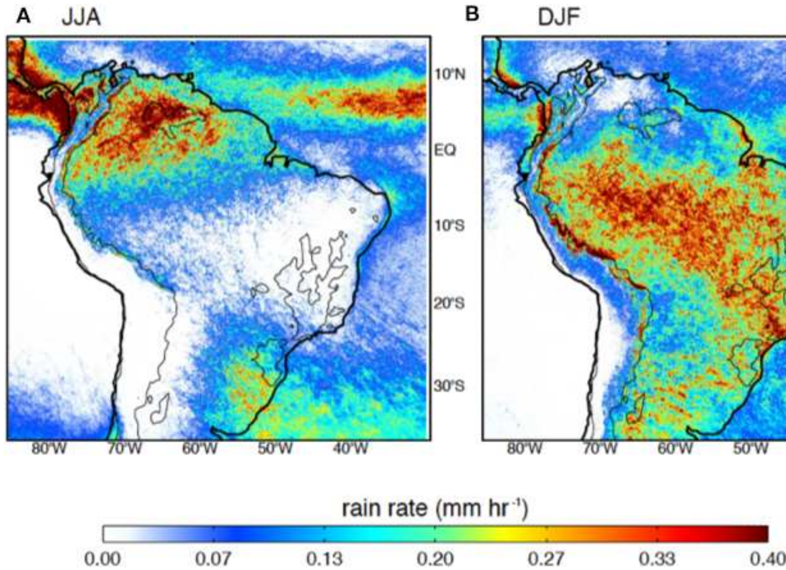

FIGURE 4 | Average rain rate from TRMM distinguishable rain areas during the months of **(A)** JJA and **(B)** DJF from 1998 to 2013. The black thin contour characterizes the 700 m elevation. Adapted from Houze et al. (2015).

After convective systems get organized, they migrate away from the topography. Usually, the migration of organized convective systems is favored by the prevailing mid- to upper level wind. Over northern western Colombia and southern Panama, organized systems tend to move westward away from the topography toward the east Pacific Ocean by the easterly flow (Mapes et al., 2003; Zuluaga and Houze, 2015). Some authors attribute the speed of flow to a gravity wave triggered by the afternoon heating of the Andes (Mapes et al., 2003), and others to the easterly wave migration over the east Pacific (Rydbeck and Maloney, 2015).

Northern South America is also affected by synoptic-scale processes favoring convective organization over the tropical Andes such as the African Easterly Waves (AEWs). These perturbations are associated with convective activity and the occurrence of storm events in northern Colombia and Venezuela (León et al., 2001; Poveda et al., 2002; Dominguez et al., 2020). To the west of the tropical Andes (north of Peru and Ecuador), rain is associated with an onshore westerly low-level flow from the equatorial Pacific, which triggers convection forced by orographic lifting of the Andes (e.g., Takahashi, 2004).

The most active regions of lightning in the world are found in the low-lands of the tropical Andes of Colombia and Venezuela (Albrecht et al., 2016), with flash rate density (FRD) of 233 flashes per km^2 per year (**Figure S3**). Lightning flash density is inversely correlated with altitude along the Andes of Colombia (Herrera et al., 2018), causing high human and livestock mortality (Cristancho et al., 2017), with 757 deaths from 2000 to 2009, or 1.78 per million per year (Cruz et al., 2013; Navarrete-Aldana et al., 2014). Also, between 2003 and 2012, 282 casualties were reported among soldiers of the Colombian Army in 149 events with 72 deaths and 210 injuries. Lightning also affect the power transmission systems in Colombia (Aranguren et al., 2017).

Southern Tropical Andes

Most of moisture reaching the Andes highlands come from the Atlantic Ocean and the Amazon River basin via easterly aerial rivers (Poveda et al., 2014). Westerly winds from the Pacific are not infrequent over the Andes from Colombia to Peru, and occur following the seasonal movement of the ITCZ and the strength of the Bolivian High Sakamoto et al. (2011); Poveda et al. (2014); Makowski Giannoni et al. (2016); Trachte (2018); Espinoza et al. (2020). Boers et al. (2015a,b, 2016) studied different types of extreme storms events over the southern tropical Andes, and found that events north of 20°S are typically generated in the Amazon Basin, whereas storms over the foothills of the eastern Andes south of 20°S, including the Puna High Plateau, originate over the southeastern part of the continent. Such propagation during the monsoon season (December to March) is explained by mid-latitude alternating pressure anomalies embedded in a westerly Rossby wave-train in combination with a low-pressure center located over northwestern Argentina, creating favorable conditions for intense storms (Liebmann et al., 2004; Espinoza et al., 2012a; Boers et al., 2015b; Paccini et al., 2017). Over the northern part of the south tropical Andes (10°S-5°N), the eastward propagation of the MJO convective core during the Austral summer (DJF), modulates sub-seasonal precipitation, producing positive rainfall anomalies up to 50% compared with the climatology (Recalde-Coronel et al., 2020).

Extreme rainfall in the valleys of the southern tropical Andes results from the interplay between the Amazon and the Pacific Ocean flows, influenced by orography (Junquas et al., 2016, 2018; Trachte, 2018). Kumar et al. (2019) show that

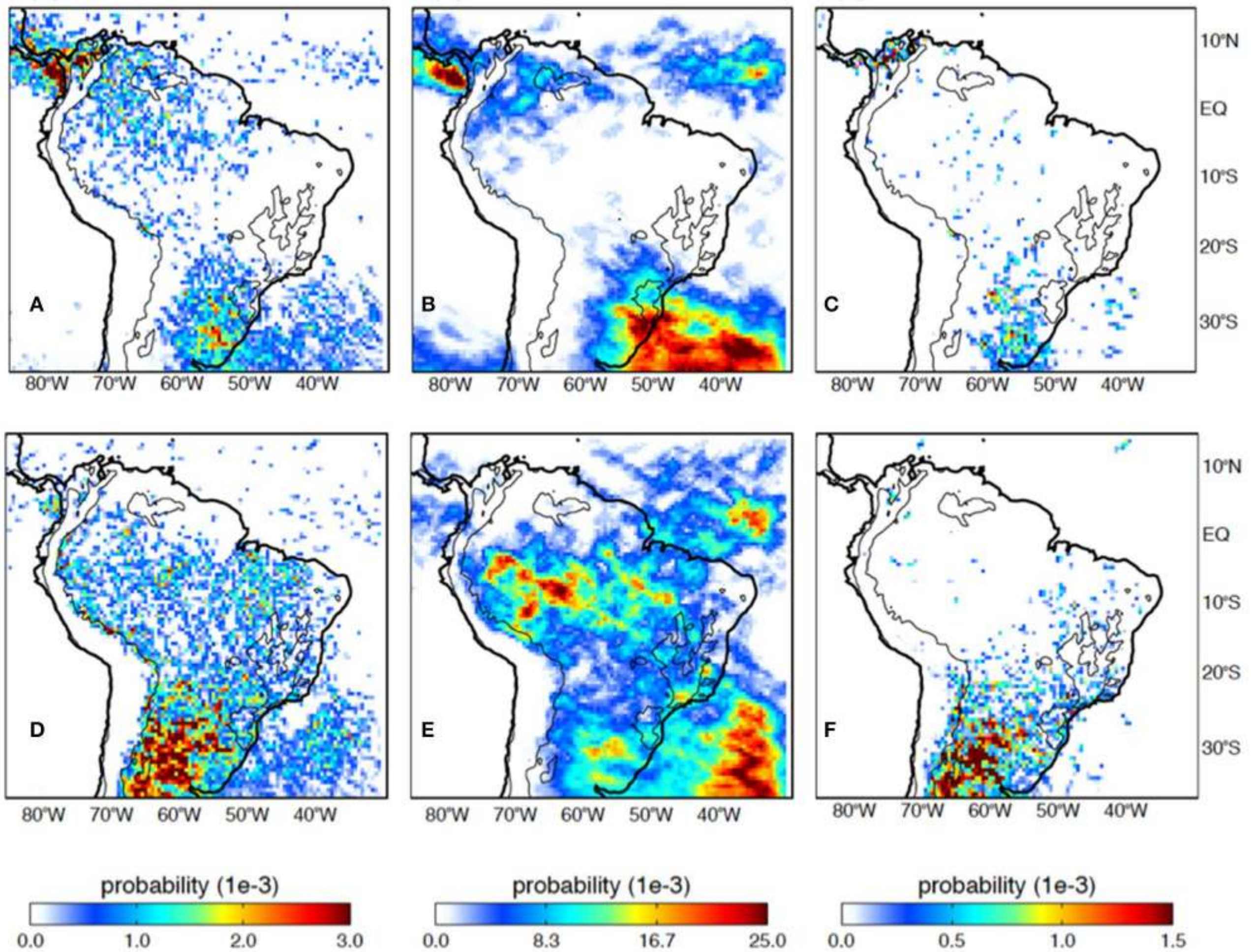

FIGURE 5 | Geographical distribution of the probability of finding **(A)** a wide convective core; **(B)** a broad stratiform region; and **(C)** a deep convective core during the months of JJA from 1998 to 2003. **(D)** same as **(A)**; **(E)** same as **(B)**; and **(F)** same as **(C)** but for DJF, respectively. The black contour inside the continental regions represents the 700 m elevation. Figure adapted from Zuluaga and Houze (2015).

precipitating cloud systems (PCs) in the Andes and western Amazon are largely affected by the directional surface flows. In particular, larger PCs (>2,000 km^2) are more frequent at the western flank of the Andes during southerly and easterly surface flows, while along the eastern flank, northerly and easterly surface winds are predominant during high and large PCs (**Figures 6A–D**). According to Villalobos et al. (2019), convection and cloud systems are deeper over the central Andes regions than in the Amazon-Andes transition region. The central Andes witness convective (30%) and stratiform (70%) precipitation, contributing with 63.3 and 36.7% of total rain, whereas in the Amazon-Andes transition those percentages and the contribution to cumulative rain attain similar values (31 and 69%, respectively). Over the central Peruvian Andes, and using a vertically pointed profile rain radar installed in the Mantaro Basin, Kumar et al. (2020) show that most of the bright band height (an indication for the melting zone) over this region vary between 4.3 and 4.7 km. An example of the vertical profile of radar reflectivity is shown in **Figures 6E,F**.

The eastern Andes foothills located at windward conditions are among the rainiest regions in the Amazon basin (4,000–7,000 mm yr^{-1}; Roche et al., 1990; Espinoza et al., 2015), resulting from the interaction between large-scale humidity transport from the Atlantic Ocean, Amazonian evapotranspiration and moisture recycling, and the steep Andes topography (Killeen et al., 2007; Espinoza et al., 2009; Zemp et al., 2014). Highest values of this orographic rainfall are located along the foothills of the eastern Andes of Peru and Bolivia (e.g., **Figure 6B**), mainly during the austral summer (Romatschke and Houze, 2010; Espinoza et al., 2015). Most rainfall intensification has been associated to the direction of 850 hPa winds (**Figure 6G**), with excessive rainfall during a north-easterly wind regime originating in subtropical South America (Garreaud and Wallace, 1998; Laurent et al., 2002; Rickenbach et al., 2002; Espinoza et al., 2015; Chávez and Takahashi, 2017; Kumar et al., 2019; Moya-Álvarez et al.,

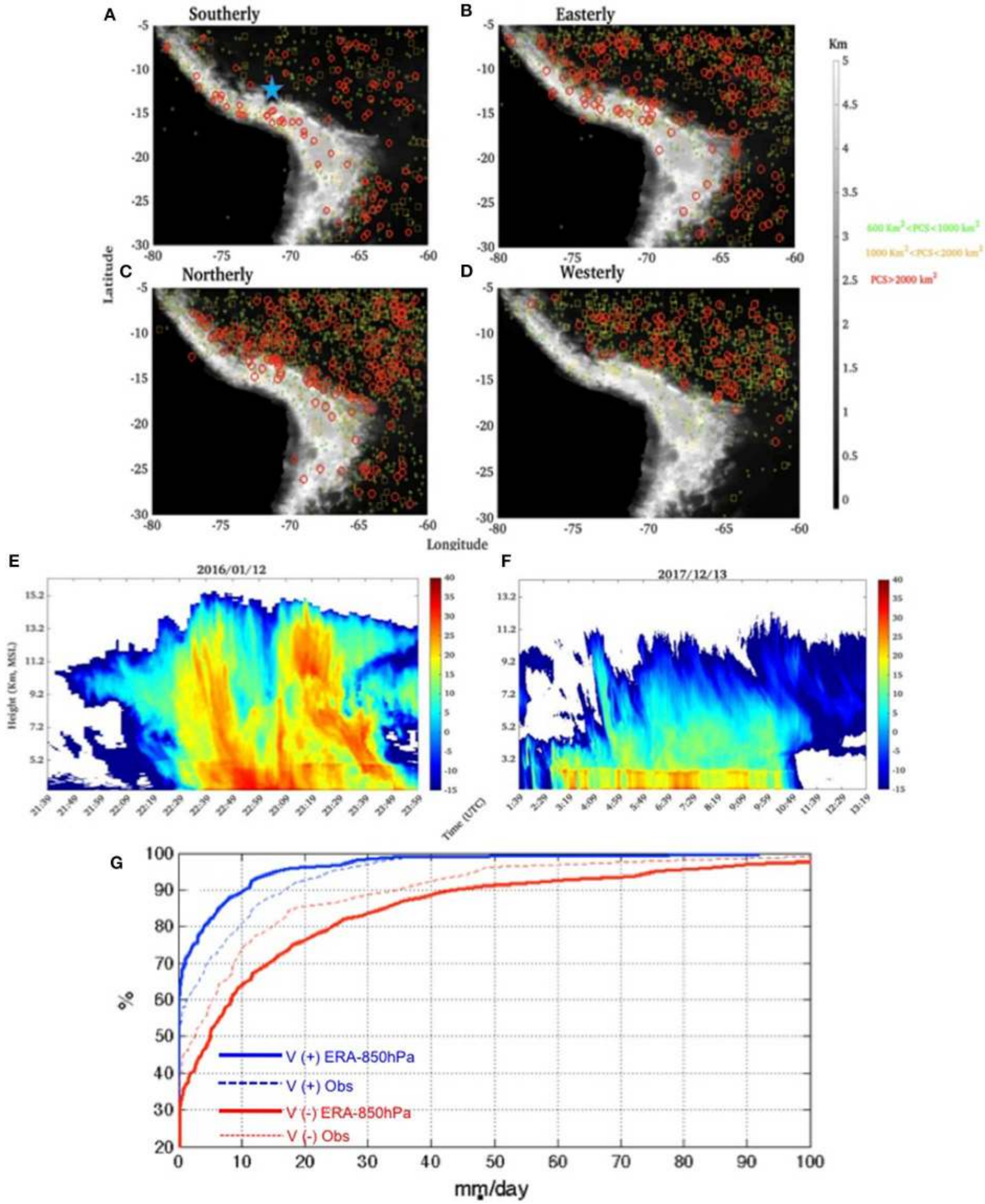

FIGURE 6 | Locations of the precipitation cloud systems for different wind regimes: **(A)** Southerly, **(B)** Easterly, **(C)** Northerly, and **(D)** Westerly. The size of the precipitation cloud systems is represented by different colors (in red, precipitation cloud systems larger than 2,000 km^2). Source: Kumar et al. (2019). © Atmospheric Research. Reprinted by permission from Elsevier. **(E,F)** Radar reflectivity measured by a meteorological Ka band cloud radar installed in the Mantaro Basin, Peru (12.04°S, 75.32°W, 3,322 m a.s.l.) during **(A)** a convective rainfall event (12 January 2016), and **(B)** a stratiform rainfall (13 February 2017). Source Kumar et al. (2020). © Atmosphere – MDPI. CC license. **(G)** Probability distribution function of June-August rainfall over the Quincemil-San Gabán stations in the Amazon-Andes transition zone, southern Peru (blue star, **A**) during different regimes: southerly (V+, blue line), and northerly (V–, red line). 850 hPa winds from ERA-40 and from the meteorological station at Iquitos, Peru, are used to estimate wind regimes (solid and dashed lines, respectively). Adapted from Espinoza et al. (2015). © Water Resources Research. Reprinted by permission from John Wiley and Sons.

2019). Wet episodes over these regions are frequently related to large and medium MCSs, triggered by the orographic lifting of the moist South American low-level jet (SALLJ, Bendix et al., 2009; Giovannettone and Barros, 2009; Romatschke and Houze, 2013; Junquas et al., 2018). Below 2000 m, intraseasonal rainfall variability is mainly modulated by the interplay between SALLJ, cross-equatorial low-level flow and southern winds intrusion toward low latitudes (Wang and Fu, 2002; Espinoza et al., 2015; Chávez and Takahashi, 2017). In the north-western Amazon-Andes transition region (Peru, Ecuador and Colombia) intense storms are more frequent under southerly low-level winds regime, particularly from June to November (Wang and Fu, 2002; Paccini et al., 2017).

Figure 5D shows how the Andes foothills region in Central South America witness localized maxima of storms containing wide convective cores (WCC). These storms are organized at the mesoscale, producing the accumulated rainfall concentrated in the hotspots shown in **Figure 5B**). The region also experiences storms with extensive broad areas of stratiform rain (BSR) as shown in **Figure 5E**, mainly localized in the Andes foothills south of Peru and northern Bolivia. Diurnal analysis of the occurrence of these storms show how WCC peaks during the evening hours while storms containing BSRs peak in the early morning, which suggest that both are part of similar MCSs in either early or later stages of their convective life cycles (Romatschke and Houze, 2010). Chávez and Takahashi (2017) found that surface precipitation over these rainfall "hotspots" at the eastern flank of the Peruvian Andes is characterized by maximum values at 01–06 LT and organizes into MCSs that represent with at least 50% of daily rainfall. Few storms containing deep convective elements are found in the central Andes foothills region (**Figure 5F**), which suggests the orographically-driven moderate convective nature of storms. This observation agrees with the notion that convection here is highly influenced by the proximity to the convection in the Amazon basin, which tends to have less deep, more maritime-like and weaker convection (Houze et al., 2015).

MCSs in the region are observed in about 86% of the cases (Jaramillo et al., 2017) by the moisture transport that converges in the Andes foothills, in association with a stronger SALLJ. In the Central Andes, MCSs mainly occur from December to March, as in the northern part of the La Plata River basin (Jaramillo et al., 2017). The other 14% of the cases are associated with cold surges coming from south-eastern South America. These MCSs show a strong relationship with the diurnal cycle of rainfall in the Amazon-Andes transition region; in the upper Andes and lower Amazon precipitation tends to peak in the afternoon (Killeen et al., 2007), On the eastern slopes of the Andes (800–2,000 m a.s.l.), convection is developed and organized into MCSs during the night and a peak of precipitation is observed at 01–06 LT. These then move downslope ($\sim$700 m) and precipitation declines during the morning (Chávez and Takahashi, 2017).

Extratropical Andes

Intense precipitation events over the extratropical Andes are different than those over the northern and central Andes, and occur both in summer and winter. Most precipitation is delivered by deep stratiform clouds rooted along frontal systems (Falvey and Garreaud, 2007; Viale and Nuñez, 2011), although deep convection associated with cut-off lows (COL) also occur. These weather systems reach the extratropical Andes year-round, and are strongly distorted by the mountains (Barrett et al., 2009). In particular, the cordillera produces a west-east precipitation gradient such that precipitation increases by a factor 2–4 over the western slope of the Andes to sharply decrease to the east of the continental divide (Viale and Garreaud, 2014). The upstream precipitation enhancement and downstream rain shadow across the southern Andes cordillera creates one of the most extreme precipitation gradients on Earth. In frontal cases, the amount of precipitation over the mountains and adjacent lowlands scales directly with the integrated water vapor transported by the westerly winds toward the western Andes (Falvey and Garreaud, 2007). Recent research shows that such transport maximizes in the core of atmospheric rivers (Ralph et al., 2016; Nieto et al., 2019) that landfall between 35 and 45° along the west coast of South America 3–4 times per month (Viale et al., 2018). After making landfall, the ARs face the Andes cordillera where they deliver most of their precipitating. Thus, ARs account for up to 50% of the precipitation in the western slope of the Andes and are associated with about half of the extreme precipitation events in this region (Viale et al., 2018), thus being responsible for the majority of extreme precipitation events along the west slopes of the extratropical Andes (Valenzuela and Garreaud, 2019). A dramatic example of this situation is illustrated with the integrated water vapor and accumulated rainfall on Dec. 17, 2017, which triggered a major flooding causing more than 20 fatalities in the Santa Lucia village in southern Chile (**Figure 7**).

The thermal structure of weather systems is also relevant in triggering extreme hydrological events over the extratropical Andes. In most storms (at least two thirds of the events) precipitation over the central valleys begins almost simultaneously with the arrival of the cold front, so the bulk of the storm accumulation occurs under cold conditions (post-frontal precipitation) with a freezing level altitude around 2,200 m (Garreaud, 2013). This level is well below the Andes crest height between 27 and 37°S (>5,000 m a.s.l.), contributing to the build-up of a seasonal snow pack that eventually melt during spring-summer. Indeed, many cold fronts arriving to central Chile during winter produce a minor increase in the flow of the rivers draining the Andes cordillera. A few winter storms, however, feature warm conditions causing a freezing level as high as 4,000 m a.s.l. and increasing the pluvial area up to a factor 4 relative to average conditions. This winter warm storm, often associated with an AR, can cause large floods downstream (Garreaud, 2013).

Cut-off lows (COL) can cause substantial precipitation near the western slope of the Andes, because the ascent in its leading edge is reinforced by the forced ascent over the terrain. In contrast to cold fronts, COLs can reach subtropical latitudes (northern Chile to southern Peru). An extraordinary COL situation happened in March 22–24, 2015, after warm waters established along the western coast of South America since early March, providing ample moisture in this otherwise dry region. The result was a major rainstorm over the Atacama region, the most arid desert in the world: up to

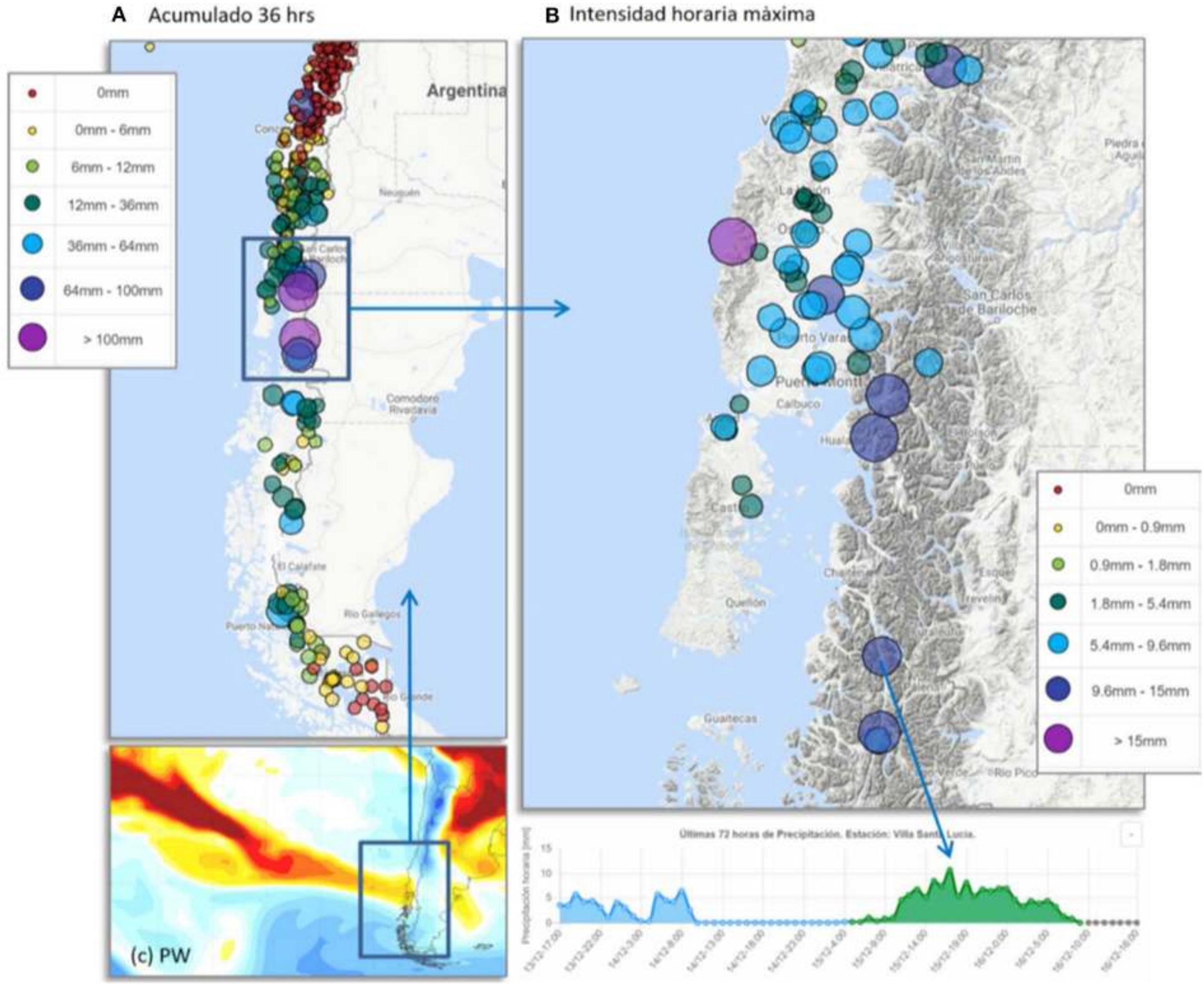

FIGURE 7 | Key aspects of the atmospheric river causing a major flooding in southern Chile. **(A)** Accumulated precipitation during Dec. 16, 2017. **(B)** Maximum rain rate (mm/h) that day. (c) Precipitable water MIMICS estimates). Red colors are precipitable water values in excess of 50 mm.

100 mm during 3 days and rainfall intensities in excess of 10 mm/h at some stations (**Figure 8**). The 2015 Atacama flooding episode is among the worst hydrometeorological disasters in Chile in terms of losses of human lives (more than 60 fatalities) and infrastructure damage (Bozkurt et al., 2016).

Convective rainfall events also occur during dry austral summer months in the northern sector of the extratropical Andes (30–40°S), when liquid precipitation occur as high as 4,000 m a.s.l, triggering landslides and debris flows and damaging infrastructure and international highways (Sepúlveda and Padilla, 2008; Garreaud and Viale, 2014). The synoptic conditions for these summer events are characterized by easterly winds atop of the Andes, opposing the climatological westerly flow that transport moist air toward the mountains (**Figure 9**). The approach of an upper level trough (or COL) is necessary to overcome the large-scale subsidence, thus contributing to exacerbate the intensity of storms (Garreaud and Rutllant, 1997; Viale and Garreaud, 2014).

The southern region of South America experience one of the deepest, and most intense convective systems on Earth (Zipser et al., 2006; Rasmussen et al., 2016), mainly over the region of Mendoza, along the Andes of Argentina. Most of this precipitation occurs in the austral spring and summer (e.g., **Figure 5B**), and concentrates to the east of the Andes in the La Plata River basin (Zipser et al., 2006; Salio et al., 2007; Romatschke and Houze, 2010; Rasmussen and Houze, 2011, 2016). An on-going research effort is under way to monitor and understand the life cycle of convective storms associated with high impact weather in the lee side of the Andes of Argentina (Provinces of Córdoba and Mendoza), known as RELAMPAGO (Remote sensing of Electrification, Lightning, And Mesoscale/microscale Processes with Adaptive Ground Observations; https://www.eol.ucar.edu/field_projects/

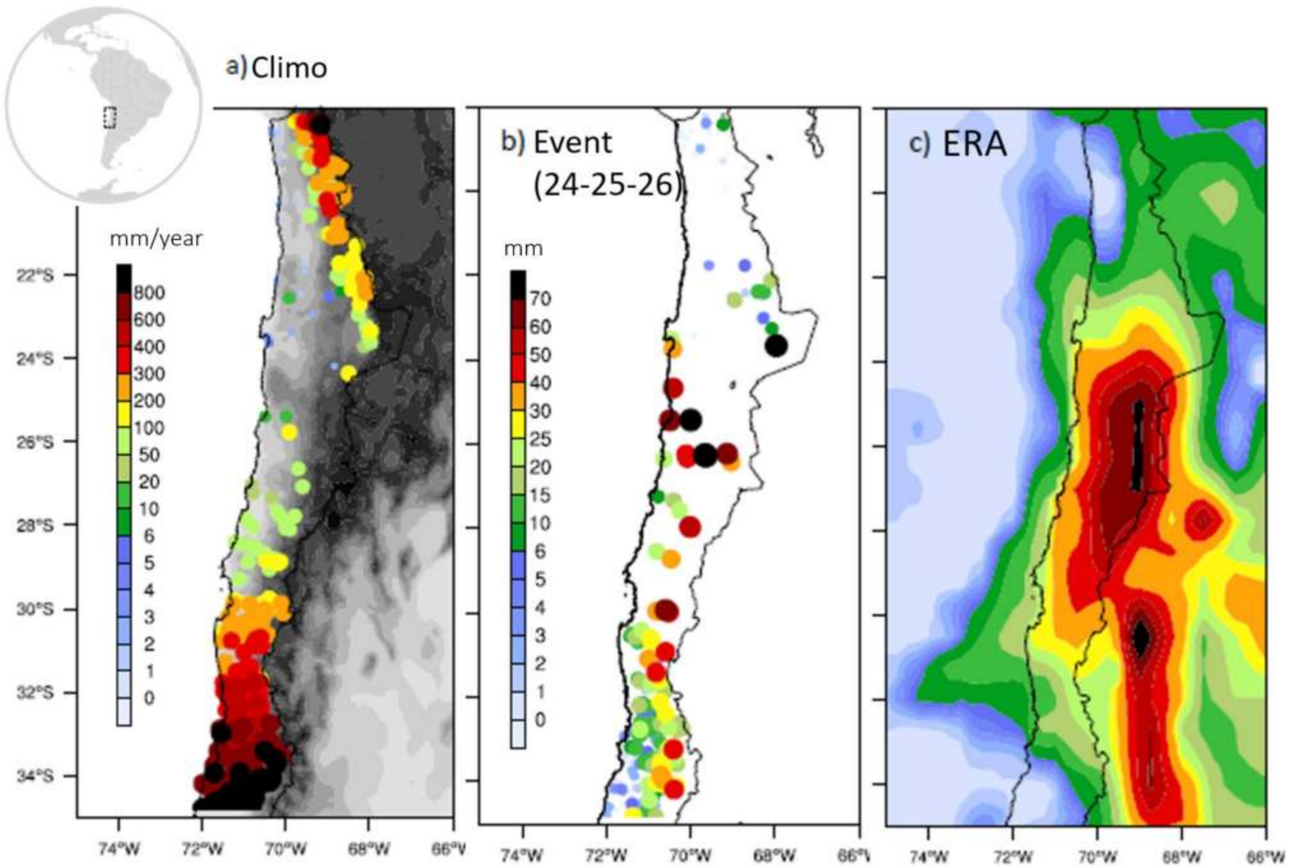

FIGURE 8 | (A) Annual mean precipitation along north-central Chile. **(B)** Station-records of accumulated precipitation during the Atacama storm (March 23–25, 2015). **(C)** ERA-5 analysis of accumulated precipitation during the Atacama storm (March 23–25, 2015). Note that the hyper-arid Atacama Desert is characterized by mean values below 5 mm/year but during the March 2015 storm some stations accumulated more than 70 mm in just three days. Based on data from Bozkurt et al. (2016).

relampago). It is a joint effort between USA, Brazil and Argentina which had an Extended Observing Period from June 1st 2018 to April 30th, 2019, and an Intensive Observing Period from November 1st to December 18th, 2018. This region experiences multicellular storms which rank among the most intense convective systems in the world, exhibiting high tops, large hail, and strong lightning activity. Most of the storms initiate and develop in the early afternoon and late evening hours near and just east of the Sierras de Córdoba, and are predominant during the austral summer (December to February), with large CAPE and weak low-level vertical wind shear (Mulholland et al., 2018). The RELAMPAGO project involve collaboration with CACTI (Clouds, Aerosols, and Complex Terrain Interactions), a USA funded project to study orographic clouds and their representation in multi-scale models (Varble et al., 2019).

Farther downstream of the extratropical Andes, the lowlands of the La Plata River Basin region experience an exceptionally number of localized and widespread convective storms near the La Plata River basin, just east of the Andes ranges (**Figures 5D–F**). There exists a preference for initial deep convective cells to be triggered near the foothills of the Andes close to Sierra de Cordoba in Argentina (e.g., DCCs shown in **Figure 5F**), under a strong topographically-driven convective initiation and maintenance. Although the Amazonian moisture source for the SALLJ does not seem to be as significant as originally thought (Yang and Dominguez, 2019), it is sometimes capped by leeside subsidence of the midlevel dry air that flows over the Andes from the eastward synoptic disturbances. The breaking of this cap triggers the release of convective instability and deep convection leading to tornadoes, hail and floods along the plains between the Andes and the Atlantic coast (Grandoso, 1966; Nascimento and Marcelino, 2005; Matsudo and Salio, 2011; Rasmussen and Houze, 2011; Mezher et al., 2012; Rasmussen et al., 2014). Associated mechanisms of hail occurrence include intense convection with sufficiently high warm and moist updrafts to increase super-cooled water content in the cloud, convergence of moist enthalpy near the ground, and the passage of cold fronts that trigger instabilities favoring upward motion on the warm side of the front, and facilitating the growth of deep convection (Teitelbaum and D'Andrea, 2015).

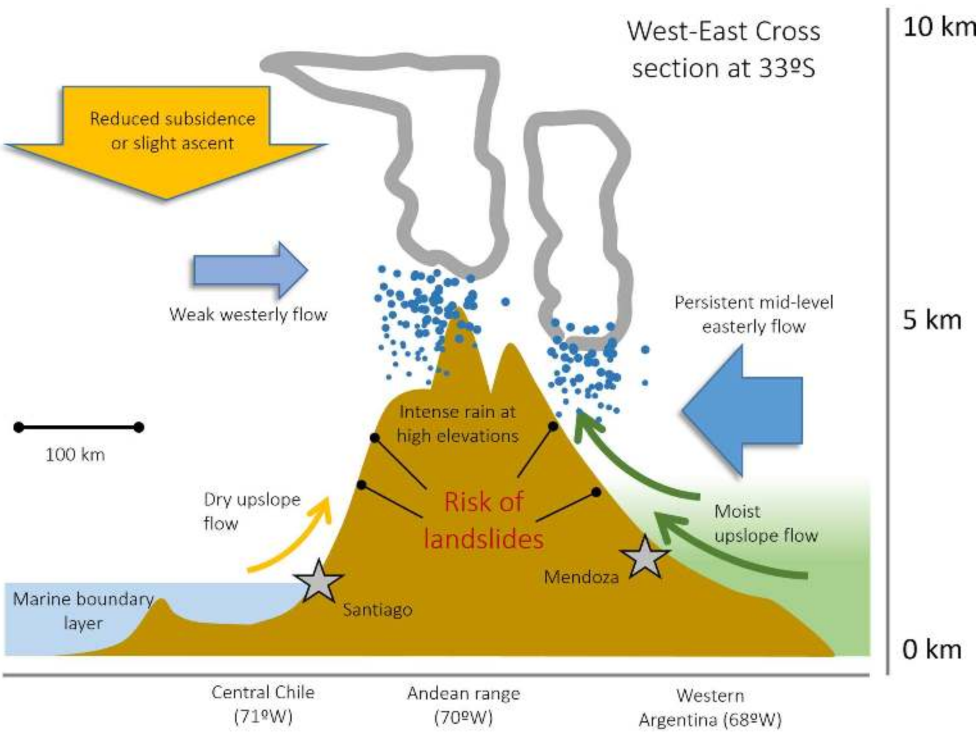

FIGURE 9 | Schematic west-east cross section during summer storms over the extratropical Andes (30-37°S). This is the most frequent type of storm (2/3) associated with an approaching weak trough aloft and easterly winds over the Argentinean side. Adapted from Viale and Garreaud (2014).

COLD SPELLS, FROSTS, AND HIGH WINDS

Northern Tropical Andes

Higher elevations in the tropical Andes pose a challenge for their communities which have to adapt to the occurrence of frosts, as is the case in the northern Andes of Colombia above 2,500 m a.s.l. Such events are typical during dry seasons due to intense radiative cooling of the ground during the night in association with very low cloud cover (**Figure S4**). The occurrence of intense frosts events causes large economic losses to agricultural communities in the Andes by destroying crops and pastures (Bermúdez, 1990; Holmann et al., 2005).

Southern Tropical Andes

Metz et al. (2013) find that along the Andes corridor, extreme cold events reduce 925-hPa temperatures up to 17°C below normal. During these events 925-hPa southerly winds are intensified from 0 to 10 m s^{-1} and the 925–700 hPa lapse rates is low (−3°C km^{-1}). Cold surges, also known as *Friajes* or *Surazos* in Spanish (*Friagems*, in Portuguese), propagate equatorward reaching the Bolivian and southern Peruvian Amazon, causing sudden and severe drops in temperature, up to 10°C in few hours, affecting people, livestock and crops (Marengo, 1983; Ronchail, 1989a,b; Marengo et al., 1997; Garreaud and Wallace, 1998; Pezza and Ambrizzi, 2005; Quispe, 2010; Sulca et al., 2018). Incursions of low-level cold southerly winds from southern South America are also associated with rainy episodes on the Amazon-Andes transition region (Chávez and Takahashi, 2017; Paccini et al., 2017), as well as formation of thick clouds in the Zongo glacier region in Bolivia (16°S, 5,060 m a.s.l.), particularly during the austral winter and spring (Sicart et al., 2015). Hurley et al. (2015) showed that around 70% of the total accumulated snow on the Quelccaya glacier (Peruvian Andes; 5,680 m) is associated with these southern cold air intrusions.

In the central Peruvian Andes, radiative frosts are a major hazard to agriculture. They are caused by low cloud cover, surface air humidity, and soil moisture (Saavedra and Takahashi, 2017), and tend to occur at night times and early morning of the dry and cold seasons (June–August) (Saavedra and Takahashi, 2017; Sulca et al., 2018). During the austral summer, extreme cold events in the Mantaro Valley (central Peruvian Andes, around 500–5,300 m a.s.l.) are caused by intrusions of air masses along the east of the Andes through equatorward displacement of extratropical Rossby waves, negative temperature advection and southeasterly surface wind anomalies, positive OLR anomalies, and possibly influenced by the Madden-Julian Oscillation.

Extratropical Andes

Severe weather events associated with intense downslope wind episodes are observed in the eastward slope of the subtropical Andes and are commonly referred to as Zonda wind events (Norte, 2015). Zonda is a high-speed warm and very dry downslope wind occurring on the lee side of the Andes characterized by very strong wind-gusts affecting several western Argentina areas. Zonda episodes are more frequent during winter and spring. The occurrence of Zonda events is often associated with large damages on a variety of systems. These damages can be either socio-economical or ecological, such as blowing off roofs, toppling of trees, downing of power electricity supply and communication lines, among others. Because of its association with dry and very warm conditions, it also favors the occurrence of fire events and damage in crops. At high altitudes over the mountains, its occurrence affects the hydrological cycle, by accelerating snow melt and evaporation, and may trigger the occurrence of avalanches (Norte et al., 2008). The classical Zonda episode, described in Norte (2015) occurs in a synoptic environment characterized by a cold front approaching the western coast of South America and the associated migratory depression, as well as a moderate northern flow over central Argentina associated with the presence of the north-western Argentinean low and a warm front located over north-eastern Argentina. These ingredients induce strong baroclinicity, intense vertical wind shear and strong wind components that are transversal to the Andes. In addition, the presence of a warm front downstream the region where the Zonda develops favors its dynamics. Hence, the Zonda is produced by the topographically and dynamically forced ascent of humid air upslope of the Andes and a subsequent orographic descent of a prefrontal air mass which is strongly baroclinic. On the basis of the knowledge of the favorable conditions for Zonda events occurrence, Otero et al. (2018) have constructed a probability index for surface Zonda wind occurrence at the city of Mendoza (Argentina), including the estimation of the onset of the event, as a tool for predicting its probability of occurrence. However, Zonda events have been less investigated over the northern part of the extratropical Andes, where several strong episodes were identified (Otero et al., 2018).

ENSO IMPACTS ON EXTREME EVENTS

El Niño-Southern Oscillation (ENSO) is the most important modulator of the global hydro-climatology at interannual timescales. Its two phases, El Niño and La Niña, trigger a large suite of hydrological and meteorological extreme events worldwide (McPhaden et al., 2006), and particularly in South America and the Andean region (Aceituno, 1988; Waylen and Poveda, 2002; Aceituno et al., 2009; Cai et al., 2020), affecting the livelihoods of societies and imposing a huge socio-economic and environmental burden to the region.

Northern Tropical Andes

During El Niño, the Andes of Colombia experience long and intense droughts, heat waves, and forest fires, while La Niña triggers intense storms, landslides, floods, avalanches and inundations (Poveda and Mesa, 1996, 1997; Poveda et al., 2001a, 2006, 2011; Hoyos et al., 2013; Bedoya-Soto et al., 2018, 2019). **Figure 10** shows the annual cycle of the probability distribution function (box-plots) of maximum intensity 1-h rainfall events in 19 rain gauges on the Colombian Andes (Poveda et al., 2002), including monthly maximum events during both extreme ENSO phases, and also *maxima* events (MME). In general, maximum rainfall intensities are larger (smaller) during La Niña (El Niño), although the MME are not necessarily directly associated with either ENSO phase. Similar conclusions are obtained for storm durations from 1 to 24 h (Poveda et al., 2002). El Niño and La Niña also affect the diurnal cycle of rainfall over the Colombian Andes, by increasing (decreasing) the amplitude during La Niña (El Niño), although the phase remains unchanged (Poveda et al., 2005).

Soil moisture over the Andes of Colombia is affected consistently by both phases of ENSO. **Figure 11** shows soil moisture data gathered at nearby plots covered by shaded coffee, sunlit coffee and secondary forest. Results indicate that the annual seasonal cycle exhibits a strong coupling to interannual (ENSO) variability. Soil moisture exhibited minimum values during the two drier seasons (July through September 1997, and December 1997 through March 1998), amidst the 1997–1998 El Niño event. On the other hand, the bi-modal annual cycle of soil moisture disappeared during the following 1998–1999 La Niña event, exhibiting saturation values throughout the rest of that year. Sunlit coffee plants exhibited stronger water deficits than forest and shaded coffee plants, thus pointing out the relevance of vegetation and land use in controlling water stress (Poveda et al., 2001a, 2011).

Atmospheric teleconnections are part of the physical mechanisms that explain the establishment and persistence of drought in the northern Andes (Poveda et al., 2006, 2011). For instance, droughts in the Andes of Ecuador during El Niño (La Niña) are associated with clear-cut westerly (easterly) surface wind anomalies over the central tropical Pacific and the reverse flow in the higher troposphere (Wang, 2002; Vicente-Serrano et al., 2017). The significant negative correlation between SST anomalies in the central tropical Pacific and precipitation anomalies over the glaciers of Ecuador showcase their strong dependence to both phases of ENSO (Favier et al., 2004; Francou et al., 2004; Vuille et al., 2008; Rabatel et al., 2013).

Southern Tropical Andes

The general effect of ENSO on precipitation in the Southern Tropical Andes tends to be the opposite to the Northern Tropical Andes, with positive (negative) anomalies during El Niño (La Niña). Different ENSO types involve a large range of impacts worldwide through atmospheric teleconnections, in addition to land-atmosphere feedbacks (e.g., Larkin and Harrison, 2005; Ashok et al., 2007; Sun et al., 2013; Bedoya-Soto et al., 2018). In Peru, rainfall anomalies are associated with different types of ENSO, usually denoted as with the EP (Eastern Pacific) and CP (Central Pacific) indices (Yu and Kao, 2007; Kao and Yu, 2009; Takahashi et al., 2011; Lavado-Casimiro and Espinoza, 2014; Sulca et al., 2017; Takahashi and Martínez, 2019). SST warming in the eastern (central) equatorial Pacific is frequently associated with enhanced (reduced) coastal (Andean and Amazonian) rainfall, which can occur, with varying relative magnitudes, during El Niño or, with opposite sign, during La Niña (Lagos et al., 2008; Lavado-Casimiro et al., 2013; Lavado-Casimiro and Espinoza, 2014; Rau et al., 2016; Sulca et al., 2017; Imfeld et al., 2019). Both EP and CP indices are associated with weakened upper-level easterly flow over Peru, more so over the central/southern Peruvian Andes (Sulca et al., 2017). Moreover, during EP El Niño events extreme droughts in the southern

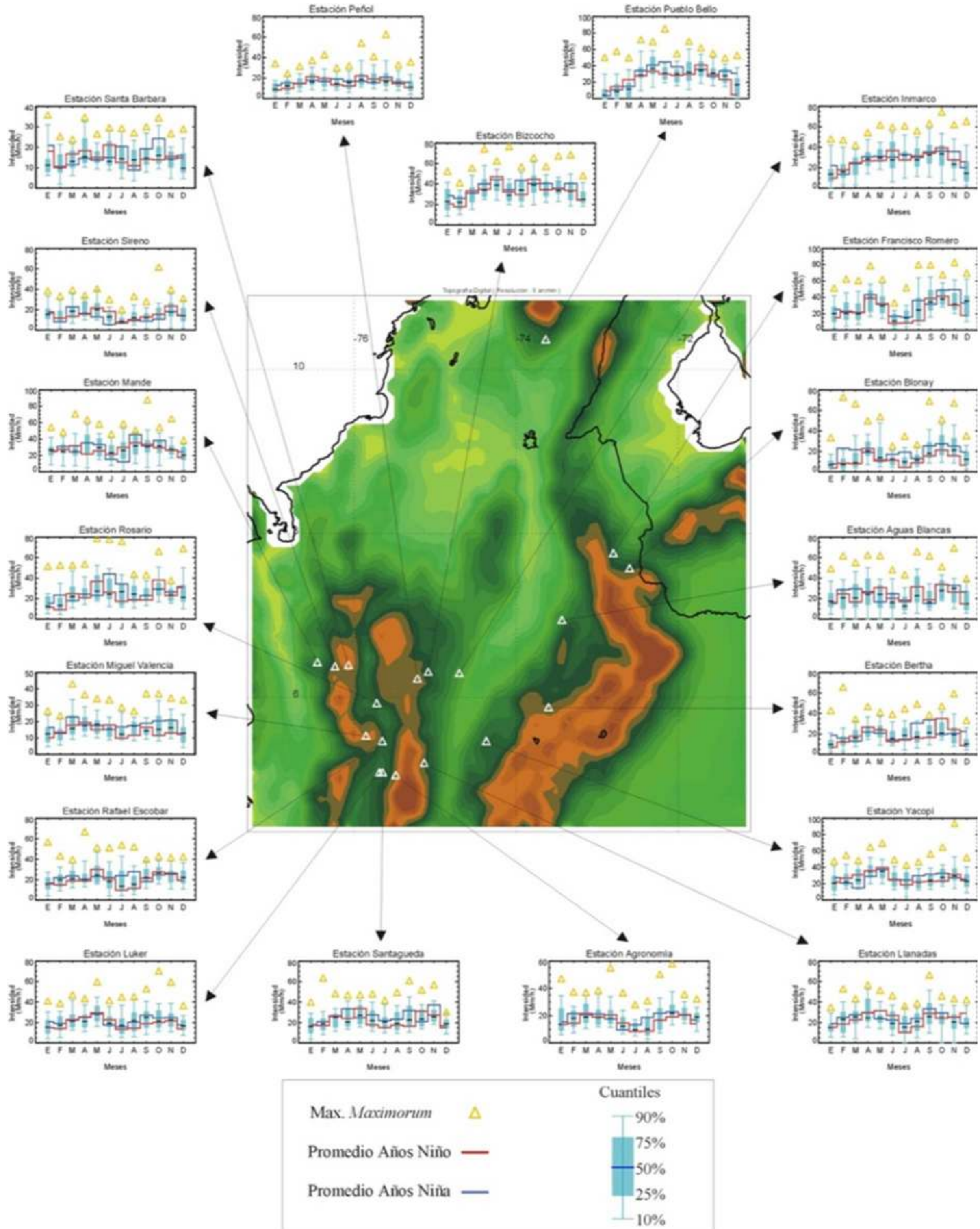

FIGURE 10 | Long-term mean annual cycle of the probability distribution function of 1 h rainfall events, including average values during El Niño (red line) and La Niña (blue line), and maxima values (yellow triangles) recorded at selected rain gauges along the Colombian Andes. Source: Poveda et al. (2002).

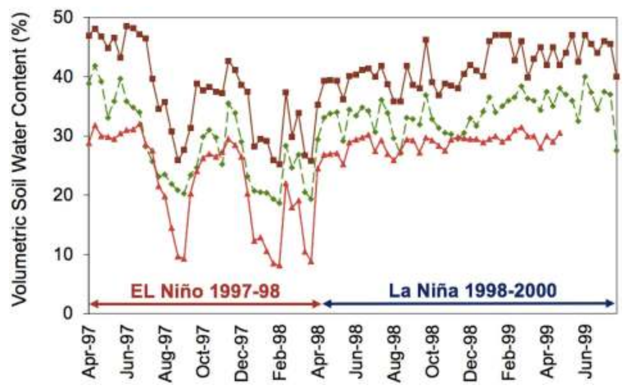

FIGURE 11 | Temporal dynamics of 10-day mean values of volumetric soil water content at 40 cm depth, recorded at three nearby parcels in the Central Andes of Colombia under different vegetation types: shaded coffee (brown), secondary forest (green), and sunlit coffee (red). The studied period (March 1997–August 1999) was under the influence of the 1997–98 El Niño and 1998–99 La Niña events. Adapted from Poveda et al. (2001b).

Peruvian Andes are associated with a stronger warming in the troposphere above the central Pacific Ocean (Imfeld et al., 2019). However, not all extreme droughts over the region are explained by El Niño. The Bolivian High and moisture advection from the Amazon play an important role (e.g., Segura et al., 2016, 2020; Imfeld et al., 2019).

Over the Peruvian coast, El Niño is the main modulator of rainfall variability at interannual scale. The strong 1982–83 and 1997–98 El Niño events were characterized by an enhancement of convective activity in the eastern Pacific (Takahashi et al., 2011; Takahashi and Dewitte, 2016; Jauregui and Takahashi, 2017), and intense storms leading to floods in the central and northern Peruvian coast (e.g., Woodman, 1985, 1999; Lavado-Casimiro et al., 2013; Bourrel et al., 2015; Rau et al., 2016). Rainfall and streamflow records in the Piura River basin (5.2°S, 80.6°W, 40 m a.s.l.; **Figure 12A**) characterize El Niño impacts (e.g., Deser and Wallace, 1987; Takahashi and Martínez, 2019). For instance, while the mean annual discharge is around 28 m^3/s (Lavado et al., 2012), it reached values of 442 m^3/s and 364 m^3/s during the 1998 and 1983 El Niños, respectively (Takahashi and Martínez, 2019). Accordingly, during extreme El Niño events suspended sediment yield in the Peruvian coast increases by 3 to 60 times compared to the 1968–2012 multiyear average (**Figure 12B**; Morera et al., 2017). In turn, Rodriguez-Morata et al. (2018) estimated that 21% of the total hydro-geomorphic disasters reported in Peru during the 1970–2013 period (including generic rainfall-related damage such as muddy areas, structural damage, holes, etc.) were related to the 1972–1973, 1982–1983, and 1997–1998 El Niño events. The 1997–1998 El Niño-driven flood damages were estimated to be around USD 1 billion, primarily along the northern coast of Peru (OPS, 2000).

A complex relationship is observed between ENSO variability and rainfall over the Peruvian coast (Bourrel et al., 2015). The so-called "coastal El Niño" strongly impacts the hydrology of Peru, such as in 1891, 1925, and 2017, characterized by warm SST anomalies over the easternmost tropical Pacific, and cold SST anomalies in the central tropical Pacific. Costal El Niño events of 1925 and 2017 are documented in Takahashi and Martínez (2019) and in Garreaud (2018a), respectively. According to Rodriguez-Morata et al. (2019) the 2017 Coastal El Niño produced rainfall records in northern Peru that can only be compared to the extraordinary El Niño events of the last 40 years, namely 1982–83 and 1997–98.

Over the Altiplano a dominant negative (positive) relationship between El Niño (La Niña) and summer (DJF) rainfall has been identified (Vuille et al., 2000; Garreaud et al., 2009). This signal becomes rather weak to the north of the Altiplano and to the sub-Andean valleys of the southwestern Amazon below 1,500 m a.s.l. (Ronchail and Gallaire, 2006). The ENSO-Altiplano rainfall emerges from the changes in the zonal wind atop of the Andes during austral summer. During El Niño years the subtropical jet stream is enhanced thus reducing the transport of moist air from the continent toward the mountains (Garreaud, 1999). The opposite situation occurs during La Niña years, when weaker westerlies in the mid troposphere foster the intrusion of moist air from the eastern lowlands toward the Altiplano. In a recent study, a second mechanism associated with upward motion over the western Amazon, has been proposed to explain the interannual precipitation variability over the Altiplano (Segura et al., 2020). The authors show a slight increase in rainfall over the past two decades, in association with the strengthening of upward motion over the western Amazon.

Seiler et al. (2013) investigated interannual climate variability in Bolivia. Temperatures were found to be higher in the Andes during El Niño, as well as during the positive phase of PDO and the Antarctic Oscillation (AAO). During the positive phase of the PDO the total annual rainfall and the frequency of intense storms were higher, regardless of ENSO phase in the lowlands. During December-February, El Niño was associated with drier conditions in the Andes with more variable precipitation.

Extratropical Andes

ENSO is a major modulator of interannual precipitation along the extratropical Andes (25–40°S), exhibiting positive (negative) anomalies during the occurrence of El Niño (La Niña). While most precipitation in this area occurs during austral winter, it does not coincide with the peak of ENSO. Yet, the correlation coefficient between Niño3.4 index and annual rainfall is about 0.6 across this region (Montecinos and Aceituno, 2003), which mostly relies on rainfall over the western slope of the Andes (central Chile). In this region, the probability of having an extreme precipitation event (>40 mm/day) is twice as large during El Niño events compared to neutral conditions. Contrary, the probability of extreme events does not decrease substantially during La Niña events.

On the eastern side of the Andes, El Niño (La Niña) is associated with positive (negative) anomalies in precipitation, river runoff and landslides (Compagnucci and Vargas, 1998; Moreiras, 2005) during both winter and summer months. Significant differences in the frequency of occurrence of extreme precipitation events have also been identified over western Argentina during winter and late spring, with increased

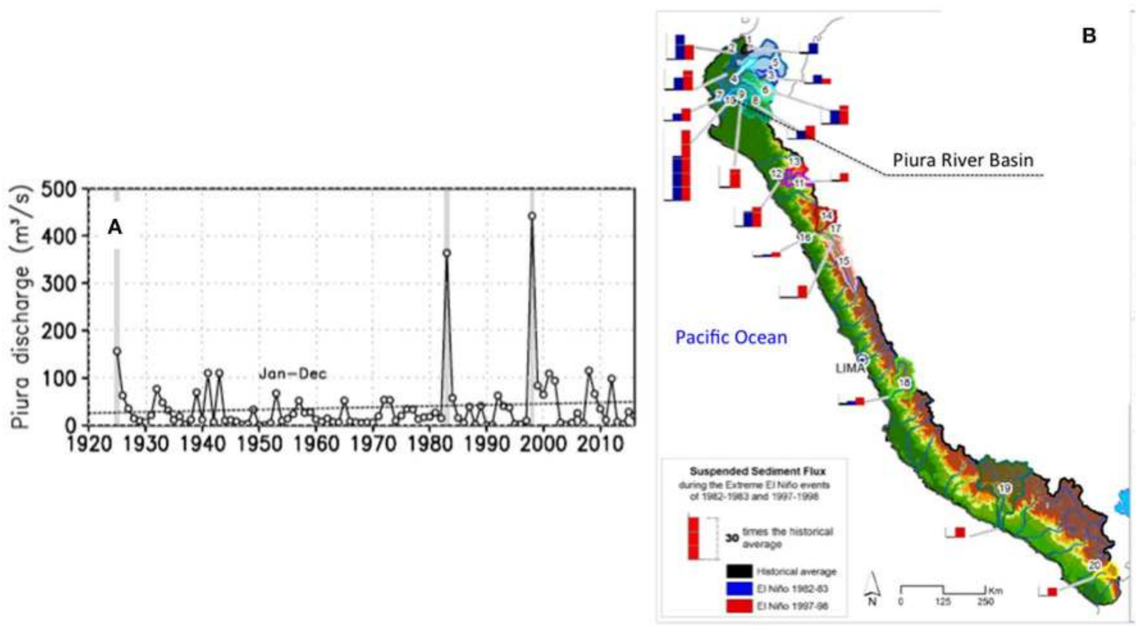

FIGURE 12 | (A) January-December mean discharge of the Piura River during the 1925–2015 period. The linear trend is indicated in dashed line. Vertical gray lines indicate the strong El Niño events of 1925, 1983, and 1998. Adapted from Takahashi and Martínez (2019). © Springer Nature. CC license. **(B)** Suspended sediment flux observed in the Peruvian coast. Black bars represent climatological sediment flux, red and blue bars display sediment flux during El Niño years of 1982–83 and 1997–98, respectively. Each cube on the bar represents the sediment flux transported over 10 normal years. Adapted from Morera et al. (2017). © Springer Nature. CC license.

(decreased) number of extreme events during El Niño (La Niña) (Grimm and Tedeschi, 2009).

FLOODS

Northern Tropical Andes

Colombia ranks first in Latin America and the Caribbean in losses and damages (per 100,000 inhabitants), from natural hazards during 1999–2013 (UNISDR, 2016). Most of them are associated with massive flooding during La Niña events (Poveda and Mesa, 1996, 1997; Poveda et al., 2001a, 2002, 2006; Hoyos et al., 2013; Bedoya-Soto et al., 2018). During the 2010–11 La Niña event, widespread flooding caused damages and losses in excess of 6 Billion US dollars, or 2% of Colombia's GDP for 2011. One reason is the intensification of the CHOCO low-level jet during La Niña, which transport large amounts of atmospheric moisture from the far eastern Pacific onshore, thus providing extra moisture for the development of MCSs and intense storms that can lead to widespread flooding along the Andes of Colombia and Ecuador. Typically, such steep river basins witness intense storms that produce flash floods, as the Guayas River in Ecuador during El Niño years (Frappart et al., 2017). Flooding mechanisms in tropical Andean cities depend on the preceding 24-h rainfall, baseflow, urbanization patterns, soil types and saturation conditions, as in the case of Quito (Perrin et al., 2001).

On the other hand, flash flood emergencies have also been observed to occur in periods with negative monthly precipitation anomalies associated with El Niño conditions as was the case of 18 May, 2015 in La Liboriana basin in the Municipality of Salgar, Colombia, causing more than 100 casualties and significant infrastructural damage. The meteorological factors associated with the emergency showed the role of successive precipitation pulses in relatively short periods that were intensified as deep convective cores interacted with the steep topography (Hoyos et al., 2019). These results show the challenges to opportunely pinpoint convective intensification over complex mountainous terrain from observations and forecast models to improve local risk reduction strategies over vulnerable regions of the tropical Andes.

Southern Tropical Andes

Floods in the central Andes can be triggered by intense storms and/or rapid glacier melting during the spring-summer of the austral hemisphere (Huggel et al., 2015). Flash floods commonly originate in moraine-dammed lakes threatening communities located in the Cordillera Blanca of Peru (Emmer, 2017). In addition, urbanization is increasing the risks of flash floods (Bourges et al., 1995; Méndez et al., 2016). In the valleys of Urubamba and Vilcanota in the Cuzco region, extreme rainfall and floods occurred in January and February 2010 causing USD 200M in damages and losses (Lavado-Casimiro et al., 2010) See **Figure S5**.

In the Peruvian Coast and most of the western flank of the Peruvian Andes, extreme floods have been associated with El Niño dating back to pre-Inca societies (e.g., Takahashi, 2004;

Manners et al., 2007; Lavado-Casimiro and Espinoza, 2014; Rau et al., 2016). Three distinctive flooding responses to El Niño have been found over the western Andes of the Chancay River north of Lima (Peru): coastal desert, Lomas, and mountain desert. The mountain desert and valleys of the Pacific slopes are devastated by catastrophic floods and torrential rains during El Niño. However, less abundant precipitation is observed in Lomas, favoring the development of vegetation during the austral winter (Kalicki et al., 2014).

Besides the strong impacts of El Niño on the Peruvian coast, extreme rainfall in Peru has also been reported during La Niña and neutral conditions in the equatorial Pacific (Ronchail et al., 2002; Espinoza et al., 2012b; Lavado-Casimiro and Espinoza, 2014; Sulca et al., 2017; Recalde-Coronel et al., 2020). Indeed, excessive rainfall over the central and western Amazon have been related to La Niña events, and to warm anomalies in the tropical South Atlantic Ocean (TSA), in association with extreme rainfall and floods, as reported in 2009, 2012 and 2014 (Ronchail et al., 2005; Marengo et al., 2010, 2011, 2013; Satyamurty et al., 2013). Rodriguez-Morata et al. (2018) documented that more than 36% of the hydro-geomorphic disasters reported in Peru during the 1970–2013 period were associated with La Niña and neutral conditions in the equatorial Pacific. The very unusual wet 2014 austral-summer period originated in the eastern slope of the Peruvian and Bolivian Andes and flooded the southern Amazon (Espinoza et al., 2014; Ovando et al., 2016; **Figure 13**). This exceptional event has been associated with warm anomalies in the western Pacific-Indian Ocean and over the subtropical South Atlantic Ocean.

Extratropical Andes

Highly intense and short storms regularly trigger severe flash floods in the Andes of Mendoza, Argentina. Although previous studies have been unsuccessful in simulating peak discharges, factors such as storms characteristics and soil variability (quasi-impervious areas) play a key role, along with vegetation, surface storage capacity, and antecedent soil moisture (Braud et al., 1999). Other studies have proposed that surface, perimeter, basin length, elevations, and slope can be useful to predict floods over that region (Perucca and Angilieri, 2011). Flash floods in the Patagonian Andes have been reconstructed from dendrochronological studies (Casteller et al., 2015).

Along the western slopes of the southern Andes (continental Chile) floods occurs mostly during winter storms with significant precipitation (>50 mm/day), and have warm characteristics (thus producing a high freezing level) or last for more than 3 days. Recent events have been observed in northern, central and southern Chile (Valenzuela and Garreaud, 2019) and they are associated either with atmospheric rivers (Viale et al., 2018) or cut-off lows (COLs), as described in section Extratropical Andes.

A trend analysis was performed on annual peak river flows between 1975 and 2008 for rivers in the semi-arid (29−32°S) and temperate (36−38°S) zone of the Chilean Andes (Pizarro et al., 2014). Negative trends were identified in 87% of the stations in the semi-arid zone while positive trends were found in 57% of the stations in the temperate zone. Differences in trends sign seem to be associated with the positive trend in the altitude of the zero-degree isotherm in this region.

LANDSLIDES, MUDSLIDES, AVALANCHES

The Andes, as all high mountain regions worldwide are subject to landslides, mudslides, rockslides, debris flows, and avalanches due to the steep topography, the soil and rock characteristics, land cover/land use change, and climate and weather patterns (Hermanns et al., 2012; Stahr and Langenscheidt, 2015). Intense storms, likely exacerbated by global warming and increased climate variability are the most important cause of landslides in the Andes (Moreiras, 2006; Sepúlveda and Petley, 2015).

Rainfall-triggered landslides cause large number of fatalities, damages and losses along the Andean, affecting human and animal lives, civil infrastructure, roads, crops, and the provision of public services (Nossin, 1999; Moreiras, 2006; Michoud et al., 2016; Younes-Cárdenas and Erazo-Mera, 2016), pipelines (Lee et al., 2009; Pettinger and Sykora, 2011; Bustinza et al., 2013; Contreras et al., 2013; García et al., 2013; Oliveros et al., 2017), and water supply systems. See **Figure S6**. Also, infrastructure development and construction favor the occurrence of landslides in the Andes (Brenning et al., 2015). On the other hand, meteorological conditions also determine the type and intensity of snow avalanches in the Andes of Argentina (Naaim et al., 2002).

These risks are particularly enhanced by the combined effects of rock avalanches causing temporal lakes and the ensuing dam failures (Ferrer, 1999; Hermanns et al., 2004). Intense storms exacerbate sediment production by slope movement on hillslopes, directly affecting their transport and deposition in downstream rivers and dams, as well as producing morphological changes in stream channels. The role of vegetation is critical on the stability of runoff and sediment yield and for example deforestation of the Andes plays a deleterious role (Braud et al., 2001). The Multinational Andean Project (MAP:GAC 2002–2008) have set forward regional guides for landslide studies and mapping, and have conformed the first regional group of researchers for landslide studies in the Andes (GEMMA) (Jaramillo, 2008).

Northern Tropical Andes

The combination of intense storms and steep terrain are major causes of landslides in the tropical Andes. For instance, a 3 h rainfall event (208 mm) on September 21, 1990, triggered more than 800 landslides along the Andes of Colombia (Aristizábal et al., 2015). The SHALSTAB model (Montgomery and Dietrich, 1994) was able to capture the physics involved in such landslides. López Salgado (2016) studied mass movements in the upper Coello River basin in the Central Andes of Colombia and identified that they result from the combination of high rainfall, steep slopes, and unstable volcanic ash cover.

There is also a strong connection between deforestation and land use change with erosion and landslides in the tropical Andes. Erosion rates in the Magdalena River basin, located between the central and eastern ranges of the Colombian Andes, have shown

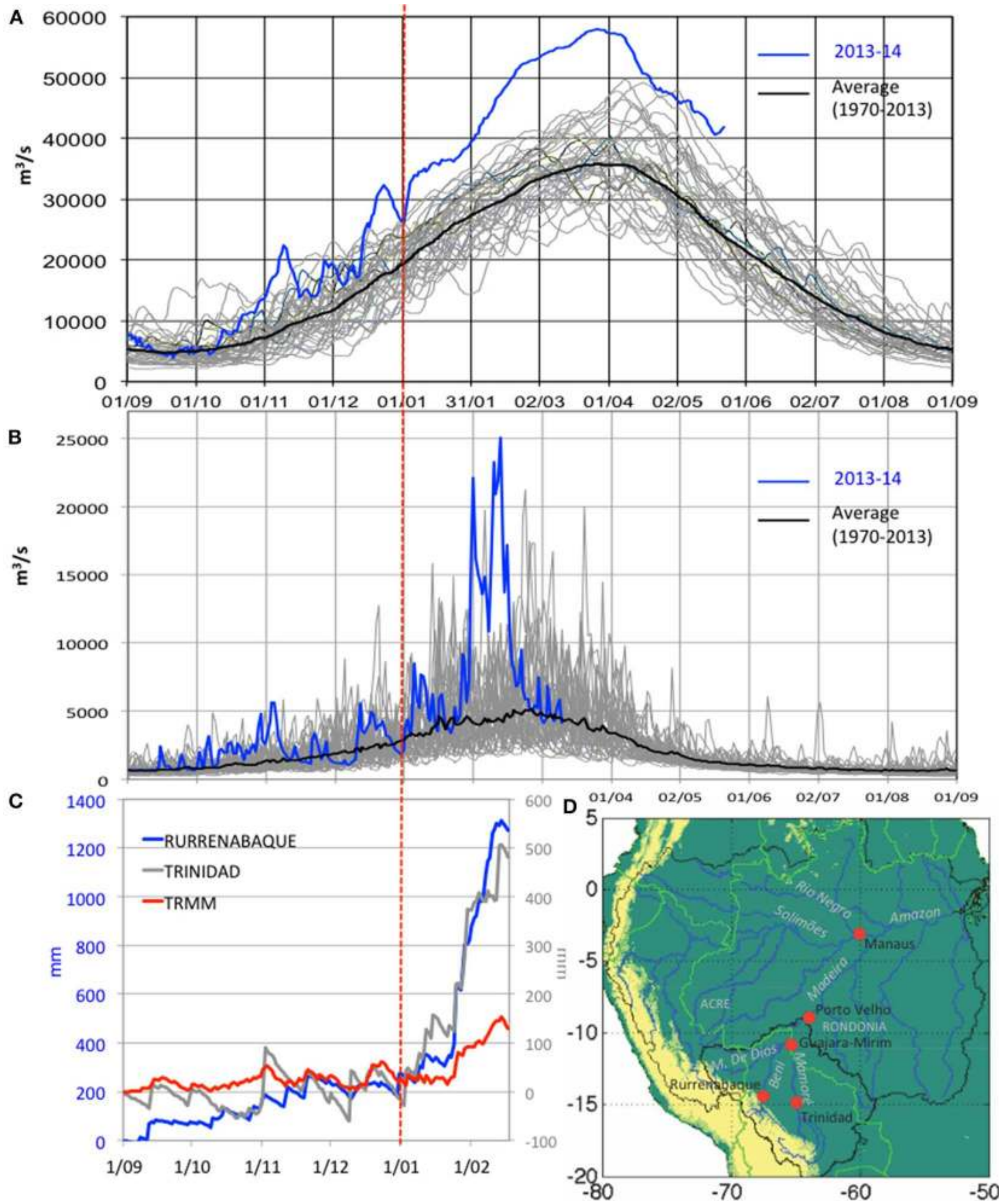

FIGURE 13 | Daily discharge at **(A)** Porto Velho on the upper Madeira River, and **(B)** Rurrenabaque on the upper Beni River during the period of 1970–2013 (gray lines). Mean discharge values and discharge during the 2013–14 hydrological year are displayed in black and blue lines, respectively. **(C)** Cumulative rainfall anomalies in Rurrenabaque (blue, left Y axis) and Trinidad (gray, right Y axis), and area average rainfall in the Porto Velho River basin computed with TRMM-RT 3B42 V7 (red, right Y axis), for the 01/09/2013–17/02/2014 period. **(D)** Location of stations and main rivers. Adapted from Espinoza et al. (2014). © ERL. CC license.

an increase from 550 ton km^{-2} y^{-1}, in the years previous to 2000, to 710 t km^{-2} y^{-1} between 2000 and 2010, as well as sediment load (average increase of 44 Mt y^{-1}), coinciding with a forest loss of 40%, and an increase of 65% in areas dedicated to agriculture and pastures (Restrepo and Escobar, 2018).

Deforestation and land use change significantly alter the landslide frequency-area distributions in the Andes of Ecuador (Guns and Vanacker, 2014). A strong increase in the frequency of small landslides in anthropogenic environments explains in part the observed enhancement in landslide denudation rates in this region (Vanacker et al., 2003, 2013; Molina et al., 2012; Guns and Vanacker, 2013, 2014). Marie and Veerle (2013) suggest that deforestation causes major changes in soil properties and hydrology, accelerating landslide activity. In other cases, vegetation contributes to destabilize slopes owing to its contribution to the organic layer mass, and promotes a new cycle of vegetation succession. Vanacker et al. (2007) show evidence that the steepness of topography contributes more than human activities or land use practices to the occurrence of infrequent large landslides over the Andes of Ecuador.

Although many landslides in the Andes are triggered by highly intense storms, Soto et al. (2017a) found that only 24% landslides in the Loja River basin (southern Ecuador) were triggered by intense storms whose return periods exceed 1 year, and less for the 76% of landslides. Also, rainfall events that are not exceptionally intense can reactivate these landslides (Soto et al., 2017b).

Erosion processes in the Andean river basins yield large concentrations of suspended sediment to the western part of the low-lying Amazonia. For example, as is the case of the Napo River in the Amazonian regions of Ecuador and Peru, where annual mean erosion rates are approximately 1,160 t km^{-2} (Laraque et al., 2009; Clark et al., 2016).

Younes-Cárdenas and Erazo-Mera (2016) developed an explanatory model to predict the degree of susceptibility of landslides along the E-20 highway in Ecuador, and concluded that the distribution of landslides was far from random, and clearly associated with several geological and environmental factors, including zones of active erosion processes, volcanic sandstones, granitic rocks and mean annual rainfall values between 1500 and 1750 mm. The non-random nature of landslides in space and time has been confirmed by Muñoz et al. (2017) who showed the multifractal space-time characteristics of landslides in the Andes of Colombia.

The main source of sediments (and nutrients) to the lower Amazon River basin is located along the Andes. Townsend-Small et al. (2008) studied the production and transport of sediments and suspended organic matter along the Chorobamba River in the central region of the Andes-Amazon transition of Peru. At least 80% of total annual suspended sediment, 74% of organic carbon, and 64% of organic nitrogen transport was concentrated in 10 days of the year, with significant seasonal changes in sources of organic matter. The latter indicates that extreme events are the main origin for this process.

Southern Tropical Andes

Global warming linked to intense storms and stronger El Niño events, along with permafrost degradation and glacier retreat promote slope instability in the Central Andes, thus increasing the frequency and intensity of landslides. These processes can modify the spatial distribution of landslides, shifting initial points of slope instability to higher altitudes, and triggering more complex and larger landslides (Moreiras and Pont, 2017). Furthermore, large mass movements that originated as rock/ice falls from the glacierized Andes can become high-volume high-velocity mud-rich debris flows, such as the 1962 and 1970 events in Nevado Huscarán (Cordillera Blanca, Peru) (Evans et al., 2009).

Landslides play an important ecological role (Restrepo et al., 2009; Smith, 2011). An inventory over the Andes of Peru indicated turn over times of 1,320 years (Clark et al., 2016), removing 264 tC km^{-2} yr^{-1} of organic carbon mostly from soils (80 %) in 25 years. A single storm event in March 2010 was responsible for 27% of the total landslide area reported, and produced 26% of the organic carbon flux associated with landslides during such 25-yr period (Huggel et al., 2015). Heavy rainfall reported during the austral summer of 2010 in Cuzco region caused economic losses estimated to be around 250 million US dollars. Landslide and flash floods destroyed around 5,000 houses, 16,300 ha of farmlands, 6.15 km of the Cusco-Machu Picchu railway line and 21 bridges (Lavado-Casimiro et al., 2010; **Figure S5**).

Lowman and Barros (2014) investigated the links between precipitation and erosion in the central Andes, and estimated mean erosion rates of 2.1–8.5 mm per year, which happens to be 1 to 2 orders of magnitude larger than long-term estimates (1,000 to 1 million years) for the central Andes. On the other hand, erosion rates in the Eastern Cordillera (northern Bolivia) have been estimated as 5–14 mm per year (Blodgett and Isacks, 2007).

The ratio of sediment transport between hillslopes and channels in the Peruvian Andes influences geomorphological features and the morphology and dynamics along the channel network (Schneider et al., 2008). The headwaters of river channel networks exhibit rough and high-relief surfaces with deep incisions and dense drainage density. Thus, storminess influences the production and transport of sediments on hillslopes and channels, reflected into landscape morphometry.

Extratropical Andes

Rock avalanches along the northwest Andes of Argentina are produced by active tectonics, in addition to lithologic, structural and topographic conditions, and climate change (Hermanns and Niedermann, 2006). Landslides in the Andes of Argentina and Chile have been linked to intense summer storms, in particular during El Niño (Trauth et al., 2000; Espizua and Bengochea, 2002; Marwan et al., 2003; Moreiras, 2005; Sepúlveda et al., 2014a,b; Moreiras and Sepúlveda, 2015; Moreiras et al., 2018). The most dangerous are caused by the zero-isotherm lifting in smaller basins exhibiting debris-rock glaciers, so-called "ENSO-climate change" landslides (ECCL; Moreiras et al., 2018).

The melting of snow accumulated in the winter conductive to saturation of soils and landslides in the following spring and summer seasons (December to February) is the major cause of slope instability in the Aconcagua Park, as evidenced in the high significant correlation between landslides and river discharges, and a weak relationship between landslide and temperature records (Moreiras et al., 2012).

DROUGHTS, HEAT WAVES, AND FIRES

ENSO is a major driver of droughts in various regions of South America (Zhou and Lau, 2001; Kane, 2006; McPhaden et al., 2010; Cai et al., 2020), in particular El Niño is associated with droughts over large parts of Colombia, Venezuela, some regions of the high Andes of Ecuador, Peru and Bolivia (Francou, 1985; Caviedes and Endlicher, 1989). At the same time, La Niña is associated with droughts in other regions of Ecuador, Bolivia, Chile and Argentina.

Northern Tropical Andes

Multiple studies have shown that droughts in the northern tropical Andes are associated with the occurrence of El Niño (section ENSO Impacts on Extreme Events, Northern Tropical Andes) through changes in the Hadley circulation (Poveda et al., 2006, 2011; Arias et al., 2015), the Walker circulation (Kousky et al., 1984; Vuille, 1999; Vuille et al., 2000; Francou et al., 2004; Poveda et al., 2006, 2011; Vicente-Serrano et al., 2011a,b, 2017), as well as to land surface-atmosphere feedbacks (Poveda and Mesa, 1997; Bedoya-Soto et al., 2018, 2019). Such droughts have deleterious impacts on water supply for humans and livestock, crops failure, and contribute to intensify forest fires, heat waves, as well as outbreaks of malaria, dengue and other vector-borne diseases, and electricity shortages owing to the importance of hydropower generation.

Tropical cloud forests are facing huge threats from fires, deforestation and climate change (Mutke et al., 2017). Deforestation and land use/land change also affect the dynamics of soil moisture in the Andes of Colombia, reducing water storage capacity and leading to higher peak flows (Ramírez et al., 2017).

The frequency and duration of dry periods in Quito has been increasing since the middle of the last century, compared to the last 400 years (Domínguez-Castro et al., 2018). The strongest dry periods occurred in 1692–1701 (the severest one), 1718–723, 1976–1980, 1990–1993, and 2001–2006. The great drought that lasted from 1692 to 1701 caused generalized famine in Quito and affected the majority of population of the central Andes. Such dry periods affect water supply, agriculture and have strong ecological impacts (Chirino et al., 2017).

The unique tundra ecosystems above 3,500 m in the neotropical Andes, *páramos*, play a fundamental ecological and hydrological role below the snow line in the high Andes, in terms of ecosystem services, such as water retention for human and animal consumption, irrigation, and hydropower. Droughts have a strong impact on the hydrological dynamics of *páramos*, such that the recovery from droughts are fundamentally determined by the aridity index (Iñiguez et al., 2016).

The dynamics of fires in the Andes of Colombia is highly controlled by the occurrence of El Niño (Becerra and Poveda, 2006). On the other hand, fires in Ecuador, Peru and Bolivia (Paramo, Yungas, and Puna, respectively) do not show a significant relation to ENSO, but to periodic weather patterns of precipitation: increased rainfall the year before fire-peak seasons followed by very dry periods and unusual low temperatures during the fire-pike (Román-Cuesta et al., 2011, 2014).

Southern Tropical Andes

Over the Altiplano region century-scale dry periods have been identified using a 707-yr dendrochronological reconstruction (Morales et al., 2012). A persistent negative trend in precipitation has been identified from 1930s to date. At interannual to multidecadal time scales, those authors also identified an ENSO-like pattern. Severe drought condition in the Altiplano region were reported during 1983 and 1992 El Niño years (Garreaud et al., 2003; Segura et al., 2016). During the 2015–2016 El Niño event, extreme dry conditions were reported over the Altiplano (Marengo et al., 2017). Severe drought affected central and southern Bolivia, with deficits of rainfall surpassing 30%. Low river discharges were documented in the northern part of the Titicaca basin (Peru) (Jiménez-Muñoz et al., 2016).

The Western Amazon has suffered three periods of extreme droughts since the beginning of the XXI Century (2005, 2010, and 2016; Espinoza et al., 2011; Jiménez-Muñoz et al., 2016), with deleterious ecological consequences (Maeda et al., 2015).

During extreme drought years, impacts on the vegetation have been identified over this region, such as reduction in vegetation activity (measured using NDVI index) and forest fires during the 2005, 2010, and 2016 droughts (Fernandes et al., 2011; Espinoza et al., 2016; Jiménez-Muñoz et al., 2016). Peaks of active fires in Amazonia have been more related to extreme drought than deforestation (Aragão et al., 2018), although the intense fire 2019 summer season was indeed related with deregulation policies in the Brazilian Amazon and the concomitant deforestation (Amigo, 2000; Lovejoy and Nobre, 2019; MAAP, 2019; Wheeling, 2019). These fires and the resulting smoke and soot can reach the highest Andes, contributing to accelerate their on-going rapid melting and disappearance (Allen, 2020). Espinoza et al. (2019) documented an increase in the dry day frequency (DDF) over the central and southern Peruvian Amazon, as well as in the Bolivian Amazon, considering the 1981–2017 period. See also Espinoza et al. (2020).

Various studies document the demise and collapse of pre-Columbian civilizations due to extensive droughts in the Central Andes. For instance, during the sixth century, major cultural disturbances were reported on the northern Peruvian coast, including the Mochica culture that was conditioned by severe sixth-century droughts, spanning from 562 to 594 CE (Shimada et al., 1991). Likewise, the Tiwanaku state, in the south-central Andes, disintegrated between c. AD 1000–1100, after 700 years of growth and colonial expansion. Such droughts impacted irrigation-based agriculture in the low-altitude colonies and the groundwater-dependent raised-field systems in the Altiplano (Ortloff and Kolata, 1993).

In the central Peruvian Andes, dry spells during the wet season (December to March) are associated with a weakened convective activity over the western tropical Pacific, that is in accord with the impacts of El Niño over the region (Sulca et al., 2016). The authors also show that westerly wind anomalies over the upper troposphere reduce moisture flow from the Amazon basin, producing dry events over the Peruvian Andes. Reduced snowfall from suppressed frontal activity in the Central Andes of Argentina is another mechanism that propagates droughts into river flows, mainly driven by La Niña-like conditions in the Pacific Ocean (Rivera et al., 2017b).

Extratropical Andes

The semiarid, Mediterranean-like climate of the extratropical Andes (30-40°S) makes this region drought-prone. Most of the annual precipitation is concentrated in few rain events. This region exhibits high year-to-year variability and

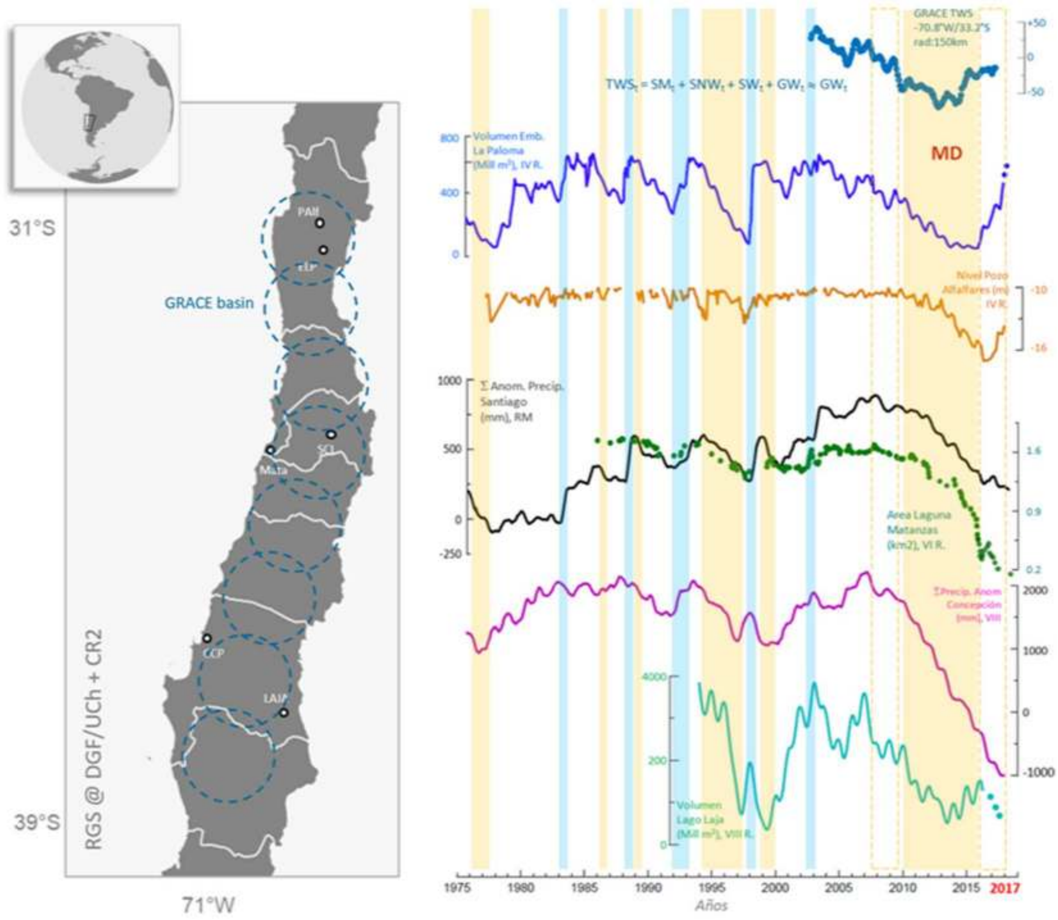

FIGURE 14 | Evolution of the water volume in selected reservoirs in central Chile (extratropical Andes) during the last four decades. Dry periods are marked by the yellow vertical bars. The ongoing megadrought is the dry spell that began in 2010.

is punctuated by severe droughts (30–60% deficits; Núñez-Cobo et al., 2018), lasting 1 year (winter season) and in some cases up to 2–3 years. An exceptional "megadrought" has been occurring in central Chile since 2010 (**Figure 14**; Garreaud et al., 2017).

Winter season droughts are accompanied by a reinforced subtropical anticyclone and deeper than average Amundsen-Bellingshausen Seas Low that conspire to weaken the westerly flow impinging in the southern Andes and restrict the number of fronts (Montecinos et al., 2011; Garreaud et al., 2017). Most drought years occur under La Niña conditions (Montecinos and Aceituno, 2003), and less under ENSO neutral conditions. Indeed, the "megadrought" has occurred mostly under near normal conditions in the equatorial Pacific and it even resisted the strong 2015–16 El Niño event (Garreaud et al., 2017).

Droughts in the southern Andes affect agriculture in central Chile and central-western Argentina (Núñez-Cobo et al., 2018), but also the water supply and hydro-electricity generation, and sets the stage for forest fires (González et al., 2018; Urrutia-Jalabert et al., 2018). The ecology of rivers flowing to the Pacific is also affected (Masotti et al., 2018), as exemplified in the summer of 2016 when the drought triggered the worst ever recorded harmful algal bloom in the coastal areas of Patagonia (Garreaud, 2018b).

Amoroso et al. (2018) developed a 525 year-long reconstruction from the Chubut River basin in Patagonia, finding the most severe droughts in 1680–1705, 1813–1828, 1900–1920, 1993–2002, and from 2011 to the present, in association with forest fires since the 1850s with a 12 year return interval, and a lack of fire for the last 94 years.

Droughts exhibit two distinct temporal regional behaviors in terms of duration and severity between North and Central Patagonia (Rivera et al., 2018). Diverse macro-climatic phenomena such as SAM, ENSO and the Pacific Decadal Oscillation (PDO) affect the interannual and interdecadal variability of droughts in Patagonia (Rivera et al., 2018). Droughts have shown to be more persistent in Argentina, with important regional differences (Minetti et al., 2010).

Extreme droughts have been on the rise in the Temperate-Mediterranean transition (TMT) zone of the Andes (35.5°-39.5°S) during the last century with respect to the previous six centuries (Christie et al., 2011). The identified changes are related to the north-south oscillations in moisture conditions between the Mediterranean and temperate Andean regions, resulting from the latitudinal position of the storm tracks forced by large-scale circulation modes. In turn, moisture conditions are linked to tropical and high-latitude ocean-atmospheric forcing, with the Palmer Drought Severity Index (PDSI) positively related to Niño-3.4 SST during spring and strongly negatively correlated with the Antarctic Oscillation (AAO) during summer. Extreme dry years exhibit a strong negative PDSI vs. AAO correlation.

In addition to droughts, years of above average moisture availability precede fire years in northern Patagonia (Veblen and Kitzberger, 2002), by enhancing the growth of herbaceous plants which increases the quantity of fine fuels during the fire season a few years later. The short-term variability of available moisture leading to massive burning is linked to El Niño, due to greater moisture availability in spring, causing fires in the following years. Warmer and drier conditions during La Niña in the spring exacerbate the drying of fuels, and fire events.

Regarding heat waves, Jacques-Coper et al. (2016) identified 201 cases in south-eastern Patagonia during 1872–2010, with mean duration of 2 weeks and temperature peak of 4.3°C on day 0 (the warmest day in the mean signal), affecting both sides of the Andes. The warming results from temperature advection and enhanced radiative heating, following a high-pressure system over southern South America, from a wave-train-like pattern along the South Pacific. Two thirds of the heat wave events are linked to enhanced ascent in the South Atlantic Convergence Zone (SACZ).

During the 2010–2015 period, the eastern flank of the southern Andes (37°S−31°S) experienced one of the most severe hydrological droughts on record with large socioeconomic impacts. Moreover, since snowmelt is the most important source of water, the reduced snowfall over the mountains propagated the drought signal through the streamflow in the adjacent foothills east of the Andes (Rivera et al., 2017a,b).

RESEARCH GAPS

There is a plethora of challenges toward understanding, modeling and, let alone, predicting the studied high impact weather events.

Much of the current knowledge about extreme climate and weather events in the Andes are based upon limited observational data in particular in the higher Andes. For instance, there are just eight permanent atmospheric sounding sites operating near or in the Andes: Palonegro and Bogotá located on the eastern Andes of Colombia, Alfonso Bonilla-Aragón near Cali (Colombia), Quito (Ecuador), Lima-Callao (Perú), Antofagasta (Chile), Mendoza (Argentina), and Santo Domingo (Chile). This is a meager set of atmospheric measurements to understand the spatiotemporal dynamics of extreme weather patterns in a region characterized by steep slopes, deep valleys, and strong ecological gradients from north to south and from west to east. The situation of meteorological radars is even worse, given the need of high spatiotemporal precipitation estimates in the Andes (Guallpa et al., 2019), and that just a few are operating in the region: Bogotá and Medellín (Colombia), the network of three radars in Cajas, Loja, and Guachaurco in southern Ecuador (Bendix et al., 2017), another in Piura that covers a small region of the north-western Peruvian Andes, three radars in the Province of Mendoza (San Martín, Tunuyan y San Rafael), and one in Jujuy, Argentina, which are active during the hail storm season (October to April).

Regarding the monitoring network of other hydrological, meteorological and climatic variables, the situation is better with respect to *in-situ* rainfall data, although large regions remain uncovered. Something similar can be said about river discharges. The network is highly deficient with respect to weather and climate data sets required to estimate evapotranspiration, and almost non-existent for soil moisture and groundwater, and for all the processes that make part of the surface energy budget. Satellite and Unmanned Aerial Vehicles (UAV) type remotely sensed observations can help improve our understanding in this region, but still require appropriate *in situ* evaluation. Satellite data alone is also insufficient to detect the occurrence and quantify the magnitude of extreme events given their short timescales and small spatial resolution. For instance, diverse ground-validation studies show the poor skill of the TRMM satellite to capture rainfall over the Andes (e.g., Ochoa et al., 2014; Zambrano-Bigiarini et al., 2017; Vallejo-Bernal et al., 2020). Our modeling efforts and the much-needed establishment of early warning systems and disaster prevention efforts are similarly limited by the lack of observational data and data networks. A thorough discussion of the observational and monitoring hydrometeorological network in the Andes is presented by Condom et al. (2020).

Many scientific questions arise about the spatiotemporal dynamics of the high impact weather and climate events discussed herein. For example, what are the dynamics and thermodynamics of the ocean-atmosphere-land interactions that explain the wettest spot on Earth over the Pacific coast of Colombia, in association with MCSs and other rainfall-generating mechanisms leading to intense storms, flooding and landsliding over the Andes of Colombia.

The very topic of rainfall-runoff processes and the formation of floods along the Andes has been largely overlooked, which is more concerning given that floods constitute the most impacting events in terms of human lives and socio-economic losses in the region. The framework of statistical scaling provides a tool to understand and predict the occurrence of floods from intense storms (Gupta and Dawdy, 1995; Menabde and Sivapalan, 2001; Furey and Gupta, 2007; Mandapaka et al., 2009; Gupta et al., 2010; Ayalew et al., 2015), but also to estimate annual peak discharges of different return periods, relevant in hydrologic design (Poveda et al., 2007). Scaling properties need to be explained in terms of the physical processes and predicted by hydrologic models (Nguyen et al., 2015; Quintero et al., 2016; Wu et al., 2017; Salazar et al., 2018; Pérez et al., 2019).

Major knowledge gaps still remain regarding the non-linear interactions and synchronicity (e.g., Boers et al., 2014, 2016; Salas et al., 2020) between the dynamics of the CHOCO, Caribbean and Orinoco LLJs, and the SALLJ with other macroclimatic phenomena and modes of variability at a wide range of temporal scales, and their association with the occurrence of extreme

TABLE 1 | Summary of High-Impact Weather Events in the Andes.

Region	Type of event	Sub-region	Leading synoptic pattern	Consequences	Seasonality	Interannual variability
Northern tropical andes	Large precipitation accumulation	Far East Pacific Ocean near Colombian and Panama Coast	Dynamics of Choco and Caribbean LLJ	Flooding, Hurricanes formation in East Pacific	Boreal summer—autumn	Decrease during El Niño years
	Large precipitation accumulation	Slopes of Tropical Andes	Dynamics of mesoscale circulations favoring MCS	Flooding, soil saturation, landslides	Boreal spring—autumn	Increase during La Niña years
	Intense rainfall rates	Slopes of Tropical Andes	Regional circulation with topographical intensification of convection	Landslides, Flash floods	Boreal spring—autumn	Strong interannual variability associated with ENSO. Location-specific
	Deep Convection	Northern Andes	Monsoonal type interaction with Caribbean Ocean	Landslides; Very intense Lighting	Summer	Increase during La Niña and decrease during El Niño
	Drought	Colombia and Ecuador	Dynamics of the CHOCO LLJ Moisture transport from Amazonia	Forest fires. Impacts on agriculture, water supply, hydroelectricity, human health, fluvial navigation	Intensified in boreal winter	Extreme cases during El Niño events
	Frost	Higher elevation of the Andes, above 2,500 m a.s.l.	Intense radiative cooling associated with low cloud cover	Negative impacts on agriculture and cattle ranching	Dry season	Increase during El Niño
Southern tropical andes	Large precipitation accumulation	Western slope of the Andes, mainly 5°S-2°N	Atmospheric Rivers; MCs	Extreme Flooding, Landslides	Austral summer	Increase during El Niño years
	Large precipitation accumulation	Eastern slope of the Andes (>2,000 masl)	Atmospheric Rivers; MCs; SA Monsoon	Flash floods, Landslides	Year round but more notable in austral summer	Increase during La Niña years
	Intense rainfall rates	Atop of South Tropical Andes (10°S–27°S)	COLs, SA Monsoon, intensification of the BH.	Landslides, hailstorms	Austral summer	Tend to coincide with La Niña
	Heavy Convection	Eastern slope of the Andes -western Amazon	MCs; Pre-frontal condition, SA Monsoon	Landslides; Lighting, flash floods	Year round but more notable in austral summer	Tend to increase during La Niña years
	Drought	Atop of South Tropical Andes (8°S-27°S, >2,000 m asl)	Reduced eastern moisture advection	Impacts on agriculture, water supply, forest fires, hydroelectricity, ecosystems	Austral summer	Tend to coincide with El Niño
	Drought	Eastern slope of the Andes -western Amazon	Reduced eastern moisture advection	Impacts on Forest fires, fluvial transport, wildlife, agriculture, water supply	Austral winter and spring	Increase during El Niño years and during warm conditions in the tropical Atlantic
	Frost	Atop of South Tropical Andes (8°S-27°S, >3,000 m)	Low cloud cover, Post frontal conditions	Negative impacts on agriculture, human health, cattle health.	Winter and spring	Unknown
	Cold spell	Eastern slope of the Andes -western Amazon	Post frontal conditions	Negative impacts human health.	Austral winter and spring	Unknown
Extratropical andes	Large precipitation accumulation	Western slope of the Andes, mainly 35–45°S	Atmospheric Rivers; Cold fronts	Flooding, extreme snow accumulation	Austral winter	Increase during El Niño years
	Intense rainfall rates	Western slope of Subtropical Andes	ARs, COLs	Landslides, hailstorms	Austral fall-winter-spring	Unknown
	Heavy Convection	Atop of Subtropical Andes (27°-37°S)	COLs, extension of the SA Monsoon	Landslides; Lighting, hailstorms	Summer	Unknown
	Drought	Subtropical Andes and adjacent lowlands	N/A	Forest fires, impacts on agriculture, water supply	Year round but more notable in winter	Tend to coincide with La Niña events
	Frost	Subtropical Andes and adjacent lowlands	Post frontal	Negative impacts on agriculture	Winter and spring	Unknown
	Wind events (Zonda winds)	East side of the subtropical Andes	Pre-frontal condition	Unseasonal heat waves, dust storms	Austral fall-winter-spring	Unknown

events, including PDO, AMO, NAO, IOD, QBO, SAM, and the Tropical Atlantic SST Dipole. Also, the interplay between high-frequency variability modes (e.g., equatorial waves, gravity waves, MJO, etc.) and ENSO, and how such interactions modulate extreme events over the Andes.

There is the need to understand the role of the diurnal cycle on the formation of storms over the Andes, and its dynamics during the aforementioned diverse modes of climate variability. In that regard, what is the role of land surface-atmosphere interactions in explaining the water and energy budgets across timescales, from the interdecadal to the diurnal, and the extraordinarily high percentage (70–90%) of precipitation recycling in the Andes (Zemp et al., 2014).

Land use changes have been intense during the last decades over the Andes and the Amazon rainforest. Deforestation, agriculture, urbanization, large infrastructure development and extractive industry exacerbate these problems, such that the tropical Andes have been identified as the most critical biodiversity hotspot worldwide (Myers et al., 2000; Marchese, 2015; Hrdina and Romportl, 2017). The functioning of the coupled Andes-Amazon system (Builes-Jaramillo and Poveda, 2018) requires a thorough investigation, including how the modification in local and regional land conditions affect: (*i*) the frequency and magnitude of extreme weather events, owing to the alteration of the hydrological cycle and the energy budget across river basins of increasing scales, and (*ii*) the vulnerability of populations under risks of avalanches, flash floods, landslides, droughts, etc.

Extreme events are most often related to a local (mesoscale) intensification of extreme conditions (e.g., high rainfall rates, strong winds) embedded in broader synoptic systems (e.g., forced convection along a cold front). Most of the research in the last decades has focused on the synoptic-scale aspects of these extreme events, but examination of their mesoscale features is largely hindered by the aforementioned shortcomings of the observational network in space and time. Thus, we do not know much yet about the triggers and mechanism behind extreme precipitation events (say, brief periods with more than 20 mm/h) over the extratropical Andes.

Another limitation is the short, limited and non-systematic record of landslides, avalanches, flash floods and other ground-level manifestations of extreme weather events. Recall that south of 20°S the Andes is sparsely populated (most people live in the lowlands immediately to the west or east of the range). The record is composed of events that somehow reached the lowlands or interrupted some roads and railways crossing the Andes. Therefore, we may face a substantial underestimation of geo-climatic hazards in this region of extremely complex terrain.

Multiple scientific questions need to be answered regarding the dynamics and spatiotemporal persistence of droughts along the Andes, including the role of vegetation, precipitation, evapotranspiration, river flows, soil moisture and groundwater, net surface radiation and the fluxes of latent and sensible heat. This is also valid for the case of wild fires and heat waves.

Given the large socio-economic toll of high impact weather events in the Andes, the need of assessing their projected changes in future climate scenarios is evident, having in mind diverse adaptation strategies. Though there are studies focusing on the impacts of climate change in the Andes (e.g., Pabón-Caicedo et al., 2020), there is a lack of studies focusing on projected changes of high impact weather events over the region. One of the reasons for this may be the lack of reliability of climate models in reproducing the current climate conditions. Models exhibit large biases mostly in near-surface variables such as temperature, winds and precipitation and, hence, large discrepancies may be found when looking at extreme weather events. Consequently, there is a clear need on assessing the quality of climate models in reproducing high-impact events in the Andes and on assessing how these events are expected to change under future warmer conditions. The state-of-the-art climate models, either Global or Regional, operating at horizontal resolutions in a range from 100 to 20 km, are not expected to capture the high-impacts events themselves, but the large scale forcings and their interaction with the complex orography. Hence, there is also the need to evaluate the skill of convection-permitting models in terms and their capability in reproducing triggering synoptic-scale mechanisms, and the occurrence of diverse extreme events.

FINAL REMARKS

We have provided an in-depth review of the most important high impact weather events along the Andes, summarized in **Table 1**. It is not possible to overstate their socio-economic, environmental and ecological deleterious impacts. Such knowledge is fundamental to assess the relevant knowledge gaps and monitoring needs, but also toward the development of associated human capabilities, the implementation of scientific networks that involve the Andean scientific community and the transfer of scientific knowledge to public policies, which are particularly necessary and particularly challenging amidst population growth and climate change, as well as deforestation and urbanization trends throughout the Andes.

AUTHOR CONTRIBUTIONS

All authors listed have made a substantial, direct and intellectual contribution to the work, and approved it for publication.

FUNDING

GP was supported by Universidad Nacional de Colombia at Medellín. JE was supported by the French AMANECER-MOPGA project funded by ANR and IRD (ref. ANR-18-MPGA-0008). MZ was supported by Patrimonio Autónomo Fondo Nacional de Financiamiento para la Ciencia, la Tecnología y la Innovación, Francisco José de Caldas (ref. 80740-128-2019). Support for the Twentieth Century Reanalysis Project version 3 dataset is provided by the U.S. Department of Energy, Office of Science Biological and Environmental Research (BER), by the National Oceanic and Atmospheric Administration Climate Program Office, and by the NOAA Earth System Research Laboratory Physical Sciences Division.

ACKNOWLEDGMENTS

We are grateful to the Global Water and Energy Exchanges Programme (GEWEX) of WCRP, in particular to Fernande Vervoort, and also to Universidad Nacional de Colombia at Medellín, and to Centro de Ciencia del Clima y la Resiliencia (CR)^2 of Universidad de Chile in Santiago (FONDAP Grant 15110009), for supporting the three regional workshops of ANDEX (https://www.gewex.org/project/andex/home/), as a prospective Regional Hydroclimate Project (RHP).

SUPPLEMENTARY MATERIAL

The Supplementary Material for this article can be found online at: https://www.frontiersin.org/articles/10.3389/feart.2020.00162/full#supplementary-material

REFERENCES

Aceituno, P. (1988). On the functioning of the southern oscillation in the South American sector: surface, climate. *Mon. Weather. Rev.* 116, 505–524.

Aceituno, P., Prieto, M. D. R., Solari, M. E., Martínez, A., Poveda, G., and Falvey, M. (2009). The 1877-1878 El Niño episode: associated impacts in South America. *Clim. Change* 92, 389–416. doi: 10.1007/s10584-008-9470-5

Albrecht, R. I., Goodman, S. J., Buechler, D. E., Blakeslee, R. J., and Christian, H. J. (2016). Where are the lightning hotspots on Earth? *Bull. Am. Meteor. Soc.* 97, 2051–2068. doi: 10.1175/BAMS-D-14-00193.1

Allen, M. (2020, January 13). Amazon fires contribute to Andean glacier melting. *Eos*.

Amigo, I. (2000). The Amazon's fragile future. *Nature* 578, 505–507. doi: 10.1038/d41586-020-00508-4

Amoroso, M. M., Speer, J. H., Daniels, L. D., Villalba, R., Cook, E., Stahle, D., et al. (2018). South American dendroecological field week 2016: exploring dendrochronological research in Northern Patagonia. *Tree Ring Res.* 74, 120–131. doi: 10.3959/1536-1098-74.1.120

Aragão, L. E. O. C., Anderson, L. O., Fonseca, M. G., Rosan, T. M., Vedovato, L. B., Wagner, F. H., et al. (2018). 21st Century drought-related fires counteract the decline of Amazon deforestation carbon emissions. *Nat. Commun.* 9:536. doi: 10.1038/s41467-017-02771-y

Aranguren, D., González, J., Cruz, A., Inampués, J., Torres, H., and Pérez-Tobón, P. S. (2017). "Lightning strikes on power transmission lines and lightning detection in Colombia," in *International Symposium on Lightning Protection, XIV SIPDA 2017* (Natal), 273–278.

Arias, P. A., Fu, R., Vera, C., and Rojas, M. (2015). A correlated shortening of the North and South American monsoon seasons in the past few decades. *Clim. Dyn.* 45, 3183–3203. doi: 10.1007/s00382-015-2533-1

Aristizábal, E., García, E., and Martí-nez, C. (2015). Susceptibility assessment of shallow landslides triggered by rainfall in tropical basins and mountainous terrains. *Nat. Hazards* 78, 621–634. doi: 10.1007/s11069-015-1736-4

Ashok, K., Behera, S., Rao, S. A., Weng, H., and Yamagata, T. (2007). El Niño modoki and its possible teleconnection. *J. Geophy. Res.* 112:3798. doi: 10.1029/2006JC003798

Ayalew, T. B., Krajewski, W. F., and Mantilla, R. (2015). Analyzing the effects of excess rainfall properties on the scaling structure of peak discharges: insights from a mesoscale river basin. *Water Resour. Res.* 51, 3900–3921. doi: 10.1002/2014WR016258

Barrett, B., Garreaud, R., and Falvey, M. (2009). Impacts of the Andes cordillera on precipitation from a midlatitude cold front. *Mon. Weather Rev.* 9, 3092–3109. doi: 10.1175/2009MWR2881.1

Becerra, A., and Poveda, G. (2006). Variabilidad anual, interanual y escalamiento temporal de los incendios forestales en la Amazonía. *Meteorol. Colombiana* 10, 121–131. Available online at: http://gfnun.unal.edu.co/fileadmin/content/geociencias/revista_meteorologia_colombiana/numero10/10_11.pdf

Bedoya-Soto, J. M., Aristizábal, E., Carmona, A. M., and Poveda, G. (2019). Seasonal shift of the diurnal cycle of rainfall over Medellin's valley, central Andes of Colombia (1998–2005). *Front. Earth Sci.* 7:92. doi: 10.3389/feart.2019.00092

Bedoya-Soto, J. M., Poveda, G., Trenberth, K., and Vélez, J. J. (2018). Interannual hydroclimatic variability and the 2009–2011 extreme ENSO phases in Colombia: from Andean glaciers to Caribbean lowlands. *Theor. Appl. Climatol.* 135, 1531–1544. doi: 10.1007/s00704-018-2452-2

Bendix, J., Fries, A., Zárate, J., Trachte, K., Rollenbeck, R., Pucha-Cofrep, F., et al. (2017). RadarNet-Sur first weather radar network in tropical high mountains. *Bull. Am. Meteor. Soc.* 98, 1235–1254. doi: 10.1175/BAMS-D-15-00178.1

Bendix, J., Trachte, K., Cermak, J., Rollenbeck, R., and Naub, T. (2009). Formation of convective clouds at the foothills of the tropical eastern Andes (South Ecuador). *J. Appl. Meteorol. Climatol.* 48, 1682–1695. doi: 10.1175/2009JAMC2078.1

Bermúdez, O. (1990). "Study into frosts in the Bogota savanna," in *Economic and Social Benefits of Meteorological and Hydrological Services. Proceedings Conference* (Geneva), 409–412.

Blodgett, T. A., and Isacks, B. L. (2007). Landslide erosion rate in the eastern cordillera of northern Bolivia. *Earth Interact.* 11, 1–30. doi: 10.1175/2007EI222.1

Boers, N., Barbosa, H. M. J., Bookhagen, B., Marengo, J. A., Marwan, N., and Kurths, J. (2015b). Propagation of strong rainfall events from southeastern South America to the Central Andes. *J. Clim.* 28, 7641–7658. doi: 10.1175/JCLI-D-15-0137.1

Boers, N., Bookhagen, B., Barbosa, H. M., Marwan, N., Kurths, J., and Marengo, J. A. (2014). Prediction of extreme floods in the eastern Central Andes based on a complex networks approach. *Nat. Commun.* 5:5199. doi: 10.1038/ncomms6199

Boers, N., Bookhagen, B., Marengo, J., Marwan, N., Storch, J. -S. V., and Kurths, J. (2015a). Extreme rainfall of the South American monsoon system: a dataset comparison using complex networks. *J. Clim.* 28, 1031–1056. doi: 10.1175/JCLI-D-14-00340.1

Boers, N., Bookhagen, B., Marwan, N., and Kurths, J. (2016). Spatiotemporal characteristics and synchronization of extreme rainfall in South America with focus on the Andes mountain range. *Clim. Dyn.* 46, 601–617. doi: 10.1007/s00382-015-2601-6

Bourges, J., Ribstein, P., Dietze, C., Guyot, J. -L., and Hoorelbeck, R. (1995). Flows and exceptional floods on a small Andean river, or the negative impact of urbanisation [Flux et crues singulieres d'un petit cours d'eau andin ou les effets pervers de l'urbanisation]. *Rev. Geogr. Alpine* 83, 111–126. doi: 10.3406/rga.1995.3793

Bourrel, L., Rau, P., Dewitte, B., Labat, D., Lavado, W., Coutaud, A., et al. (2015). Low-frequency modulation and trend of the relationship between ENSO and precipitation along the northern to centre Peruvian Pacific coast. *Hydrol. Process.* 29, 1252–1266. doi: 10.1002/hyp.10247

Bozkurt, D., Rondanelli, R., Garreaud, R., and Arriagada, A. (2016). Impact of warmer eastern tropical Pacific SST on the March 2015 Atacama floods. *Mon. Weather Rev.* 144, 4441–4460. doi: 10.1175/MWR-D-16-0041.1

Braud, I., Fernandez, P., and Bouraoui, F. (1999). Study of the rainfall-runoff process in the Andes region using a continuous distributed model. *J. Hydrol.* 216, 155–171. doi: 10.1016/S0022-1694(98)00292-3

Braud, I., Vich, A. I. J., Zuluaga, J., Fornero, L., and Pedrani, A. (2001). Vegetation influence on runoff and sediment yield in the Andes region: observation and modelling. *J. Hydrol.* 254, 124–144. doi: 10.1016/S0022-1694(01)00500-5

Brenning, A., Schwinn, M., Ruiz-Páez, A. P., and Muenchow, J. (2015). Landslide susceptibility near highways is increased by 1 order of magnitude in the Andes of southern Ecuador, Loja province. *Nat. Hazard Earth Syst.* 15, 45–57. doi: 10.5194/nhess-15-45-2015

Builes-Jaramillo, L. A., and Poveda, G. (2018). Conjoint analysis of surface and atmospheric water balances in the Andes-Amazon system. *Water Resour. Res.* 54, 3472–3489. doi: 10.1029/2017WR021338

Bustinza, J. A., Rocca, R. J., Zeballos, M. E., and Terzariol, R. E. (2013). "Rerouting of a pipeline due to landslide reactivation in an Andean valley," in *ASME 2013 International Pipeline Geotechnical Conference (IPG)* (Bogotá).

Cai, W., McPhaden, M., Grimm, A., Rodrigues, R., Taschetto, A., Garreaud, R., et al. (2020). Climate impacts of El Niño-Southern Oscillation on South America. *Nat. Rev. Earth Environ.* 1, 215–231. doi: 10.1038/s43017-020-0040-3

Casteller, A., Stoffel, M., Crespo, S., Villalba, R., Corona, C., and Bianchi, E. (2015). Dendrogeomorphic reconstruction of flash floods in the Patagonian Andes. *Geomorphology* 228, 116–123. doi: 10.1016/j.geomorph.2014.08.022

Caviedes, C., and Endlicher, W. (1989). The precipitation in northern Peru during the El Nino oscillation of 1983 [Die Niederschlagsverhaltnisse in Nordperu wahrend des El-Nino oscillation-ereignisses von 1983]. *Erde* 120, 81–87.

Chávez, S. P., and Takahashi, K. (2017). Orographic rainfall hotspots in the Andes-Amazon transition according to the TRMM precipitation radar and *in situ* data. *Geophys. Res. Atmos*. 122, 5870–5882. doi: 10.1002/2016JD026282

Chirino, E., Ruiz-Yanetti, S., Vilagrosa, A., Mera, X., Espinoza, M., and Lozano, P. (2017). Morpho-functional traits and plant response to drought conditions in seedlings of six native species of Ecuadorian ecosystems. *Flora* 233, 58–67. doi: 10.1016/j.flora.2017.05.012

Christie, D. A., Boninsegna, J. A., Cleaveland, M. K., Lara, A., Le Quesne, C., Morales, M. S., et al. (2011). Aridity changes in the Temperate-Mediterranean transition of the Andes since AD 1346 reconstructed from tree-rings. *Clim. Dyn*. 36, 1505–1521. doi: 10.1007/s00382-009-0723-4

Clark, K. E., West, A. J., Hilton, R. G., Asner, G. P., Quesada, C. A., Silman, M. R., et al. (2016). Storm-triggered landslides in the Peruvian Andes and implications for topography, carbon cycles, and biodiversity. *Earth Surf. Dyn*. 4, 47–70. doi: 10.5194/esurf-4-47-2016

Compagnucci, R. H., and Vargas, W. (1998). Inter-annual variability of the Cuyo rivers' streamflow in the Argentinean Andean mountains and ENSO events. *Int. J. Climatol.* 18, 1593–1609.

Condom, T., Martínez, R., Pabón, J. D., Costa, F., Pineda, L., Nieto, J. J., et al. (2020). Climatological and hydrological observations for the South American Andes: *in-situ* stations, satellite and reanalysis data sets. *Front. Earth Sci.* 8:92. doi: 10.3389/feart.2020.00092

Contreras, M. F., Vergara, C., Pereira, M., Colonia, J. D., and Garcí-a, H. (2013). "Pipeline integrity assessment and mitigation techniques in unstable soil conditions based on comparison of in line inspection results," in *ASME 2013 International Pipeline Geotechnical Conference (IPG)* (Bogotá).

Cristancho, C. J. A., Suárez, H., Urbano, Y., and Román, F. (2017). "Fatal livestock lightning accident in Colombia," in: *2017 International Symposium on Lightning Protection (XIV SIPDA)* (Natal), 295–298.

Cruz, C., Rentería, E., and Román, F. (2013). "Statistics of the Colombian National Army lightning accidents," in *2013 International Symposium on Lightning Protection (XII SIPDA)* (Belo Horizonte), 324–328.

Deser, C., and Wallace, J. M. (1987). El Niño events and their relation to the Southern Oscillation: 1925–1986. *J. Geoph. Res*. 92, 14189–14196. doi: 10.1029/JC092iC13p14189

Dominguez, C., Done, J. M., and Bruyère, C. L. (2020). Easterly wave contributions to seasonal rainfall over the tropical Americas in observations and a regional climate model. *Clim. Dyn*. 54, 191–209. doi: 10.1007/s00382-019-04996-7

Domínguez-Castro, F., Garcí-a-Herrera, R., and Vicente-Serrano, S. M. (2018). Wet and dry extremes in Quito (Ecuador) since the 17th century. *Inter. J. Clim*. 38, 2006–2014. doi: 10.1002/joc.5312

Duffaut-Espinosa, L. A., Posadas, A. N., Carbajal, M., and Quiroz, R. (2017). Multifractal downscaling of rainfall using Normalized Difference Vegetation Index (NDVI) in the Andes plateau. *PLoS ONE* 12:e0168982. doi: 10.1371/journal.pone.0168982

Emmer, A. (2017). Geomorphologically effective floods from moraine-dammed lakes in the Cordillera Blanca, Peru. *Quat. Sci. Rev*. 177, 220–234. doi: 10.1016/j.quascirev.2017.10.028

Espinoza, J. C., Chavez, S., Ronchail, J., Junquas, C., Takahashi, K., and Lavado, W. (2015). Rainfall hotspots over the southern tropical Andes: spatial distribution, rainfall intensity, and relations with large-scale atmospheric circulation, *Water Resour. Res*. 51, 3459–3475. doi: 10.1002/2014WR016273

Espinoza, J. C., Garreaud, R., Poveda, G., Arias, P. A., Molina-Carpio, J., Masiokas, M., et al. (2020). Hydroclimate of the Andes Part I: main climatic features. *Front. Earth Sci*. 8:64. doi: 10.3389/feart.2020.00064

Espinoza, J. C., Lengaigne, M., Ronchail, J., and Janicot, S. (2012a). Large-scale circulation patterns and related rainfall in the Amazon Basin: a neuronal networks approach. *Clim. Dyn*. 38:121. doi: 10.1007/s00382-011-1010-8

Espinoza, J. C., Marengo, J. A., Ronchail, J., Molina, J., Noriega, L., and Guyot, J. L. (2014). The extreme 2014 flood in south-western Amazon basin: the role of tropical-subtropical south Atlantic SST gradient. *Environ. Res. Lett*. 9:124007. doi: 10.1088/1748-9326/9/12/124007

Espinoza, J. C., Ronchail, J., Guyot, J. L., Cochonneau, G., Naziano, F., Lavado, W., et al. (2009). Spatio-temporal rainfall variability in the Amazon basin countries (Brazil, Peru, Bolivia, Colombia, and Ecuador). *Int. J. Climatol.* 29, 1574–1594. doi: 10.1002/joc.1791

Espinoza, J. C., Ronchail, J., Guyot, J. L., Junquas, C., Drapeau, G., Martinez, J. M., et al. (2012b). From drought to flooding: understanding the abrupt 2010-2011 hydrological annual cycle in the Amazonas River and tributaries. *Environ. Res. Lett.* 7:024008. doi: 10.1088/1748-9326/7/2/024008

Espinoza, J. C., Ronchail, J., Guyot, J. L., Junquas, C., Vauchel, P., Lavado, W. S., et al. (2011). Climate variability and extremes drought in the upper Solimões River (Western Amazon Basin): understanding the exceptional 2010 drought. *Geophys. Res. Lett*. 38:L13406. doi: 10.1029/2011GL047862

Espinoza, J. C., Ronchail, J., Marengo, J. A., and Segura, H. (2019). Contrasting north-south changes in Amazon wet-day and dry-day frequency and related atmospheric features (1981–2017). *Clim. Dyn.* 52, 5413–5430. doi: 10.1007/s00382-018-4462-2

Espinoza, J. C., Segura, H., Ronchail, J., Drapeau, G., and Gutierrez-Cori, O. (2016). Evolution of wet- and dry-day frequency in the western Amazon basin: relationship with the atmospheric circulation and impacts on the vegetation. *Water Resour. Res*. 52, 8546–8560. doi: 10.1002/2016WR019305

Espizua, L. E., and Bengochea, J. D. (2002). Landslide hazard and risk zonation mapping in the Rí-o Grande basin, Central Andes of Mendoza, Argentina. *Mt. Res. Dev*. 22, 177–185. doi: 10.1659/0276-4741(2002)022[0177:LHARZM]2.0.CO;2

Evans, S. G., Bishop, N. F., Fidel Smoll, L., Valderrama Murillo, P., Delaney, K. B., and Oliver-Smith, A. (2009). A re-examination of the mechanism and human impact of catastrophic mass flows originating on Nevado Huascarán, Cordillera Blanca, Peru in 1962 and 1970. *Eng. Geol*. 108, 96–118. doi: 10.1016/j.enggeo.2009.06.020

Falvey, M., and Garreaud, R. (2007). Wintertime precipitation episodes in Central Chile: associated meteorological conditions and orographic influences. *J. Hydromet*. 8, 171–193. doi: 10.1175/JHM562.1

Favier, V., Wagnon, P., Chazarin, J. -P., Maisincho, L., and Coudrain, A. (2004). One-year measurements of surface heat budget on the ablation zone of Antizana Glacier 15, Ecuadorian Andes. *J. Geophys. Res*. 109:D18105. doi: 10.1029/2003JD004359

Fernandes, K., Baethgen, W., Bernardes, S., deFries, R., DeWitt, D. G., Goddard, L., et al. (2011). North Tropical Atlantic influence on western Amazon fire season variability. *Geophys. Res. Lett*. 38:L12701. doi: 10.1029/2011GL047392

Ferrer, C. (1999). Dammed and failure of natural dams and its relations with coseismic events: some examples from the Venezuelan Andes [Represamientos y rupturas de embalses naturales (lagunas de obturación) como efectos có-smicos: algunos ejemplos en los Andes venezolanos]. *Rev. Geog. Venez*. 40, 109–121.

Francou, B. (1985). El Nino and the drought in the High Central Andes of Peru and Bolivia. [El Nino y la sequia en los altos Andes Centrales: Peru y Bolivia.] *Bull. Inst.Francais des Etudes Andines*. 14, 1–18.

Francou, B., Vuille, M., Favier, V., and Cáceres, B. (2004). New evidence for an ENSO impact on low-latitude glaciers: Antizana, Andes of Ecuador. *J Geophys. Res*. 109:D18106. doi: 10.1029/2003JD004484

Frappart, F., Bourrel, L., Brodu, N., Salazar, X. R., Baup, F., Darrozes, J., et al. (2017). Monitoring of the spatio-temporal dynamics of the floods in the Guayas watershed (Ecuadorian pacific coast) using global monitoring ENVISAT ASAR images and rainfall data. *Water* 9:12. doi: 10.3390/w9010012

Furey, P., and Gupta, V. K. (2007). Diagnosing peak-discharge power laws observed in rainfall-runoff events in Goodwin Creek experimental watershed. *Adv. Water Res*. 30, 2387–2399. doi: 10.1016/j.advwatres.2007.05.014

García, H., Nieves, C., and Colonia, J. D. (2013). "Integrity management program for geo-hazards in the OCENSA pipeline system," in *ASME 2013 International Pipeline Geotechnical Conference (IPG)* (Bogotá).

Garreaud, R. (2013). Warm winter storms in central Chile. *J. Hydrometeor*. 14, 1515–1534. doi: 10.1175/JHM-D-12-0135.1

Garreaud, R., Vuille, M., and Clement, A. (2003). The climate of the Altiplano: observed current conditions and mechanism of past changes. *Paleogeogr. Palaeoclimatol. Palaeoecol*. 194, 5–22. doi: 10.1016/S0031-0182(03)00269-4

Garreaud, R. D. (1999). Multiscale analysis of the summertime precipitation over the central Andes. *Mon. Weather. Rev.* 127, 901–921.

Garreaud, R. D. (2018a). A plausible atmospheric trigger for the 2017 coastal El Niño. *Int. J. Climatol.* 38, e1296–e1302. doi: 10.1002/joc.5426

Garreaud, R. D. (2018b). Record-breaking climate anomalies lead to severe drought and environmental disruption in Western Patagonia in 2016. *Clim. Res.*74, 217–229. doi: 10.3354/cr01505

Garreaud, R. D., Alvarez-Garreton, C., Barichivich, J., Boisier, J. P., Christie, D. A., Galleguillos, M., et al. (2017). The 2010-2015 megadrought in Central Chile: impacts on regional hydroclimate and vegetation. *Hydrol. Earth Syst. Sci.* 21, 6307–6327. doi: 10.5194/hess-21-6307-2017

Garreaud, R. D., and Rutllant, J. (1997). Precipitación estival en los Andes de Chile central: aspectos climatológicos. *Atmósfera* 10, 191–211.

Garreaud, R. D., and Viale, M. (2014). Análisis de los fenómenos meteorológicos y climáticos que afectan la cuenca del río Maipo. *Aquae Papers* 5, 17–29.

Garreaud, R. D., Vuille, M., Compagnucci, R., and Marengo, J. (2009). Present-day South American climate. *Palaeogeo. Palaeoclim. Palaeoecol*. 281, 180–195. doi: 10.1016/j.palaeo.2007.10.032

Garreaud, R. D., and Wallace, J. M. (1998). Summertime incursions of midlatitude air into subtropical and tropical South America. *Mon. Weather Rev*. 126, 2713–2733.

Giovannettone, J. P., and Barros, A. P. (2009). Probing regional orographic controls of precipitation and cloudiness in the central andes using satellite data. *J. Hydromet*. 10, 167–182. doi: 10.1175/2008JHM973.1

Gómez, J. D., and Poveda, G. (2008). Estimación del espectro multifractal para series de precipitación horaria en los Andes tropicales de Colombia. *Revista Acad. Colomb. Ci. Exact*. 32, 483–502. Available online at: http://www.accefyn.com/revista/Vol_32/125/483-502.pdf

González, M. E., Gómez-González, S., Lara, A., Garreaud, R. D., and Díaz-Hormazábal, I. (2018). The 2010-2015 Megadrought and its influence on the fire regime in central and south central Chile. *Ecosphere* 9:e2300. doi: 10.1002/ecs2.2300

Grandoso, H. N. (1966). Distribución temporal y geográfica del granizo en la Provincia de Mendoza y su relación con algunos parámetros meteorológicos. *Serie Meteorológica*. 1, 49.

Grimm, A. A., and Tedeschi, R. G. (2009) ENSO and extreme rainfall events in South America. *J. Clim.* 22,1590–1609. doi: 10.1175/2008JCLI2429.1

Guallpa, M., Orellana-Alvear, J., and Bendix, J. (2019). Tropical Andes radar precipitation estimates need high temporal and moderate spatial resolution. *Water* 11:1038. doi: 10.3390/w11051038

Guha-Sapir, D., Below, R., and Hoyois, P. (2015). *EM-DAT: The CRED/OFDA International Disaster Database*. Brussels: Université Catholique de Louvain. Retrieved from: http://www.emdat.be/database (accessed October 30, 2015).

Guns, M., and Vanacker, V. (2013). Forest cover change trajectories and their impact on landslide occurrence in the tropical Andes. *Environ. Earth Sci*. 70, 2941–2952. doi: 10.1007/s12665-013-2352-9

Guns, M., and Vanacker, V. (2014). Shifts in landslide frequency-area distribution after forest conversion in the tropical Andes. *Anthropocene* 6, 75–85. doi: 10.1016/j.ancene.2014.08.001

Gupta, V. K., and Dawdy, D. (1995). Physical interpretations of regional variations in the scaling exponents of flood quantiles. *Hydrol. Process*. 9, 347–361. doi: 10.1002/hyp.3360090309

Gupta, V. K., Mantilla, R., Troutman, B. M., Dawdy, D., and Krajewski, W. F. (2010). Generalizing a nonlinear geophysical flood theory to medium-sized river networks. *Geophys. Res. Lett*. 37:L11402. doi: 10.1029/2009GL041540

Hermanns, R. L., and Niedermann, S. (2006). Rock avalanching in the NW argentine Andes as a result of complex interactions of lithologic, structural and topographic boundary conditions, climate change and active tectonics. *Landslides* 49, 497–520. doi: 10.1007/978-1-4020-4037-5_27

Hermanns, R. L., Niedermann, S., Ivy-Ochs, S., and Kubik, P. W. (2004). Rock avalanching into a landslide-dammed lake causing multiple dam failure in las conchas valley (NW Argentina) - evidence from surface exposure dating and stratigraphic analyses. *Landslides* 1, 113–122. doi: 10.1007/s10346-004-0013-5

Hermanns, R. L., Valderrama, P., Fauqu, L., Penna, I. M., Sepúlveda, S., Moreiras, S., et al. (2012). Landslides in the Andes and the need to communicate on an interandean level on landslide mapping and research [Deslizamientos en los Andes y la necesidad de comunicar a nivel interandino sobre el mapeo y la investigación de deslizamientos]. *Rev. Assoc. Geol.* 69, 321–327. Available online at: http://ppct.caicyt.gov.ar/index.php/raga/article/view/1824

Herrera, J., Younes, C., and Porras, L. (2018). Cloud-to-ground lightning activity in Colombia: a 14-year study using lightning location system data. *Atmos. Res*. 203, 164–174. doi: 10.1016/j.atmosres.2017.12.009

Holmann, F., Rivas, L., Urbina, N., Rivera, B., Giraldo, L. A., Guzman, S., et al. (2005). The role of livestock in poverty alleviation: an analysis of Colombia. *Livest. Res. Rural Dev*. 17. Retrieved from: http://www.lrrd.org/lrrd17/1/holm17011.htm (accessed May 16, 2020).

Houze, R. A. Jr., Wilton, D. C., and Smull, B. F. (2007). Monsoon convection in the Himalayan region as seen by the TRMM precipitation radar. *Quart. J. Roy. Meteor. Soc.* 133, 1389–1411.

Houze, R. A. Jr. (2004). Mesoscale convective systems. *Rev. Geophys.* 42:150. doi: 10.1029/2004RG000150

Houze, R. A. Jr., Rasmussen, K. L., Zuluaga, M. D., and Brodzik, S. R. (2015). The variable nature of convection in the tropics and subtropics: a legacy of 16 years of Tropical rainfall measuring mission satellite. *Rev. Geophys*. 53, 994–1021. doi: 10.1002/2015RG000488

Hoyos, C. D., Ceballos, L. I., Pérez-Carrasquilla, J. S., Sepúlveda, J., López-Zapata, S. M., Zuluaga, M. D., et al. (2019). Meteorological conditions leading to the 2015 Salgar flash flood: lessons for vulnerable regions in tropical complex terrain. *Nat. Hazards Earth Syst. Sci*. 19, 2635–2665. doi: 10.5194/nhess-19-2635-2019

Hoyos, N., Escobar, J., Restrepo, J. C., Arango, A. M., and Ortiz, J. C. (2013). Impact of the 2010-2011 La Niña phenomenon in Colombia, South America: the human toll of an extreme weather event. *Appl. Geogr*. 39, 16-25. doi: 10.1016/j.apgeog.2012.11.018

Hrdina, A., and Romportl, D. (2017). Evaluating global biodiversity hotspots – very rich and even more endangered. *J. Lands Ecol*. 10, 108–115. doi: 10.1515/jlecol-2017-0013

Huggel, C., Raissig, A., Rohrer, M., Romero, G., Diaz, A., and Salzmann, N. (2015). How useful and reliable are disaster databases in the context of climate and global change? A comparative case study analysis in Peru. *Nat. Hazards Earth Syst. Sci*. 15, 475–485. doi: 10.5194/nhess-15-475-2015

Hurley, J. V., Vuille, M., Hardy, D. R., Burns, S. J., and Thompson, L. G. (2015). Cold air incursions, δ^{18}O variability, and monsoon dynamics associated with snow days at Quelccaya ice cap, Peru. *J. Geophys. Res. Atmos*. 120, 7467–7487. doi: 10.1002/2015JD023323

Hurtado, A. F., and Poveda, G. (2009). Linear and global space-time dependence and Taylor hypotheses for rainfall in the tropical Andes. *J. Geophys. Res*. 114: D10105. doi: 10.1029/2008JD011074

Imfeld, N., Schuller, C. B., Marrou, K. M. C., Jaques-Cooper, M., Sedlmeier, K., Gubler, S., et al. (2019). Summertime precipitation deficits in the southern Peruvian highlands since 1964. *Int. J. Climatol.* 39, 4497–4513. doi: 10.1002/joc.6087

Iñiguez, V., Morales, O., Cisneros, F., Bauwens, W., and Wyseure, G. (2016). Analysis of the drought recovery of Andosols on southern Ecuadorian Andean páramos. *Hydrol. Earth Sys. Sci*. 20, 2421–2435. doi: 10.5194/hess-20-2421-2016

Jacques-Coper, M., Bronnimann, S., Martius, O., Vera, C., and Cerne, B. (2016). Summer heat waves in Southeastern Patagonia: an analysis of the intraseasonal timescale. *Int. J. Climatol*. 36, 1359–1374. doi: 10.1002/joc.4430

Jaramillo, L., Poveda, G., and Mejía, J. F. (2017). Mesoscale convective systems and other precipitation features over the tropical Americas and surrounding seas as seen by TRMM. *Int. J. Climatol*. 37, 380–397. doi: 10.1002/joc.5009

Jaramillo, M. M. (2008). Guidelines for landslide hazard mapping in the Andes: speaking one language. *Geol. Soc. Spec. Publ.* 305, 53–61. doi: 10.1144/SP305.6

Jauregui, Y. R., and Takahashi, K. (2017). Simple physical-empirical model of the precipitation distribution based on a tropical sea surface temperature threshold and the effects of climate change. *Clim. Dyn*. 50:2217. doi: 10.1007/s00382-017-3745-3

Jiménez-Muñoz, J. C., Mattar, C., Barichivich, J., Santamaría-Artigas, A., Takahashi, K., Malhi, Y., et al. (2016). Record-breaking warming and extreme drought in the Amazon rainforest during the course of El Niño 2015-2016. *Sci. Rep.* 6:33130. doi: 10.1038/srep33130

Junquas, C., Li, L., Vera, C. S., Le Treut, H., and Takahashi, K. (2016). Influence of South America orography on summertime precipitation in Southeastern South America. *Clim. Dyn*. 46, 3941–3963. doi: 10.1007/s00382-015-2814-8

Junquas, C., Takahashi, K., Condom, T., Espinoza, J. C., Chavez, S., Sicart, J. E., et al. (2018). Understanding the influence of orography over the precipitation diurnal cycle and the associated atmospheric processes in the central Andes. *Clim. Dyn*. 50, 3995–4017. doi: 10.1007/s00382-017-3858-8

Kalicki, P., Kalicki, T., and Kittel, P. (2014). The influence of El Niño on settlement patterns in Lomas de Lachay, central coast, Peru. *Interdis. Archaeol*. 5, 147–160. doi: 10.24916/iansa.2014.2.5

Kane, R. P. (2006). El Niño effects on rainfall in South America: comparison with rainfalls in India and other parts of the world. *Adv. Geosci*. 6, 35–41. doi: 10.5194/adgeo-6-35-2006

Kao, H., and Yu, J. (2009). Contrasting Eastern-Pacific and Central-Pacific types of ENSO. *J. Clim.* 22, 615–632. doi: 10.1175/2008JCLI2309.1

Killeen, T. J., Douglas, M., Consiglio, T., Jørgensen, P. M., and Mejia, J. (2007). Dry spots and wet spots in the Andean hotspot. *J. Biogeogr*. 34, 1357–1373. doi: 10.1111/j.1365-2699.2006.01682.x

Kousky, V. E., Kayano, M. T., and Cavalcanti, I. F. A. (1984). A review of the Southern Oscillation: oceanic–atmospheric circulation changes and related rainfall anomalies. *Tellus Ser A* 36, 490–504. doi: 10.1111/j.1600-0870.1984.tb00264.x

Kumar, S., Castillo-Velarde, C. D., Valdivia Prado, J. M., Flores Rojas, J. L., Callañaupa Gutierrez, S. M., Moya Alvarez, A. S., et al. (2020). Rainfall Characteristics in the Mantaro Basin over tropical Andes from a vertically pointed profile rain radar and *in-situ* field campaign. *Atmosphere* 11:248. doi: 10.3390/atmos11030248

Kumar, S., Vidal, S.-Y., Moya-Álvarez, A. S., and Martínez-Castro, D. (2019). Effect of the surface wind flow and topography on precipitating cloud systems over the Andes and associated Amazon basin: GPM observations. *Atmos. Res*. 225, 193–208. doi: 10.1016/j.atmosres.2019.03.027

Kummerow, C., Barnes, W., Kozu, T., Shiue, J., and Simpson, J. (1998). The Tropical Rainfall Measuring Mission (TRMM) sensor package. *J. Atmos. Oceanic Technol.* 15, 809–817.

Kummerow, C. J., Simpson, J., Thiele, O., Barnes, W., Chang, A. T., Hou, A., et al. (2000). The status of the Tropical Rainfall Measuring Mission (TRMM) after two years in orbit. *J. Appl. Meteorol.* 39, 1965–1982. doi: 10.1175/1520-0450(2001)040<1965:TSOTTR>2.0.CO;2

Lagos, P., Silva, Y., Nickl, E., and Mosquera, K. (2008). El Niño-related precipitation variability in Perú. *Adv. Geosci.* 14, 231–237. doi: 10.5194/adgeo-14-231-2008

Laraque, A., Bernal, C., Bourrel, L., Darrozes, J., Christophoul, F., Armijos, E., et al. (2009). Sediment budget of the Napo River, Amazon Basin, Ecuador and Peru. *Hydrol. Proc*. 23, 3509–3524. doi: 10.1002/hyp.7463

Larkin, N. K., and Harrison,. D. E. (2005). Global seasonal temperature and precipitation anomalies during El Niño autumn and winter. *Geophys. Res. Lett*. 32:L13705. doi: 10.1029/2005GL022738

Laurent, H., Machado, L. A. T., Morales, C., and Durieux, L. (2002). Characteristics of the Amazonian mesoscale convective systems observed from satellite and radar during the WETAMC/LBA experiment. *J. Geophys. Res*. 107:8054. doi: 10.1029/2001JD000337

Lavado, W., Ronchail, J., Labat, D., Espinoza, J. C., and Guyot, J. L. (2012). A basin-scale analysis of rainfall and runoff in Peru (1969-2004): Pacific, Titicaca and Amazonas drainages. *Hydrol. Sci. J*. 57, 625–642. doi: 10.1080/02626667.2012.672985

Lavado-Casimiro, W., and Espinoza, J. C. (2014). Impactos de El Niño y La Niña en las lluvias del Perú (1965–2007). *Rev. Brasil. Meteo*. 29, 171–182. doi: 10.1590/S0102-77862014000200003

Lavado-Casimiro, W., Felipe, O., Silvestre, E., and Bourrel, L. (2013). ENSO impact on hydrology in Peru. *Adv. Geos*. 33, 33–39. doi: 10.5194/adgeo-33-33-2013

Lavado-Casimiro, W. S., Silvestre, E., and Pulache, W. (2010). Tendencias en los extremos de lluvias cerca a la ciudad del Cusco y su relación con las inundaciones de Enero del 2010. (Extreme rainfall trends around Cusco and its relationship with the floods in January). *Rev. Peruana Geoatmos*. 2,89–98. Available online at: https://web2.senamhi.gob.pe/rpga/pdf/2010_vol02/art8.pdf

Lee, E. M., Audibert, J. M. E., Hengesh, J. V., and Nyman, D. J. (2009). Landslide-related ruptures of the Camisea pipeline system, Peru. *Q. J. Eng. Geol. Hydrog*. 42, 251–259. doi: 10.1144/1470-9236/08-061

León, G., Zea, J., and Eslava, J. (2001). Ondas del este en Colombia y algunos aspectos relevantes de los ciclones tropicales. *Meteorol. Colomb*. 3, 137–141. Available online at: http://gfnun.unal.edu.co/fileadmin/content/geociencias/revista_meteorologia_colombiana/numero03/03_15.pdf

Liebmann, B., Kiladis, G. N., Vera, C. S., Saulo, A. C., and Carvalho, L. M. V. (2004). Subseasonal variations of rainfall in South America in the vicinity of the low-level jet east of the Andes and comparison to those in the South Atlantic convergence zone. *J. Clim.* 17, 3829–3842. doi: 10.1175/1520-0442(2004)017<3829:SVORIS>2.0.CO;2

López Salgado, H. J. (2016). "Assessing soil susceptibility to mass movements: case study of the Coello river basin, Colombia," in*: Geopedology: An Integration of Geomorphology and Pedology for Soil and Landscape Studies*, eds J. A. Zinck, G. Metternicht, G. Bocco, and H. F. Del Valle (Cham: Springer International Publisher), 411–424.

López, M. E., and Howell, W. E. (1967). Katabatic winds in the Equatorial Andes. *J. Atmos. Sci*. 24, 29–35.

Lovejoy, T., and Nobre, C. A. (2019). Winds of will: tipping change in the Amazon. *Sci. Adv.* 5:eaba2949. doi: 10.1126/sciadv.aba2949

Lowman, L. E. L., and Barros, A. P. (2014). Investigating links between climate and orography in the central Andes: coupling erosion and precipitation using a physical-statistical model. *J. Geophys. Res. Earth Surf*. 119, 1322–1353. doi: 10.1002/2013JF002940

MAAP (2019). *Major Finding - Many Brazilian Amazon Fires Follow 2019 Deforestation.* Available online at: https://maaproject.org/2019/amazon-fires-deforestation/ (accessed March 9, 2020).

Maeda, E. E., Kim, H., Aragão, L. E. O. C., Famiglietti, J. S., and Oki, T. (2015). Disruption of hydroecological equilibrium in southwest Amazon mediated by drought. *Geophys. Res. Lett*. 42, 7546–7553. doi: 10.1002/2015GL065252

Magrin, G. O., Marengo, J. A., Boulanger, J.-P., Buckeridge, M. S., Castellanos, E., Poveda, G., et al. (2014). "Central and South America," in: *Climate Change 2014: Impacts, Adaptation, and Vulnerability. Part B: Regional Aspects. Contribution of Working Group II to the Fifth Assessment Report of the Intergovernmental Panel on Climate Change*, eds V. R. Barros, C. B. Field, D. J. Dokken, M. D. Mastrandrea, K. J. Mach, T. E. Bilir, M. Chatterjee, K. L. Ebi, Y. O. Estrada, R. C. Genova, B. Girma, E. S. Kissel, A. N. Levy, S. MacCracken, P. R. Mastrandrea, and L.L. White (Cambridge, UK; New York, NY: Cambridge University Press), 1499–1566.

Makowski Giannoni, S., Trachte, K., Rollenbeck, R., Lehnert, L., Fuchs, J., and Bendix, J. (2016). Atmospheric salt deposition in a tropical mountain rainforest at the eastern Andean slopes of south Ecuador-Pacific or Atlantic origin? *Atmos. Chem. Phys*. 16, 10241–10261. doi: 10.5194/acp-16-10241-2016

Mandapaka, P. V., Krajewski, W. F., Mantilla, R., and Gupta, V. K. (2009). Dissecting the effect of rainfall variability on the statistical structure of peak flows. *Adv.Water Res.* 32, 1508–1525. doi: 10.1016/j.advwatres.2009.07.005

Manners, R. B., Magilligan, F. J., and Goldstein, P. S. (2007). Floodplain development, El Niño, and cultural consequences in a hyperarid Andean environment. *Ann. Assoc. Am. Geogr*. 97, 229–249. doi: 10.1111/j.1467-8306.2007.00533.x

Mapes, B. E., Warner, T. T., and Xu, M. (2003). Diurnal patterns of rainfall in northwestern South America. Part III: diurnal gravity waves and nocturnal convection offshore. *Mon. Weather Rev.* 131, 830–844. doi: 10.1175/1520-0493(2003)131<0830:DPORIN>2.0.CO;2

Marchese, C. (2015). Biodiversity hotspots: a shortcut for a more complicated concept. *Glob. Ecol. Conserv*. 3, 297–309. doi: 10.1016/j.gecco.2014.12.008

Marengo, J. (1983). Estudios Agroclimático de la zona de Genaro Herrera (Requena-Loreto) y climático en la selva baja norte del Perú. Tesis UNALM. *Ing. Meteorólogo. Lima.* p. 464.

Marengo, J., Cornejo, A., Satymurty, P., Nobre, C., and Sea, W. (1997). Cold surges in tropical and extratropical South America: the strong event in June 1994. *Mon. Weather Rev.* 125, 2759–2786.

Marengo, J. A., Alves, L. M., Soares, W. R., Rodriguez, D. A., Camargo, H., Paredes, M., et al. (2013). Two contrasting seasonal extremes in tropical South America in 2012: flood in Amazonia and drought in Northeast Brazil. *J. Clim*. 26, 9137–9154. doi: 10.1175/JCLI-D-12-00642.1

Marengo, J. A., Espinoza, J. C., Ronchail, J., Alves, L. M., and Baez, J. (2017). [Regional Climates] Central South America [in "State of the Climate in 2016"]. *Bull. Am. Meteorol. Soc*. 98, S187–S190. doi: 10.1175/2017BAMSStateoftheClimate.1

Marengo, J. A., Tomasella, J., Alves, L. M., Soares, W., and Rodriguez, D. A. (2011). The drought of 2010 in the context of historical droughts in the Amazon region. *Geophys. Res. Lett*. 38, 1–5. doi: 10.1029/2011GL047436

Marengo, J. A., Tomasella, J., Soares, W., Alves, L. M., and Nobre, C. A. (2010). Extreme climatic events in the Amazon basin: climatological and hydrological context of previous floods. *Theor. Appl. Climatol*. 85, 1–5. doi: 10.1007/s00704-011-0465-1

Marie, G., and Veerle, V. (2013). "Landslide controlling factors in catchments with high deforestation," in *Landslide Science and Practice.* eds C. Margottini, P. Canuti, and K. Sassa (Berlin; Heidelberg: Springer), 227–233.

Marwan, N., Trauth, M. H., Vuille, M., and Kurths, J. (2003). Comparing modern and Pleistocene ENSO-like influences in NW Argentina using nonlinear time series analysis methods. *Clim. Dyn*. 21, 317–326. doi: 10.1007/s00382-003-0335-3

Masiokas, M. H., Rabatel, A., Rivera, A., Ruiz, L., Pitte, P., Ceballos, J. L., et al. (2020). Current state and recent changes of the cryosphere in the Andes. *Front Earth Sci.* 8:99. doi: 10.3389/feart.2020.00099

Masotti, I., Aparicio-Rizzo, P., Yevenes, M. A., Garreaud, R., Belmar, L., and Farías, L. (2018). The influence of river discharge on nutrient export and phytoplankton biomass off the central Chile coast (33°-37°S): seasonal cycle and interannual variability. *Front. Mar. Sci*. 5:423. doi: 10.3389/fmars.2018.00423

Matsudo, C. M., and Salio, P. (2011). Severe weather reports and proximity to deep convection over Northern Argentina. *Atmos. Res*. 100, 523–537. doi: 10.1016/j.atmosres.2010.11.004

McPhaden, M. J., Vera, C. S., and Martnez Guingla, R. (2010). Climate variability and change in South America. *Eos* 91:473. doi: 10.1029/2010EO490006

McPhaden, M. J., Zebiak, S. E., and Glantz, M. H. (2006). ENSO as an integrating concept in Earth science. *Science* 314, 1740–1745. doi: 10.1126/science.1132588

Menabde, M., and Sivapalan, M. (2001). Linking space-time variability of river runoff and rainfall fields: a dynamic approach. *Adv. Water Res*., 24, 1001–1014. doi: 10.1016/S0309-1708(01)00038-0

Méndez, W., Rivas, L., Fernández, E., Díaz, Y., Arévalo, M., and Correa, N. (2016). Hydro-geomorphological hazard in catchments of the Waraira Repano national park south hillside, Distrito Capital, Venezuela [Amenaza hidrogeomorfológica en microcuencas de la vertiente sur del Parque Nacional Waraira Repano, Distrito Capital, Venezuela]. *Rev. Geog. Venez*. 57, 70–91. Available online at: http://www.saber.ula.ve/handle/123456789/41975

Mesa, O. J., and Peñaranda, V. M. (2015). Complejidad de la estructura espacio-temporal de la precipitación. *Rev. Acad. Colomb. Cienc. Ex. Fis. Nat*. 39, 304–320. doi: 10.18257/raccefyn.196

Metz, N. D., Archambault, H. M., Srock, A. F., Galarneau, T. J. Jr., and Bosart, L. F. (2013). A comparison of South American and African preferential pathways for extreme cold events. *Mon. Weather. Rev*. 141, 2066–2086. doi: 10.1175/MWR-D-12-00202.1

Mezher, R. N., Doyle, M., and Barros, V. (2012). Climatology of hail in Argentina. *Atmos. Res*. 114–115, 70–82. doi: 10.1016/j.atmosres.2012.05.020

Michoud, C., Baumann, V., Lauknes, T. R., Penna, I., Derron, M. - H., and Jaboyedoff, M. (2016). Large slope deformations detection and monitoring along shores of the Potrerillos dam reservoir, Argentina, based on a small-baseline InSAR approach. *Landslides* 13, 451–465. doi: 10.1007/s10346-015-0583-4

Minetti, J. L., Vargas, W. M., Poblete, A. G., de la Zerda, L. R., and Acuña, L. R. (2010). Regional droughts in southern South America. *Theor. Appl. Clim*. 102, 403–415. doi: 10.1007/s00704-010-0271-1

Molina, A., Vanacker, V., Balthazar, V., Mora, D., and Govers, G. (2012). Complex land cover change, water and sediment yield in a degraded andean environment. *J. Hydrol*. 472–473, 25–35. doi: 10.1016/j.jhydrol.2012.09.012

Montecinos, A., and Aceituno, P. (2003). Seasonality of the ENSO-related rainfall variability in central Chile and associated circulation anomalies. *J. Clim*. 16, 281–296. doi: 10.1175/1520-0442(2003)016<0281:SOTERR>2.0.CO;2

Montecinos, A., Kurgansky, M. V., Muñoz, C., and Takahashi, K. (2011). Non-ENSO interannual rainfall variability in central Chile during austral winter. *Theor. Appl. Climatol*. 106, 557–568. doi: 10.1007/s00704-011-0457-1

Montgomery, D. R., and Dietrich, W. E. (1994). A physically based model for the topographic control on shallow landsliding. *Water Resour. Res*. 30, 1153–1171. doi: 10.1029/93WR02979

Morales, M. S., Christie, D. A., Villalba, R., Argollo, J., Pacajes, J., Silva, J. S., et al. (2012). Precipitation changes in the South American Altiplano since 1300 AD reconstructed by tree-rings. *Clim. Past* 8, 653–666. doi: 10.5194/cp-8-653-2012

Moreiras, S., Lisboa, M. S., and Mastrantonio, L. (2012). The role of snow melting upon landslides in the central Argentinean Andes. *Earth Surf. Proc. Land.* 37, 1106–1119. doi: 10.1002/esp.3239

Moreiras, S. M. (2005). Climatic effect of ENSO associated with landslide occurrence in the Central Andes, Mendoza Province, Argentina. *Landslides* 2, 53–59. doi: 10.1007/s10346-005-0046-4

Moreiras, S. M. (2006). Frequency of debris flows and rockfall along the Mendoza river valley (Central Andes), Argentina: associated risk and future scenario. *Q Intern*. 158, 110–121. doi: 10.1016/j.quaint.2006.05.028

Moreiras, S. M., and Pont, I. P. V. D. (2017). Climate change driving greater slope instability in the Central Andes. *Adv. Cult. Liv. Landsl.* 5, 191–197. doi: 10.1007/978-3-319-53483-1_22

Moreiras, S. M., Pont, I. V. D., and Araneo, D. (2018). Were merely storm-landslides driven by the 2015-2016 Niño in the Mendoza River valley? *Landslides* 15:997. doi: 10.1007/s10346-018-0959-3

Moreiras, S. M., and Sepúlveda, S. A. (2015). Megalandslides in the Andes of central Chile and Argentina (32°-34°S) and potential hazards. *Geol. Soc. Spec. Publ*. 399, 329–344. doi: 10.1144/SP399.18

Morera, S. B., Condom, T., Crave, A., Steer, P., and Guyot, J. L. (2017). The impact of extreme El Niño events on modern sediment transport along the western Peruvian Andes (1968-2012). *Sci. Rep*. 7:11947. doi: 10.1038/s41598-017-12220-x

Moya-Álvarez, A. S., Martínez-Castro, D., Kumar, S., Estevan, R., and Silva, Y. (2019). Response of the WRF model to different resolutions in the rainfall forecast over the complex Peruvian orography. *Theor. Appl. Clim*. 137:2993. doi: 10.1007/s00704-019-02782-3

Mulholland, J. P., Nesbitt, S. W., Trapp, R. J., Rasmussen, K. L., and Salio, P. V. (2018). Convective storm life cycle and environments near the Sierras de Córdoba, Argentina. *Mon. Weather Rev*. 146, 2541–2557. doi: 10.1175/MWR-D-18-0081.1

Muñoz, E., Poveda, G., Ochoa, A., and Caballero, H. (2017). "Multifractal analysis of spatial and temporal distributions of landslides in Colombia," in *Advancing Culture of Living With Landslides,* eds M. Mikos, B. Tiwari, Y. Yin, K. Sassa (Cham: Springer International Publishing), 1073–1079.

Mutke, J., Bohnert, T., and Weigend, M. (2017). Climate change: save last cloud forests in western Andes. *Nature* 541:157. doi: 10.1038/541157e

Myers, N., Mittermeier, R. A., da Fonseca, C. G., Gustavo, A. B., and Kent, J. (2000). Biodiversity hotspots for conservation priorities. *Nature* 403, 853–858. doi: 10.1038/35002501

Naaim, M., Furdada, G., and Martínez, H. (2002). Calibration and application of the MN2D dynamics model to the avalanches of Las Leñas (Argentina). *Nat. Hazards Earth Sys. Sci*. 2, 221–226. doi: 10.5194/nhess-2-221-2002

Nascimento, E. L., and Marcelino, I. P. V. O. (2005). Preliminary analysis of the 3 January 2005 tornadoes in Criciuma/SC. *Bull. Braz. Meteorol. Soc*. 29, 33–44.

Navarrete-Aldana, N., Cooper, M. A., and Holle, R. L. (2014). Lightning fatalities in Colombia from 2000 to 2009. *Nat. Hazards* 74, 1349–1362. doi: 10.1007/s11069-014-1254-9

Nguyen, P., Thorstensen, A., Sorooshian, S., Hsu, K., and AghaKouchak, A. (2015). Flood forecasting and inundation mapping using hiresflood-uci and near-real-time satellite precipitation data: the 2008 Iowa flood. *J. Hydrometeorol.* 16, 1171–1183. doi: 10.1175/JHM-D-14-0212.1

Nieto, R., Ciric, D., Vázquez, M., Liberato, M. L. R., and Gimeno, L. (2019). Contribution of the main moisture sources to precipitation during extreme peak precipitation months. *Adv. Water Resour.* 131:103385. doi: 10.1016/j.advwatres.2019.103385

Norte, F. A. (2015). Understanding and forecasting Zonda wind (Andean Foehn) in Argentina: a review. *Atmos. Clim. Sci.* 5, 163–193. doi: 10.4236/acs.2015.53012

Norte, F. A., Ulke, A., Simonelli, S., and Viale, M. (2008). The severe Zonda wind event of 11 July 2006 east of the Andes Cordillera (Argentine): a case study using the BRAMS model. *Met. Atmos. Phys.* 102, 1–14. doi: 10.1007/s00703-008-0011-6

Nossin, J. J. (1999). Monitoring of hazards and urban growth in Villavicencio, Colombia, using scanned air photos and satellite imagery. *Geo J.* 49, 151–158. doi: 10.1023/A:1006939519722

Núñez-Cobo, J., Garreaud, R., and Verbist, K. (2018). "Sequias en Chile," in *Atlas de Sequía de América Latina y el Caribe.* ed J. K. Núñez Cobo (Paris; La Serena: Verbist UNESCO and CAZALAC), 204.

Ochoa, A., Pineda, L., Crespo, P., and Willems, P. (2014). Evaluation of TRMM 3B42 precipitation estimates and WRF retrospective precipitation simulation over the Pacific–Andean region of Ecuador and Peru. *Hydrol. Earth Syst. Sci.* 18, 3179-3193. doi: 10.5194/hess-18-3179-2014

Oliveros, F., Hernández, E., and Soto, G. (2017). "Application of geotechnical criteria for the occurrence of earth flows (avalanches) on the right of way of pipeline transportation system of Camisea in the coast zone of Peru," in *ASME 2017 International Pipeline Geotechnical Conference (IPG)* (Lima).

OPS (2000). *Perú: Fenómeno El Niño, 1997-1998.* Washigton, DC: Organización Panamericana de la Salud. Fenómeno El Niño, 1997-1998.

Ortloff, C. R., and Kolata, A. L. (1993). Climate and collapse: agro-ecological perspectives on the decline of the Tiwanaku State. *J. Archaeol. Sci.* 20, 195–221. doi: 10.1006/jasc.1993.1014

Otero, F., Norte, F., and Araneo, D. (2018). A probability index for surface zonda wind occurrence. *Theor. Appl. Climatol.* 131, 213. doi: 10.1007/s00704-016-1983-7

Ovando, A., Tomasella, J., Rodriguez, D. A., Martinez, J. M., Siqueira-Junior, J. L., Pinto, G. L. N., et al. (2016). Extreme flood events in the Bolivian Amazon wetlands. *J. Hydrol. Reg. Stu.* 5, 293–308. doi: 10.1016/j.ejrh.2015.11.004

Pabón-Caicedo, J. D., Arias, P. A., Carril, A. F., Espinoza, J. C., Fita, L., Goubanova, K., et al. (2020). Observed and projected hydroclimate changes in the Andes. *Front. Earth Sci.* 8:61. doi: 10.3389/feart.2020.00061

Paccini, L., Espinoza, J. C., Ronchail, J., and Segura, H. (2017). Intraseasonal rainfall variability in the Amazon basin related to large-scale circulation patterns: a focus on western Amazon-Andes transition region. *Int. J. Clim.* 38, 2386–2399. doi: 10.1002/joc.5341

Pérez, G., Mantilla, R., Krajewski, W. F., and Wright, D. B. (2019). Using physically based synthetic peak flows to assess local and regional flood frequency analysis methods. *Water Resour. Res.* 55, 8384–8403. doi: 10.1029/2019WR024827

Perrin, J. L., Bouvier, C., Janeau, J. L., Mánez, G., and Cruz, F. (2001). Rainfall/runoff processes in a small peri-urban catchment in the Andes mountains. The Rumihurcu Quebrada, Quito (Ecuador). *Hydrol. Process.* 15, 843–854. doi: 10.1002/hyp.190

Perucca, L. P., and Angilieri, Y. E. (2011). Morphometric characterization of del Molle Basin applied to the evaluation of flash floods hazard, Iglesia Department, San Juan, Argentina. *Q. Int.* 233, 81–86. doi: 10.1016/j.quaint.2010.08.007

Pettinger, A. M., and Sykora, D. W. (2011). Landslide risk assessment for pipeline systems in mountainous regions. *J. Pipeline Syst. Eng.* 10, 161–171.

Pezza, A. B., and Ambrizzi, T. (2005). Dynamical conditions and synoptic tracks associated with different types of cold surge over tropical South America. *Int. J. Climatol.* 25, 215–241. doi: 10.1002/joc.1080

Pizarro, R., Vera, M., Valdés, R., Helwig, B., and Olivares, C. (2014). Multi-decadal variations in annual maximum peak flows in semi-arid and temperate regions of Chile. *Hydrol. Sci. J.* 59, 300–311. doi: 10.1080/02626667.2013.803182

Posadas, A., Duffaut Espinosa, L. A., Yarlequé, C., Carbajal, M., Heidinger, H., Carvalho, L., et al. (2015). Spatial random downscaling of rainfall signals in Andean heterogeneous terrain, Nonlin. *Process. Geophys*. 22, 383–402. doi: 10.5194/npg-22-383-2015

Poveda, G. (2011). Mixed memory, (non) Hurst effect, and maximum entropy of rainfall in the tropical Andes. *Adv. Water Res*. 34, 243–256. doi: 10.1016/j.advwatres.2010.11.007

Poveda, G., Álvarez, D. M., and Rueda, O. A. (2011). Hydro-climatic variability over the Andes of Colombia associated with ENSO: a review of climatic processes and their impact on one of the Earth's most important biodiversity hotspots. *Clim. Dyn*. 36, 2233–2249. doi: 10.1007/s00382-010-0931-y

Poveda, G., Jaramillo, A., Gil, M. M., Quiceno, N., and Mantilla, R. I. (2001a). Seasonality in ENSO related precipitation, river discharges, soil moisture, and vegetation index (NDVI) in Colombia. *Water Resour. Res*. 37, 2169–2178. doi: 10.1029/2000WR900395

Poveda, G., Jaramillo, A., and Mantilla, R. (2001b). "Asociación Entre el Fenómeno El Niño y las anomalías de humedad de suelo y del índice "NDVI" en Colombia," in *Memorias IX Congreso Latinoamericano e Ibérico de Meteorología* (Buenos Aires), 7–11.

Poveda, G., Jaramillo, L., and Vallejo, L. F. (2014). Seasonal precipitation patterns along pathways of South American low-level jets and aerial rivers. *Water Resour. Res*. 50, 98–118. doi: 10.1002/2013WR014087

Poveda, G., and Mejía, J. F. (2004). Escalamiento espacial de sistemas convectivos de mesoescala sobre Colombia y el Pacífico Oriental en 1998 según la Misión TRMM. *Avances en Recursos Hidráulicos* 11, 131–143. Available online at: http://bdigital.unal.edu.co/6108/1/No._11-2004-4.pdf

Poveda, G., and Mesa, O. J. (1996). Las fases extremas del fenómeno ENSO (El Niño y La Niña) y su influencia sobre hidrología de Colombia. *Ing. Hidrául. Méx*. 1, 21–37.

Poveda, G., and Mesa, O. J. (1997). Feedbacks between hydrological processes in tropical South America and large scale oceanic atmospheric phenomena. *J. Clim*. 10, 2690–2702.

Poveda, G., and Mesa, O. J. (1999). La corriente de chorro superficial del oeste ("del CHOCÓ") y otras dos corrientes de chorro atmosféricas sobre Colombia: Climatología y Variabilidad durante las fases del ENSO. *Revista Acad. Colomb. Ci. Exact*. 23, 517–528.

Poveda, G., and Mesa, O. J. (2000). On the existence of Lloró (the rainiest locality on earth): enhanced ocean-land-atmosphere interaction by a low-level jet. *Geophys. Res. Lett*. 27, 1675–1678. doi: 10.1029/1999GL006091

Poveda, G., Mesa, O. J., Arias, P. A., Salazar, L. F. Moreno, H., Vieira, S. C., et al. (2005). The diurnal cycle of precipitation in the tropical Andes of Colombia. *Mon. Weather. Rev*. 133, 228–240. doi: 10.1175/MWR-2853.1

Poveda, G., Mesa, O. J., Toro, V. G., Agudelo, P. A., Álvarez, J. F., Arias, P. A., et al. (2002). Diagnostics of the anual cycle and ENSO effects on 1 to 24-hr rainfall events over the Andes of Colombia [In Spanish]. *Meteorol. Colombiana.* 5, 67–74.

Poveda, G., and Salas, H. D. (2015). Statistical scaling, Shannon entropy and generalized space-time q-entropy of rainfall fields in tropical South America. *Chaos* 25:075409. doi: 10.1063/1.4922595

Poveda, G., Vélez, J. I., Mesa, O. J., Cuartas, A., Barco, J., Mantilla, R., et al. (2007). Linking long-term water balances and statistical scaling to estimate river flows along the drainage network of Colombia. *J. Hydrol. Eng*. 12, 4–13. doi: 10.1061/(ASCE)1084-0699(2007)12:1(4)

Poveda, G., Waylen, P. R., and Pulwarty, R. (2006). Modern climate variability in northern South America and southern Mesoamerica. *Palaeogeo. Palaeoclim. Palaeoecol*. 234, 3–27. doi: 10.1016/j.palaeo.2005.10.031

Quintero, F., Krajewski, W. F., Mantilla, R., Small, S., and Seo, B. (2016). A spatial–dynamical framework for evaluation of satellite rainfall products for flood prediction. *J. Hydrometeorol.* 17, 2137-2154. doi: 10.1175/JHM-D-15-0195.1

Quispe, N. (2010). Estructura dinámica de una baja fría. *Rev. Peruana Geo-Atmos.* 1, 125–133. Available online at: https://web2.senamhi.gob.pe/rpga/pdf/2009_vol01/

Rabatel, A., Francou, B., Soruco, A., Gomez, J., Cáceres, B., Ceballos, J. L., et al. (2013). Current state of glaciers in the tropical Andes: a multi-century perspective on glacier evolution and climate change. *Cryosphere* 7, 81–102. doi: 10.5194/tc-7-81-2013

Ralph, F. M., Prather, K. A., Cayan, D., Spackman, J. R., DeMott, P., Dettinger, M., et al. (2016). CalWater field studies designed to quantify the roles of atmospheric rivers and aerosols in modulating US West Coast precipitation in a changing climate. *Bull. Am. Meteorol. Soc*. 97, 1209–1228. doi: 10.1175/BAMS-D-14-00043.1

Ramírez, B. H., van der Ploeg, M., Teuling, A. J., Ganzeveld, L., and Leemans, R. (2017). Tropical montane cloud forests in the orinoco river basin: the role of soil organic layers in water storage and release. *Geoderma* 298,14–26. doi: 10.1016/j.geoderma.2017.03.007

Rasmussen, K. L., Chaplin, M. M., Zuluaga, M. D., and Houze, R. A. Jr. (2016). Contribution of extreme convective storms to rainfall in south america. *J. Hydrometeorol.* 17, 353–367. doi: 10.1175/JHM-D-15-0067.1

Rasmussen, K. L., and Houze, R. A. Jr. (2011). Orogenic convection in subtropical South America as seen by the TRMM satellite. *Mon. Weather Rev*. 139, 2399–2420. doi: 10.1175/MWR-D-10-05006.1

Rasmussen, K. L., and Houze, R. A. Jr. (2016). Convective initiation near the Andes in subtropical South America. *Mon. Weather Rev*. 144, 2351–2374. doi: 10.1175/MWR-D-15-0058.1

Rasmussen, K. L., Zuluaga, M. D., and Houze, R. A. Jr. (2014). Severe convection and lightning in subtropical South America. *Geophys. Res. Lett*. 41, 7359–7366. doi: 10.1002/2014GL061767

Rau, P., Bourrel, L., Labat, D., Melo, P., Dewitte, B., Frappart, F., et al. (2016). Regionalization of rainfall over the Peruvian Pacific slope and coast. *Int. J. Climatol.* 37, 143–158. doi: 10.1002/joc.4693

Recalde-Coronel, G. C., Zaitchik, B., and Pan, W. K. (2020). Madden–Julian oscillation influence on sub-seasonal rainfall variability on the west of South America. *Clim. Dyn.* 54, 2167–2185. doi: 10.1007/s00382-019-05107-2

Restrepo, C., Walker, L. R., Shiels, A. B., Bussmann, R., Claessens, L., Fisch, S., et al. (2009). Landsliding and its multiscale influence on mountainscapes. *Bioscience* 59, 685–698. doi: 10.1525/bio.2009.59.8.10

Restrepo, J. D., and Escobar, H. A. (2018). Sediment load trends in the Magdalena River basin (1980–2010): anthropogenic and climate-induced causes. *Geomorphology* 302, 76–91. doi: 10.1016/j.geomorph.2016.12.013

Rickenbach, T. M., Ferreira, R. N., Halverson, J. B., Herdies, D. L., and Silva Dias, M. A. F. (2002). Modulation of convection in the southwestern Amazon basin by extratropical stationary fronts. *J. Geophys. Res.* 107:8040. doi: 10.1029/2000JD000263

Rivera, J. A., Araneo, D. C., and Peñalba, O. C. (2017a). Threshold level approach for streamflow drought analysis in the Central Andes of Argentina: a climatological assessment. *Hydrol. Sci. J*. 62, 1949–1964. doi: 10.1080/02626667.2017.1367095

Rivera, J. A., Araneo, D. C., Penalba, O. C., and Villalba, R. (2018). Regional aspects of streamflow droughts in the Andean rivers of Patagonia, Argentina. Links with large-scale climatic oscillations. *Hydrol. Res*. 49, 134–149. doi: 10.2166/nh.2017.207

Rivera, J. A., Penalba, O. C., Villalba, R., and Araneo, D. C. (2017b). Spatio-temporal patterns of the 2010-2015 extreme hydrological drought across the Central Andes, Argentina. *Water* 9:652. doi: 10.3390/w9090652

Roche, M. A., Aliaga, A., Campos, J., Pena, J., Cortes, J., and Rocha, N. (1990). "Hétérogénéité des précipitations sur la cordillère des Andes boliviennes," in *Hydrology in Mountainous Regions: International Association of Hydrological Sciences,* ed H. Lang (Wallingford: IAHS Publication), 381–388.

Rodriguez-Morata, C., Ballesteros-Canovas, J. A., Rohrer, M., Espinoza, J. C., Beniston, M., and Stoffel, M. (2018). Linking atmospheric circulation patterns with hydro geomorphic disasters in Peru. *Int. J. Climatol.* 38, 3388–3404. doi: 10.1002/joc.5507

Rodriguez-Morata, C., Díaz, H. F., and Ballesteros-Canovas, J. A. (2019). The anomalous 2017 coastal El Niño event in Peru. *Clim Dyn*. 52, 5605–5622. doi: 10.1007/s00382-018-4466-y

Rollenbeck, R., and Bendix, J. (2011). Rainfall distribution in the Andes of southern Ecuador derived from blending weather radar data and meteorological field observations. *Atmos. Res*. 99, 277–289. doi: 10.1016/j.atmosres.2010.10.018

Román-Cuesta, R. M., Carmona-Moreno, C., Lizcano, G., New, M., Silman, M., Knoke, T., et al. (2014). Synchronous fire activity in the tropical high Andes: an indication of regional climate forcing. *Glob. Change Biol*. 20, 1929–1942. doi: 10.1111/gcb.12538

Román-Cuesta, R. M., Salinas, N., Asbjornsen, H., Oliveras, I., Huaman, V., Gutiérrez, Y., et al. (2011). Implications of fires on carbon budgets in Andean cloud montane forest: the importance of peat soils and tree resprouting. *Forest Ecol. Manag*. 261, 1987–1997. doi: 10.1016/j.foreco.2011.02.025

Romatschke, U., and Houze, R. A. (2013). Characteristics of precipitating convective systems accounting for the summer rainfall of tropical and subtropical South America. *J. Hydrometeorol.* 14, 25–46. doi: 10.1175/JHM-D-12-060.1

Romatschke, U., and Houze, R. A. Jr. (2010). Extreme summer convection in South America. *J. Clim.* 23, 3761–3791. doi: 10.1175/2010JCLI3465.1

Romatschke, U., Medina, S., and Houze, R. A. Jr. (2010). Regional, seasonal, and diurnal variations of extreme convection in the South Asian region. *J. Climate* 23, 419–439. doi: 10.1175/2009JCLI3140.1

Ronchail, J. (1989a). Advections Polaires en Bolivie: mise en évidence et caractérisation des effets climatiques. *Hydrol. Cont*. 4, 49–56.

Ronchail, J. (1989b). "Climatological winter effects of southern advections in Bolivia and north-west Brazil (1973–1984)," *Paper Read at Third International Conference on Southern Hemisphere Meteorology and Oceanography.* (Buenos Aires).

Ronchail, J., Bourrel, L., Cochonneau, G., Vauchel, P., Phillips, L., Castro, A., et al. (2005). Climate and inundations in the Mamoré basin (South-Western Amazon-Bolivia). *J. Hydrol.* 302, 223–238. doi: 10.1016/j.jhydrol.2004.07.005

Ronchail, J., Cochonneau, G., Molinier, M., Guyot, J. -L., de Miranda Chaves, G. A., Guimarães, V., et al. (2002). Interannual rainfall variability in the Amazon Basin and sea surface temperatures in the equatorial Pacific and the tropical Atlantic Oceans. *Int. J. Climatol*. 22, 1663–1686. doi: 10.1002/joc.815

Ronchail, J., and Gallaire, R. (2006). ENSO and rainfall along the Zongo Valley (Bolivia) from the Altiplano to the Amazon Basin. *Int. J. Climatol*. 26, 1223–1236. doi: 10.1002/joc.1296

Rydbeck, A. V., and Maloney, E. D. (2015). On the Convective coupling and moisture organization of east Pacific easterly waves. *J. Atmos. Sci*. 72, 3850–3970. doi: 10.1175/JAS-D-15-0056.1

Saavedra, M., and Takahashi, K. (2017). Physical controls on frost events in the central Andes of Peru using in situ observations and energy flux models. *Agric. For. Met.* 239, 58–70. doi: 10.1016/j.agrformet.2017.02.019

Sakamoto, M. S., Ambrizzi, T., and Poveda, G. (2011). Moisture sources and life cycle of convective systems over western Colombia. *Adv. Meteorol.* 2011:890759. doi: 10.1155/2011/890759

Salas, H. D., Poveda, G., Mesa, O. J., and Marwan, N. (2020). Generalized synchronization between ENSO and hydrological variables in Colombia: a recurrence quantification approach. *Front. Appl. Math. Stat*. 6:3. doi: 10.3389/fams.2020.00003

Salazar, J. F., Villegas, J. C., Rendón, A. M., Rodríguez, E., Hoyos, I., Mercado-Bettín, D., et al. (2018). Scaling properties reveal regulation of river flows in the Amazon through a "forest reservoir". *Hydrol. Earth Syst. Sci.* 22, 1735–1748. doi: 10.5194/hess-22-1735-2018

Salio, P., Nicolini, M., and Zipser, E. J. (2007). Mesoscale convective systems over southeastern South America and their relationship with the South American low-level jet. *Mon. Weather Rev*. 135, 1290–1309. doi: 10.1175/MWR3305.1

Satyamurty, P., da Costa, C. P. W., Manzi, A. O., and Candido, L. A. (2013). A quick look at the 2012 record flood in the Amazon basin. *Geophys. Res. Lett*. 40, 1396–1401. doi: 10.1002/grl.50245

Schneider, H., Schwab, M., and Schlunegger, F. (2008). Channelized and hillslope sediment transport and the geomorphology of mountain belts. *Int. J. Earth Sci.* 97, 179–192. doi: 10.1007/s00531-006-0164-9

Schoolmeester, T., Saravia, M., Andresen, M., Postigo, J., Valverde, A., Jurek, M., et al. (2016). "*Outlook on Climate Change Adaptation in the Tropical Andes mountains*," in *Mountain Adaptation Outlook Series.United Nations Environment Programme, GRID-Arendal and CONDESAN.* Nairobi, Arendal, Vienna and Lima. Available online at: www.unep.org, www.grida.no, www.co.

Segura, H., Espinoza, J. C., Junquas, C., Lebel, T., Vuille, M., and Garreau, R. (2020). Recent changes in the precipitation-driving processes over the southern tropical Andes/western Amazon. *Clim. Dyn.* 54, 2613-2631. doi: 10.1007/s00382-020-05132-6

Segura, H., Espinoza, J. C., Junquas, C., and Takahashi, K. (2016). Evidencing decadal and interdecadal hydroclimatic variability over the central Andes. *Environ. Res. Lett.* 11:094016. doi: 10.1088/1748-9326/11/9/094016

Seiler, C., Hutjes, R. W. A., and Kabat, P. (2013). Climate variability and trends in Bolivia. *Jour. Appl. Meteorol. Clim*. 52, 130–146. doi: 10.1175/JAMC-D-12-0105.1

Sepúlveda, S. A., Moreiras, S. M., Lara, M., and Alfaro, A. (2014a). Debris flows in the Andean ranges of central Chile and Argentina triggered by 2013 summer storms: characteristics and consequences. *Landslides* 12, 115–133. doi: 10.1007/s10346-014-0539-0

Sepúlveda, S. A., and Padilla, C. (2008). Rain-induced debris and mudflow triggering factors assessment in the Santiago cordilleran foothills, Central Chile. *Nat. Hazards* 47, 201–215. doi: 10.1007/s11069-007-9210-6

Sepúlveda, S. A., and Petley, D. N. (2015). Regional trends and controlling factors of fatal landslides in Latin America and the Caribbean. *Nat. Hazards Earth Syst. Sci.* 15, 1821–1833. doi: 10.5194/nhess-15-1821-2015

Sepúlveda, S. A., Rebolledo, S., McPhee, J., Lara, M., Cartes, M., Rubio, E., et al. (2014b). Catastrophic, rainfall-induced debris flows in Andean villages of Tarapacá, Atacama desert, northern Chile. *Landslides* 11, 481–491. doi: 10.1007/s10346-014-0480-2

Shimada, I., Schaaf, C. B., Thompson, L. G., and Mosley-Thompson, E. (1991). Cultural impacts of severe droughts in the prehistoric Andes: application of a 1,500-year ice core precipitation record. *World Archaeol.* 22, 247–270. doi: 10.1080/00438243.1991.9980145

Sicart, J. E., Espinoza, J. C., Queno, L., and Medina, M. (2015). Radiative properties of clouds over a tropical Bolivian glacier: seasonal variations and relationship with regional atmospheric circulation. *Int. J. Clim.* 36, 3116–3128. doi: 10.1002/joc.4540

Smith, M. D. (2011). The ecological role of climate extremes: current understanding and future prospects. *J. Ecol.* 99, 651–655. doi: 10.1111/j.1365-2745.2011.01833.x

Soto, J., Galve, J. P., Palenzuela, J. A., Azaín, J. M., Tamay, J., and Irigaray, C. (2017b). A multi-method approach for the characterization of landslides in an intramontane basin in the Andes (Loja, Ecuador). *Landslides* 14, 1929–1947. doi: 10.1007/s10346-017-0830-y

Soto, J., Palenzuela, J. A., Galve, J. P., Luque, J. A., Azaín, J. M., Tamay, J., et al. (2017a). Estimation of empirical rainfall thresholds for landslide triggering using partial duration series and their relation with climatic cycles. An application in southern Ecuador. *Bull. Eng. Geol. And Environ.* doi: 10.1007/s10064-017-1216-z

Stahr, A., and Langenscheidt, E. (2015). *Landforms of High Mountains*. Berlin; Heidelberg: Springer-Verlag.

Stäubli, A., Nussbaumer, S. U., Allen, S. K., Huggel, C., Arguello, M., Costa, F., et al. (2017). "Analysis of weather- and climate-related disasters in mountain regions using different disaster databases," in: *Climate Change, Extreme Events and Disaster Risk Reduction. Sustainable Development Goals Series.* eds S. Mal, R. Singh, and C. Huggel (Cham: Springer), 17–41.

Sulca, J., Takahashi, K., Espinoza, J. C., Vuille, M., and Lavado-Casimiro, W. (2017). Impacts of different ENSO flavors and tropical Pacific convection variability (ITCZ, SPCZ) on austral summer rainfall in South America, with a focus on Peru. *Int. J. Climatol.* 38, 420–435. doi: 10.1002/joc.5185

Sulca, J., Vuille, M., Roundy, P., Takahashi, K., Espinoza, J. C., Silva, Y., et al. (2018). Climatology of extreme cold events in the central Peruvian Andes during austral summer: origin, types, and teleconnections. *Q J. R Meteorol. Soc.* 144, 2693–2714. doi: 10.1002/qj.3398

Sulca, J., Vuille, M., Silva, Y., and Takahashi, K. (2016). Teleconnections between the Peruvian central Andes and Northeast Brazil during extreme rainfall events in austral summer. *J. Hydrometeorol.* 17, 499–515. doi: 10.1175/JHM-D-15-0034.1

Sun, D., Xue, F., and Zhou, T. J. (2013). Impacts of two types of El Niño on atmospheric circulation in the Southern Hemisphere. *Adv. Atmos. Sci.* 30, 1732–1742. doi: 10.1007/s00376-013-2287-9

Takahashi, K. (2004). The atmospheric circulation associated with extreme rainfall events in Piura, Peru, during the 1997–1998 and 2002 El Niño events. *Ann. Geophys.* 22, 3917–3926. doi: 10.5194/angeo-22-3917-2004

Takahashi, K., and Dewitte, B. (2016). Strong and moderate nonlinear El Niño regimes. *Clim. Dyn.* 46, 1627–1645. doi: 10.1007/s00382-015-2665-3

Takahashi, K., and Martínez, A. G. (2019). The very strong coastal El Niño in 1925 in the far-eastern Pacific. *Clim. Dyn.* 52, 7389–7415. doi: 10.1007/s00382-017-3702-1

Takahashi, K., Montecinos, A., Goubanova, K., and Dewitte, B. (2011). ENSO regimes: reinterpreting the canonical and Modoki El Niño. *Geophys. Res. Lett.* 38:L10707. doi: 10.1029/2011GL047364

Teitelbaum, H., and D'Andrea, F. (2015). Deep convection east of the Andes Cordillera: four hailstorm cases. *Tellus* 67:26806. doi: 10.3402/tellusa.v67.26806

Townsend-Small, A., McClain, M. E., Hall, B., Noguera, J. L., Llerena, C. A., and Brandes, J. A. (2008). Suspended sediments and organic matter in mountain headwaters of the Amazon River: results from a 1-year time series study in the central Peruvian Andes. *Geochim. Cosmochim. Acta* 72, 732–740. doi: 10.1016/j.gca.2007.11.020

Trachte, K. (2018). Atmospheric moisture pathways to the highlands of the tropical Andes: analyzing the effects of spectral nudging on different driving fields for regional climate modeling. *Atmosphere* 9:456. doi: 10.3390/atmos9110456

Trachte, K., Rollenbeck, R., and Bendix, J. (2010). Nocturnal convective cloud formation under clear-sky conditions at the eastern Andes of south Ecuador. *J. Geophys. Res. Atmos.* 115D:24203. doi: 10.1029/2010JD014146

Trauth, M. H., Alonso, R. A., Haselton, K. R., Hermanns, R. L., and Strecker, M. R. (2000). Climate change and mass movements in the NW Argentine Andes. *Earth Planet. Sci. Lett.* 179, 243–256. doi: 10.1016/S0012-821X(00)00127-8

UNISDR (2016). *Oficina de las Naciones Unidas para la Reducción del Riesgo de Desastres 2016: Impacto de los Desastres en América Latina y El Caribe, 1990-2013.* Agencia Española de Cooperación Internacional para el Desarrollo y Corporación OSSO.

Urrutia-Jalabert, R., González, M. E., González-Reyes, Á., Lara, A., and Garreaud, R. (2018). Climate variability and forest fires in central and south-central Chile. *Ecosphere* 9:e02171. doi: 10.1002/ecs2.2171

Valenzuela, R. A., and Garreaud, R. D. (2019). Extreme daily rainfall in central-southern Chile and its relationship with low-level horizontal water vapor fluxes. *J. Hydrometeorol.* 20, 1829–1850. doi: 10.1175/JHM-D-19-0036.1

Vallejo-Bernal, S. M., Urrea, V., Bedoya-Soto, J. M., Posada, D., Olarte, A., Cárdenas-Posso, Y., et al. (2020). Ground validation of TRMM 3B43 V7 precipitation estimates over Colombia. Part I: Monthly and seasonal timescales. *Int. J. Climatol.* doi: 10.1002/joc.6640

Vanacker, V., Balthazar, V., and Molina, A. (2013). Anthropogenic activity triggering landslides in densely populated mountain areas. *Landslide Sci.Pract.* 4, 163–167. doi: 10.1007/978-3-642-31337-0_21

Vanacker, V., Molina, A., Govers, G., Poesen, J., and Deckers, J. (2007). Spatial variation of suspended sediment concentrations in a tropical Andean river system: the Paute River, southern Ecuador. *Geomorphology* 87, 53–67. doi: 10.1016/j.geomorph.2006.06.042

Vanacker, V., Vanderschaeghe, M., Govers, G., Willems, E., Poesen, J., Deckers, J., et al. (2003). Linking hydrological, infinite slope stability and land-use change models through GIS for assessing the impact of deforestation on slope stability in high Andean watersheds. *Geomorphology* 52, 299–315. doi: 10.1016/S0169-555X(02)00263-5

Varble, A., Nesbitt, S., Salio, P., Avila, E., Borque, P., deMott, P., et al. (2019). *Cloud, Aerosol, and Complex Terrain Interactions (CACTI) Field Campaign Report.* Ed Stafford R (ARM user facility). DOE/SC-ARM-19-028.

Veblen, T. T., and Kitzberger, T. (2002). Inter-hemispheric comparison of fire history: the Colorado Front Range, U.S.A., and the northern Patagonian Andes, Argentina. *Plant Ecol.* 163, 187–207. doi: 10.1023/A:1020905823901

Velasco, I., and Fritsch, J. M. (1987). Mesoscale convective complexes in the Americas. *J. Geophys. Res. Atmos.* 92, 9591–9613. doi: 10.1029/JD092iD08p09591

Viale, M., and Garreaud, R. (2014). Summer precipitation events over the western slope of the subtropical Andes. *Mon. Weather Rev.* 142, 1074-1092. doi: 10.1175/MWR-D-13-00259.1

Viale, M., and Nuñez, M. N. (2011). Climatology of winter orographic precipitation over the subtropical central Andes and associated synoptic and regional characteristic. *J. Hydrometeorol.* 12, 481–507. doi: 10.1175/2010JHM1284.1

Viale, M., Valenzuela, R., Garreaud, R., and Ralph, F. (2018). Impacts of atmospheric rivers on precipitation in Southern South America. *J. Hydrometeorol.* 19, 1671–1686. doi: 10.1175/JHM-D-18-0006.1

Vicente-Serrano, S. M., Aguilar, E., Martínez, R., Martín-Hernández, N., Azorin-Molina, C., Sanchez-Lorenzo, A., et al. (2017). The complex influence of ENSO on droughts in Ecuador. *Clim. Dyn.* 48, 405–427. doi: 10.1007/s00382-016-3082-y

Vicente-Serrano, S. M., Beguería, S., and López-Moreno, J. I. (2011b). Comment on "Characteristics and trends in various forms of the Palmer Drought Severity Index (PDSI) during 1900–2008" by A. *Dai. J. Geophys. Res. Atmos.* 116:D19112. doi: 10.1029/2011JD016410

Vicente-Serrano, S. M., López-Moreno, J. I., Gimeno, L., Nieto, R., Morán-Tejeda, E., Lorenzo-Lacruz, J., et al. (2011a) A multi-scalar global evaluation of the impact of ENSO on droughts. *J. Geophys. Res. Atmos.* 116:D20109. doi: 10.1029/2011JD016039

Villalobos, E. E., Martinez-Castro, D., Kumar, S., Silva, Y., and Fashe, O. (2019). Study of convective storms in the Peruvian central Andes using PR-TRMM and KuPR-GPM radars (In Spanish). *Rev. Cubana Meteorol.* 25, 59–75. Available online at: http://rcm.insmet.cu/index.php/rcm/article/view/454/673

Vuille, M. (1999). Atmospheric circulation over the Bolivian Altiplano during dry and wet periods and extreme phases of the southern oscillation. *Int. J. Climatol.* 19, 1579–1600.

Vuille, M., Bradley, R., and Keimig, F. (2000). Interannual climate variability in the central Andes and its relation to tropical Pacific and Atlantic forcing. *J. Geophys. Res. Atmos.* 105, 12447–12460. doi: 10.1029/2000JD900134

Vuille, M., Francou, B., Wagnon, P., Juen, I., Kaser, G., Mark, B., et al. (2008). Climate change and tropical Andean glaciers: past, present and future. *Earth Sci. Rev*. 89, 79–86. doi: 10.1016/j.earscirev.2008.04.002

Wang, C. (2002). Atmospheric circulation cells associated with the El Niño–Southern Oscillation. *J. Climate* 15, 399–419. doi: 10.1175/1520-0442(2002)015<0399:ACCAWT>2.0.CO;2

Wang, H., and Fu, R. (2002) Cross-equatorial flow and seasonal cycle of precipitation over South America. *J. Clim.* 15, 1591–1608. doi: 10.1175/1520-0442(2002)015<1591:CEFASC>2.0.CO;2

Waylen, P. R., and Poveda, G. (2002). El Niño-Southern oscillation and aspects of western South America hydro-climatology. *Hydrol. Process*. 16, 1247–1260. doi: 10.1002/hyp.1060

Wheeling, K. (2019, October 10). Deforestation could Exacerbate Drought in the Amazon. *Eos*.

Woodman, R. F. (1985). "Recurrencia del Fenòmeno del Niño con intensidad comparable a la del Niño 1982–1983. El Fenòmeno El Niño," in *Proceedings of the Seminario Regional Ciencia, Tecnología y Agresiòn Ambiental* (Lima: CONCYTEC), 301–332.

Woodman, R. F. (1999). "Modelo estadístico de pronòstico de las precipitaciones en la costa norte del Perú. El Fenòmeno El Niño. Investigaciòn para una prognosis," in *1er encuentro de Universidades del Pacífico Sur: Memoria* (Lima), 93–108.

Wu, H., Adler, R. F., Tian, Y., Gu, G., and Huffman, G. J. (2017). Evaluation of quantitative precipitation estimations through hydrological modeling in floods river basins. *J. Hydrometeorol.* 18, 529–553. doi: 10.1175/JHM-D-15-0149.1

Yang, Z., and Dominguez, F. (2019). Investigating land surface effects on the moisture transport over south america with a moisture tagging model. *J. Clim.* 32, 6627–6644. doi: 10.1175/JCLI-D-18-0700.1

Yarleque, C., Vuille, M., Hardy, D. R., Posadas, A., and Quiroz, R. (2016). Multiscale assessment of spatial precipitation variability over complex mountain terrain using a high-resolution spatiotemporal wavelet reconstruction method. *J. Geophys. Res. Atmos.* 121, 198–216. doi: 10.1002/2016JD025647

Yepes, J., Poveda, G., Mejía, J. F., Moreno, L., and Rueda, C. (2019). CHOCO-JEX: a research experiment focused on the Chocó low-level jet over the far eastern Pacific and western Colombia. *Bull. Am. Meteorol. Soc.* 100, 779–796. doi: 10.1175/BAMS-D-18-0045.1

Younes-Cárdenas, N., and Erazo-Mera, E. (2016). Landslide susceptibility analysis using remote sensing and GIS in the western Ecuadorian Andes. *Nat. Hazards* 81, 1829–1859. doi: 10.1007/s11069-016-2157-8

Yu, J. -Y., and Kao, H. -Y. (2007). Decadal changes of ENSO persistence barrier in SST and ocean heat content indices: 1958–2001. *J. Geophys. Res*. 112:D13106. doi: 10.1029/2006JD007654

Zambrano-Bigiarini, M., Nauditt, A., Birkel, C., Verbist, K., and Ribbe, L. (2017). Temporal and spatial evaluation of satellite-based rainfall estimates across the complex topographical and climatic gradients of Chile. *Hydrol. Earth Syst. Sci*. 21, 1295–1320. doi: 10.5194/hess-21-1295-2017

Zemp, D., Schleussner, C. -F., Barbosa, H., van Der Ent, R., Donges, J. F., Heinke, J., et al. (2014). On the importance of cascading moisture recycling in South America. *Atmos. Chem. Phys*. 14, 13337–13359. doi: 10.5194/acp-14-13337-2014

Zhou, J., and Lau, K.-M. (2001). Principal modes of interannual and decadal variability of summer rainfall over South America (2001). *Int. J. Clim*. 21, 1623–1644. doi: 10.1002/joc.700

Zipser, E. J., Liu, C., Cecil, D. J., Nesbitt, S. W., and Yorty, D. P. (2006). Where are the most intense thunderstorms on Earth? *Bull. Am. Meteorol. Soc*. 87, 1057–1071. doi: 10.1175/BAMS-87-8-1057

Zuluaga, M. D., and Houze, R. A. Jr. (2015). Extreme convection of the near-equatorial Americas, Africa, and adjoining oceans as seen by TRMM. *Mon. Weather Rev*. 143, 298–316. doi: 10.1175/MWR-D-14-0 0109.1

Conflict of Interest: The authors declare that the research was conducted in the absence of any commercial or financial relationships that could be construed as a potential conflict of interest.